



Terms and Conditions of Use of Digitised Theses from Trinity College Library Dublin

Copyright statement

All material supplied by Trinity College Library is protected by copyright (under the Copyright and Related Rights Act, 2000 as amended) and other relevant Intellectual Property Rights. By accessing and using a Digitised Thesis from Trinity College Library you acknowledge that all Intellectual Property Rights in any Works supplied are the sole and exclusive property of the copyright and/or other IPR holder. Specific copyright holders may not be explicitly identified. Use of materials from other sources within a thesis should not be construed as a claim over them.

A non-exclusive, non-transferable licence is hereby granted to those using or reproducing, in whole or in part, the material for valid purposes, providing the copyright owners are acknowledged using the normal conventions. Where specific permission to use material is required, this is identified and such permission must be sought from the copyright holder or agency cited.

Liability statement

By using a Digitised Thesis, I accept that Trinity College Dublin bears no legal responsibility for the accuracy, legality or comprehensiveness of materials contained within the thesis, and that Trinity College Dublin accepts no liability for indirect, consequential, or incidental, damages or losses arising from use of the thesis for whatever reason. Information located in a thesis may be subject to specific use constraints, details of which may not be explicitly described. It is the responsibility of potential and actual users to be aware of such constraints and to abide by them. By making use of material from a digitised thesis, you accept these copyright and disclaimer provisions. Where it is brought to the attention of Trinity College Library that there may be a breach of copyright or other restraint, it is the policy to withdraw or take down access to a thesis while the issue is being resolved.

Access Agreement

By using a Digitised Thesis from Trinity College Library you are bound by the following Terms & Conditions. Please read them carefully.

I have read and I understand the following statement: All material supplied via a Digitised Thesis from Trinity College Library is protected by copyright and other intellectual property rights, and duplication or sale of all or part of any of a thesis is not permitted, except that material may be duplicated by you for your research use or for educational purposes in electronic or print form providing the copyright owners are acknowledged using the normal conventions. You must obtain permission for any other use. Electronic or print copies may not be offered, whether for sale or otherwise to anyone. This copy has been supplied on the understanding that it is copyright material and that no quotation from the thesis may be published without proper acknowledgement.

DEVELOPING NOVEL THERAPEUTIC APPROACHES IN CHEMORESISTANT OVARIAN CANCER PATIENTS

VOLUME I



*A Thesis Submitted to the University of Dublin for the Degree of
Doctor of Philosophy (Ph.D.)*

By

Lynda Marie McEvoy (B.A., B.Sc.)

Supervisor: Prof. John O'Leary

Department of Histopathology and Morbid Anatomy

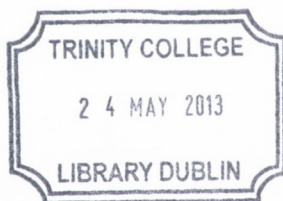
University of Dublin

Trinity College

March 2012

Declaration

I hereby certify that the work in this thesis has not been submitted for any other degree or diploma at this, or any other university, and that all the work described herein is entirely my own except where otherwise acknowledged. This thesis may be made available from the library for lending, consultation or copying.



Thesis 10061.1

Lynda McEvoy

Lynda McEvoy

Summary

Ovarian cancer is the fifth most common cause of cancer death in women and is the leading cause of death from gynaecological malignancy in the Western world. A recent study by the National Cancer Registry, Ireland has shown that between 2004 and 2009, ovarian cancer was the fourth most common cause of cancer death in women in Ireland. It also found that Ireland has the 4th highest incidence of, and the highest mortality rate from, ovarian cancer in Europe. Ovarian cancer is associated with poor long-term survival due to late diagnosis and development of chemoresistance. While approximately 80% of patients respond well to platinum/taxane-based chemotherapy initially, a large proportion suffer recurrent disease and become chemoresistant.

Tumour hypoxia is characterized by a low level of tumour oxygenation, and is associated with many features of tumour aggressiveness including increased cellular proliferation, inhibition of apoptosis, increased invasion and metastasis, and chemoresistance. Most of the functions of hypoxia are mediated through HIF-1 α . While HIF-1 α has been associated with platinum resistance in a variety of cancers, including ovarian, relatively little is known about the importance of the duration of hypoxia. Similarly, the gene pathways activated in ovarian cancer which cause chemoresistance as a result of hypoxia are poorly understood.

This study aimed to firstly investigate the effect of hypoxia duration on resistance to cisplatin (platinum) and paclitaxel (taxane) in an ovarian cancer chemoresistance cell line model. Secondly, we aimed to identify genes whose expression was associated with hypoxia-induced chemoresistance, and thirdly, we wished to select hypoxia-associated biomarkers and evaluate their expression in ovarian tumours.

Cisplatin-sensitive (A2780) and cisplatin-resistant (A2780cis) ovarian cancer cell lines were exposed to various combinations of hypoxia and/or chemotherapeutic drugs as part of a 'hypoxia matrix' designed to cover clinically relevant scenarios in terms of tumour hypoxia. Response to cisplatin and paclitaxel was measured by the MTT assay. RNA was extracted from cells treated as part of the hypoxia

matrix at the point which gave the most consistent and largest changes in chemoresistance, and was interrogated on Affymetrix Human Gene ST 1.0 arrays. Differential gene expression was analysed for cells exposed to hypoxia and/or treated with cisplatin and four potential markers of chemoresistance were selected for evaluation in a cohort of ovarian tumour samples by RT-PCR.

We found that resistance to cisplatin increases over time in A2780 cells cultured in hypoxia, while in A2780cis, cisplatin resistance is not increased to the same degree as in A2780 cells. There was a trend towards increased paclitaxel resistance over time in A2780 cells while the paclitaxel resistance profile of A2780cis did not change in hypoxia. A plethora of genes were differentially expressed in cells exposed to hypoxia and cisplatin which could be associated with chemoresistance. Expression of potential/known biomarkers of hypoxia in ovarian cancer was evaluated by RT-PCR in ovarian tumour samples – BDNF, ANGPTL4, HER3 and HIF-1 α . High expression of ANGPTL4 trended towards reduced progression-free and overall survival. High expression of HER3 trended towards increased progression-free but reduced overall survival, while high expression of HIF-1 α trended towards increased progression-free and reduced overall survival. BDNF was expressed in a small percentage of tumour samples and requires further study.

In conclusion, this study has further characterized the relationship between hypoxia and chemoresistance in an ovarian cancer model. We have also identified many potential biomarkers of hypoxia and platinum resistance and provided an initial validation of a subset of these markers in ovarian cancer tissues.

Acknowledgements

I wish to sincerely thank my supervisor, Professor John O’Leary, for all your help and guidance over the past three years. Your enthusiasm for research was hugely motivating over the course of the thesis.

Thank you to the Emer Casey Foundation for all your support over the years. I hope you are really proud of what you have achieved in Emer’s memory.

A very big thank you to my co-supervisor, Dr. Sharon O’Toole, for all your knowledge, support and patience during this PhD. I really appreciate everything you have done over the years.

A special thank you to Prof. Orla Sheils for all your help, particularly when times were hard, you always knew what to do!

Thank you to Dr. Cara Martin for all your advice and input into the project.

Thank you to Dr. Cathy Spillane for all your knowledge, advice and chats over the years! Our red wine night will finally happen!

Thank you to everyone in the lab in CPL, especially Emma, Gary, Paul, Lisa, Gordon, Niamh, Darragh and Ruth for all your friendship, coffees and Friday lunches.

Thank you to Jean Freeman for all administrative support in CPL.

Thank you to Dr. Gordon Blackshields for your bioinformatics knowledge!

Thanks to everyone in the Coombe Molecular Pathology lab for all your friendship and my ‘first home’ including Mic, Jamie, Yvonne, Salah, Helen, Christine, Aoife Cooke, and Aoife Canney.

Thanks to all in Obs & Gynae for all the chats, advice and friendship, including Dr. Lucy Norris, Dr. Lynne Kelly, Dr. Feras Abu Saadeh, Dr. Ream Langhe, Ms. Christina Boccardo, and Ms. Valerie Ashe.

Thank you to Dr. Britta Stordal for help with Western Blots.

Thank you to Alo McGoldrick, UCD, for sectioning the patient tumour samples and isolating RNA.

Thank you to Cathy in cytology, SJH, for the purple lids and to Ronan Ward in histology for help arranging materials.

Thank you to Dr. Noreen Gleeson, Dr. Tom D’Arcy and all the registrars, SHOs and interns on the gynae-oncology team in St. James’s Hospital for help in collecting patient specimens.

Thank you to everyone in the compounding unit in St. James’s Hospital for provision of cytotoxic drugs.

Thank you to Actavis for donation of the vehicle control for paclitaxel.

Thank you to Dr. Louise Kehoe and Jacqui Barry-O’Crowley from histology in the Coombe for everything histology-related!

To the girls – Erin, Lisa, Nell, Sarah, Siobhan, Carmel, Maeve, Niamh, Roisin, Oonagh, Steph and Stacey – thank you so much for being great friends, always listening and having a laugh!

To Mam and Dad, thank you for always being there, and for all your help throughout the course of the PhD. It’s finally time for me to get a real job!

Michael, I couldn’t have done this without you.

'For Mam and Dad'

List of Tables

1.1	Hypotheses Regarding the Aetiology of Ovarian Cancer	20
1.2	FIGO Classification of Ovarian Cancer	25
1.3	Classification of Platinum Resistance	29
1.4	Effects of Hypoxia on Chemoresistance	37
2.1	Concentrations of Supplements Added to RPMI 1640 media for Cell Culture of A2780 and A2780cis Cell Lines.....	43
2.2	Cell Densities for A2780 and A2780cis Cell Lines as Set Out by the ECACC Guidelines	44
2.3	Controls for MycoAlert® assay for Mycoplasma Contamination of Cell Culture	46
2.4	List of Concentrations of Poly-A Controls.....	62
2.5	First Strand cDNA Master Mix Components	63
2.6	Second-Strand Master Mix Components	64
2.7	IVT Master Mix Components.....	64
2.8	cRNA Binding Mix Components.....	65
2.9	Second-Cycle Master Mix Components	67
2.10	cDNA Binding Mix Components	68
2.11	Fragmentation Reaction Component	69
2.12	Fragmentation Master Mix Components	70
2.13	Labelling Master Mix Components.....	70
2.14	Hybridization Cocktail Master Mix	71
2.15	Components of Reverse Transcription Master Mix	76
2.16	Components of Taqman® Master Mix.....	76
2.17	Modified RIPA used for Protein Extraction	80

2.18	Concentrations of BSA in the BCA Assay Standards	82
2.19	Components of Separating and Stacking Gels for Western Blot	83
2.20	Components of Electrophoresis Running Buffer	83
2.21	Components of Laemmli (Loading) Buffer	84
2.22	Components of Transfer Buffer	85
2.23	Components of Wash Buffer	85
3.1	Components of Vehicle Controls for Cisplatin and Paclitaxel	99
3.2	List of Seeding Densities Assayed to Determine the Optimum Cell Concentration for Cytotoxicity Assays	100
3.3	Concentrations of Cytotoxic Drugs Cisplatin and Paclitaxel	101
3.4	Hypoxia Matrix Conditions	103
3.5	Antibodies for HIF-1 α Timecourse	105
3.6	IC50 Values Obtained When Treating A2780 and A2780cis with Cisplatin and Paclitaxel for Various Timepoints	112
4.1	Differential Gene Expression Summary Characteristics of A2780 vs. A2780cis	173
4.2	Top Five Significantly Up-Regulated Pathways in A2780cis Compared to A2780	176
4.3	Top Five Significantly Up-Regulated Pathways in A280cis Compared to A2780	177
4.4	Summary of the Gene Expression Changes Induced by Hypoxia in A2780 and A2780cis	182
4.5	Top Five Up-Regulated Pathways in A2780 Cells Exposed to Hypoxia	187

4.6	Top Five Down-Regulated Pathways in A2780 Cells Exposed to Hypoxia	187
4.7	Top Five Up-Regulated Pathways in A2780cis Cells Exposed to Hypoxia	188
4.8	Top Five Down-Regulated Pathways in A2780cis Cells Exposed to Hypoxia	188
4.9	Significantly Enriched Pathways from Commonly Up-Regulated Genes in A2780 and A2780cis in Response to Hypoxia	191
4.10	Top Five Significantly Enriched Pathways from Commonly Down-Regulated Genes in A2780 and A2780cis in Response to Hypoxia	191
4.11	Commonly Up-Regulated Pathways in A2780 Cells Exposed to Hypoxia and A2780cis	194
4.12	Commonly Down-Regulated Pathways in A2780 Cells Exposed to Hypoxia and A2780cis	194
4.13	Commonly Dysregulated Genes in A2780 Cells Exposed to Hypoxia and A2780cis which are Linked to Cisplatin Resistance in the Literature	194
4.14	Summary of Differential Gene Expression Characteristics for A2780 Cells Treated with Cisplatin for 72 hours in Normoxia or Hypoxia	208
4.15	Top Four Significantly Up-Regulated Pathways in A2780 Cells Treated with Cisplatin in Normoxia	212
4.16	Top Four Significantly Down-Regulated Pathways in A2780 Cells Treated with Cisplatin in Normoxia	212
4.17	Top Four Significantly Up-Regulated Pathways in A2780 Cells Treated with Cisplatin in Hypoxia	213
4.18	Top Four Significantly Down-Regulated Pathways in A2780 Cells Treated with Cisplatin in Hypoxia	213
4.19	Pathway Analysis of Up-Regulated Genes in A2780 Cells Treated with Cisplatin in Hypoxia Only	216

4.20	Pathway Analysis of Down-Regulated Genes in A2780 Cells Treated with Cisplatin in Hypoxia Only.....	217
4.21	Dysregulated Genes in the Hypoxic Response to Cisplatin in A2780 which have been Directly Linked to Cisplatin Resistance	218
4.22	Summary of Differential Gene Expression Characteristics of A2780cis Treated with Cisplatin in Normoxia and Hypoxia	219
4.23	Top Five Significantly Up-Regulated Pathways in A2780cis Treated with Cisplatin in Normoxia	223
4.24	Top Five Significantly Down-Regulated Pathways in A2780cis Treated with Cisplatin in Normoxia.....	223
4.25	Top Three Significantly Up-Regulated Pathways in A2780cis Treated with Cisplatin in Hypoxia	224
4.26	Top Three Significantly Down-Regulated Pathways in A2780cis Treated with Cisplatin in Hypoxia	224
4.27	Pathway Analysis of Up-Regulated Genes in the A2780cis Hypoxic Response to Cisplatin	226
4.28	Pathway Analysis of Down-Regulated Genes in the A2780cis Hypoxic Response to Cisplatin	226
4.29	Dysregulated Genes in A2780cis Hypoxic Only Response to Cisplatin Linked to Cisplatin Resistance in the Literature.....	227
4.30	Significant Commonly Up-Regulated Pathways in the A2780 and A2780cis 'Hypoxic Only' Response to Cisplatin	228
4.31	Significant Commonly Down-Regulated Pathways in the A2780 and A2780cis 'Hypoxic Only' Response to Cisplatin.....	228
4.32	Commonly Dysregulated Genes in the A2780 and A2780cis Hypoxic Only Response to Cisplatin	

	which have been Directly Linked to Cisplatin Resistance	229
5.1	List of Samples Used for Validation Based on the Hypoxia Matrix.....	248
5.2	List of Patient/Tumour Characteristics.....	248
5.3	List of Probes for Taqman® PCR	249
5.4	Classification of Tumour Samples Based on Response to Chemotherapy	250
5.5	Breakdown of High and Low Gene Expression	251
5.6	Comparison of Fold-Changes in Validation Genes in Array and Taqman®(TM).....	254
5.7	Summary of Kaplan-Meier Analysis.....	266

List of Figures

1.1	Six Hallmarks of Cancer.....	4
1.2	The Cell Cycle.....	6
1.3	Fas Signalling Pathway	7
1.4	Tumour Angiogenesis	9
1.5	Emerging Hallmarks of Cancer	11
1.6	Histology of Epithelial Ovarian Cancer Subtypes	16
1.7	Histology of Type I and Type II Ovarian Tumours	21
1.8	Computed Tomography Scan of Advanced Ovarian Cancer	23
1.9	Summary of HIF-1-mediated Processes	32
2.1	INVIVO2 400 Hypoxia Workstation	48
2.2	Sample Graphs Obtained Using MTT Assay.....	49
2.3	Electropherograms Produced From Analysis of RNA Samples by the Bionalyzer Expert Software	53
2.4	Regions of the Electropherogram Analysed on the Bioanalyzer Expert Software to Generate a RIN Value for RNA Samples	54
2.5	Bioanalyzer Chip Priming Station	56
2.6	Differences in Gene Change Capture between 3' Assay and WT Assays	57
2.7	Comparison of Detection of Fold Changes of Gene Expression Across Varying Concentrations of RNA	58

2.8	Synthesis of GeneChip Arrays.....	59
2.9	Outline of the Three Day Protocol for Array Analysis	61
2.10	Affymetrix GeneChip Array.....	72
2.11	Overview of the Taqman® PCR Process	75
2.12	Setting the Threshold for PCR Reactions	78
3.1	Structure of Cisplatin.....	90
3.2	Structure of Paclitaxel	95
3.3	Schematic of Hypoxia Matrix Conditions	104
3.4	Light Images of A2780 and A2780cis Cell Lines	108
3.5	Light Images of A2780 and A2780cis Cells Exposed to Hypoxia	109
3.6	Optimal Seeding Density for A2780 and A2780cis Cell Lines	111
3.7	Treatment Periods for A2780 Cells with Cisplatin and Paclitaxel.....	113
3.8	Treatment Periods for A2780cis Cells with Cisplatin and Paclitaxel.....	114
3.9	Effect of Cisplatin on Morphology of A2780 in Normoxia and Hypoxia	117
3.10	Effect of Cisplatin on Morphology of A2780cis in Normoxia and Hypoxia	118
3.11	A2780cis are more Resistant to Cisplatin than A2780.....	119
3.12	A2780 and A2780cis Show Similar Resistance Profiles to Paclitaxel.....	120

3.13	Acute Hypoxia Increases Resistance to Cisplatin in A2780	121
3.14	Acute Hypoxia Increases Resistance to Paclitaxel in A2780.....	122
3.15	Chronic Hypoxia Increases Resistance to Cisplatin in A2780	124
3.16	Chronic Hypoxia Increases Resistance to Paclitaxel in A2780.....	125
3.17	Treating A2780 in Hypoxia Increases Resistance to Cisplatin	127
3.18	Treating A2780 in Hypoxia Increases Resistance to Paclitaxel.....	128
3.19	Acute Hypoxia Increases Resistance to Cisplatin in A2780cis	130
3.20	Acute Hypoxia does not Increase Resistance to Paclitaxel in A2780cis.....	131
3.21	Chronic Hypoxia Increases Resistance to Cisplatin in A2780cis	133
3.22	Chronic Hypoxia does not Increase Resistance to Paclitaxel in A2780cis.....	134
3.23	Treating A2780cis in Hypoxia Increases Resistance to Cisplatin	136
3.24	Treating A2780cis in Hypoxia does not Increase Resistance to Paclitaxel	137
3.25	Timecourse of expression of HIF-1 α in A780 and A2780cis	139
4.1	Location of B2 Oligo Positive Control on GeneChip Arrays	166

4.2	Probe Summarization Quality Control Metrics	168
4.3	Control Signal Quality Control Metrics	169
4.4	Pearson's Correlation of Samples Analysed on Affymetrix Arrays	171
4.5	Clustering Denogram of Hierarchical Clustering Analysis of Gene Expression Profiles of A2780 and A2780cis Cells With/Without Exposure to Hypoxia and Treatment with Cisplatin	172
4.6	Chromosomal Location Plot of Differentially Expressed Genes in A2780cis Compared to A2780	174
4.7	Overview of Gene Expression Changes in A2780 and A2780cis	175
4.8	Chromosomal Location Plots of Genes Differentially Expressed by Hypoxia in A2780 and A2780cis Cells	184
4.9	Volcano Plot and Heat Map of Gene Expression Changes in A2780 Cells in Response to Hypoxia	185
4.10	Volcano Plot and Heat Map of Gene Expression Changes in A2780cis Cells in Response to Hypoxia	186
4.11	Summary of Common Differential Gene Changes in A2780 and A2780cis Cells Exposed to Hypoxia	190
4.12	Comparison of Gene Expression Changes Induced by Hypoxia and Repeated Cisplatin Exposure in A2780.....	193

4.13	Chromosomal Location Plots for Differentially Expressed Genes in A2780 Cells in response to Cisplatin Treatment in Normoxia and Hypoxia	209
4.14	Differences in Gene Expression Patterns Between Untreated and Cisplatin Treated A2780 Cells in Normoxia	210
4.15	Differences in Gene Expression Patterns Between Untreated and Cisplatin Treated A2780 cells in Hypoxia	211
4.16	Comparison of Differential Gene Expression Changes in A2780 Cells Treated with Cisplatin in Normoxia and Hypoxia	215
4.17	Chromosomal Location Plots for Differentially Expressed Genes in A2780cis in Response to Cisplatin Treatment in Normoxia and Hypoxia	220
4.18	Volcano Plot and Heat Map Depicting Gene Expression Changes in Response to Cisplatin in A2780cis in Normoxia.....	221
4.19	Volcano Plot and Heat Map Depicting Gene Expression Changes in Response to Cisplatin in A2780cis in Hypoxia.....	222
4.20	Comparison of Gene Expression Changes in A2780cis Treated with Cisplatin in Normoxia and Hypoxia	225
5.1	Comparison of Taqman® Analysis and Array Data	255
5.2	Comparison of Array and Taqman® Fold Changes for Cisplatin Response	256

5.3	Changes in Gene Expression in A2780 in the Hypoxia Matrix	259
5.4	Changes in Gene Expression in A2780cis in the Hypoxia Matrix	260
5.5	Expression of ANGPTL4 in Cohort of Tumour Samples.....	263
5.6	Expression of HER3 in Cohort of Tumour Samples	264
5.7	Expression of HIF-1 α in Cohort of Tumour Samples	265
A1	Comparison of Untreated Cells with Cells Treated with Vehicle Control Solutions	xxxix

Abbreviations

ADP	Adenosine Diphosphate
AGCC	Affymetrix GeneChip Command Console
ALCAM	Activated Leukocyte Cell Adhesion Molecule
AMPS	Ammonium Persulphate
ANGPT1	Angiopoietin-1
ANGPTL4	Angiopoietin-like 4
AP	Alkaline Phosphatase
APC	Adenomatous Poliposis Coli
ARHI	Aplasia Ras Homolog member 1
ATP	Adenosine Triphosphate
AUC	Area under the Curve
BCA	Bicinchoninic Acid
BCI2L1	BCI-2 like 1
BDNF	Brain-Derived Neurotrophic Factor
BIRC3	Baculoviral IAP Repeat Containing 3
BMP4	Bone Morphogenetic Protein 4
BOLD	Blood Oxygen Level Dependent
BPH	Benign Prostatic Hyperplasia
BRCA	Breast Cancer 1, Early Onset
BSA	Bovine Serum Albumin
CA9	Carbonic Anhydrase 9
CAM	Cell Adhesion Molecule
CAV1	Caveolin-1
CCNU	1-(2-chloroethyl)-3-cyclohexyl-1nitrosurea
CDK	Cyclin-Dependent Kinase

cDNA	Complementary DNA
CGH	Comparative Genomic Hybridization
CHO	Chinese Hamster Ovary
Cis	Cisplatin
CKI	Cyclin-Dependent Kinase Inhibitor
CLL	Chronic Lymphocytic Leukaemia
cRNA	Complementary RNA
CSC	Cancer Stem Cell
CO ₂	Carbon Dioxide
CoCl ₂	Cobalt Chloride
COL6A3	Collagen Type VI Alpha3
CT	Computed Tomography
C _T	Threshold Cycle
CXADR	Coxsackie Virus and Adenovirus Receptor
DAVID	Database for Annotation, Visualization and Integrated Discovery
DDIT3	DNA Damage Inducible Transcript 3
DISC	Death Inducing Signalling Complex
DII4	Delta-like 4
DMSO	Dimethylsulfoxide
DNA	Deoxyribonucleic Acid
dTTP	Deoxythymidine Triphosphate
DUSP	Dual Specificity Phosphatase
dUTP	Deoxyuracil Triphosphate
ECACC	European Collection of Cell Cultures
ECM	Extracellular Matrix

EGFR	Epidermal Growth Factor Receptor
EORTC	European Organization of Research and Treatment of Cancer
EPR	Electron Paramagnetic Resonance
5-FU	5-Fluorouracil
FADD	Fas-Associated Death Domain
FA	Fanconi's Anaemia
FANC	Fanconi's Anaemia Complementation Group
Fara-A	9-Beta-D-Arabinofuranosyl-2-Fluoroadenine
FasL	Fas Ligand
FAZA	Fluoro-azomycinarabino-furanoside
FBS	Foetal Bovine Serum
FDR	False Discovery Rate
FET	Fluorescent Energy Transfer
FGF	Fibroblast Growth factor
FIAF	Fasting Induced Adipose Factor
FIGO	International Federation of Obstetricians and Gynaecologists
FIH	Factor inhibiting HIF-1
FWER	Familywise Error Rate
GADD45A	Growth Arrest and DNA Damage Inducible Protein
GAPDH	Glyceraldehyde 3-Phosphate Dehydrogenase
GLUT1	Glucose Transporter 1
GOG	Gynecologic Oncology Group
GPC3	Glypican 3
GST	Glutathione-S-Transferase
HBOS	Hereditary Breast/Ovarian Syndrome

hCG	Human Chorionic Gonadotropin
HFARP	Hepatic Fibrinogen/Angiopoietin-Related Protein
HGF	Hepatocyte Growth Factor
HIF	Hypoxia Inducible Factor
HLA	Human Leukocyte Antigen
HNCC	Hereditary Nonpolyposis Colorectal Cancer
HPV	Human Papillomavirus
HR	Homologous Recombination
HRE	Hypoxia Regulated Element
Hyp	Hypoxia
HX4	(3-[¹⁸ F] fluoro-2(4-((2-nitro-1H-imidazol-1-yl)methyl)-1H-1,2,3-triazol-1-yl)
IC ₅₀	Inhibitory Concentration 50
IDO	Indoleamine 2,3-Deoxygenase
IGF1R	Insulin Like Growth Factor 1 Receptor
iHOP	Information Hyperlinked Over Proteins
IVT	In Vitro Transcription
JNK	c-Jun N Terminal Kinase
KITLG	KIT Ligand
LAMP	Lysosomal Associated Membrane Protein
LDH	Lactate Dehydrogenase
LOH	Loss of Heterozygosity
LMP	Latent Membrane Protein
MAP	Microtubule Associated Protein
MAPK	Mitogen-Activated Protein Kinase
MCJ	Methylation Controlled J Protein

MCM	Minichromosome Maintenance Protein
MCP	Monocyte Chemoattractant Protein
MDR1	Multidrug Resistance Protein 1
miRNA	Micro RNA
MEK	Mitogen/Extracellular Signal Related Kinase
MMP	Matrix Metalloprotease
MRI	Magnetic Resonance Imaging
MTT	3-(4,5-dimethylthiazol2-yl)-2,5-diphenyltetrazolium bromide
N ₂	Nitrogen
NCRI	National Cancer Registry, Ireland
NER	Nucleotide excision Repair
Norm	Normoxia
NOSE	Normal Ovarian Surface Epithelium
NTC	No Template Control
O ₂	Oxygen
ODD	Oxygen Dependent Degradation
OS	Overall Survival
PAS	Per Arnt Sim
PBS	Phosphate Buffered Saline
PBST	PBS-Tween
PCOS	Polycystic Ovarian Syndrome
PCR	Polymerase Chain Reaction
PDGF	Platelet Derived Growth Factor
PEG3	Paternally Expressed 3
PET	Positron Emission Tomography

PFS	Progression-Free Survival
PGAR	PPARgamma Angiopoietin Related
PGF	Placental Growth Factor
PHD	Prolyl Hydroxylase
PIAMP	Phorbos-12-Myristate-13-Acetate-Induced Protein 1
PIN	Prostatic Intraepithelial Neoplasia
PM	Perfect Match
PMSF	Phenylmethanesulfonylfluoride
PPP1R3C	Protein Phosphatase 1, Regulatory Subunit 3C
pRb	Retinoblastoma Protein
PTEN	Phosphatase and Tensin Homologue
RASGRP1	Ras Guanyl Releasing Protein 1
REAL	Revised European-American Lymphoma
RIN	RNA Integrity Number
RIPA	Radioimmunoprecipitation Buffer
RLE	Relative Log Expression
RMA	Robust Multi-Array Average
RNA	Ribonucleic Acid
ROC	Receiver Operating Characteristic
ROCK1	Rho-Associated Coiled Coil Containing Protein 1
ROS	Reactive Oxygen Species
RT-PCR	Reverse Transcription PCR
SD	Standard Deviation
SDS	Sodium Dodecyl Sulphate
SNP	Single Nucleotide Polymorphism
STAT	Signal Transducer and Activator of Transcription

TAM	Tumour Associated Macrophage
Taq	<i>Thermus aquaticus</i>
TEA	Tocopherol Ether Acetic Acid Analogue
TGF α	Transforming Growth Factor α
TGF β	Transforming Growth Factor β
THBS1	Thrombospondin-1
TIMP3	Metallopeptidase Inhibitor 3
T _m	Melting Temperature
TMED	N, N, N', N'-Tetramethyl-Ethane-1,2-Diamine
TNF	Tumour Necrosis Factor
TPZ	Tirapazamine
UNG	Uracil-DNA Glycosylase
Unt	Untreated
USP22	Ubiquitin Specific Peptidase 2
VEGF	Vascular Endothelial Growth Factor
VHL	Von Hippel Lindau Protein
XIAP	X-Linked Inhibitor of Apoptosis
XPA	Xeroderma Pigmentosum, Complementation Group A

List of Units

°C	Degrees Celsius
g	Gram
H	Hour
L	Litre
μL	Microlitre
μM	Micromolar
mL	Millilitre
mM	Millimolar
Min	Minute
ng	nanogram
nM	Nanomolar
PSI	Pounds per Square Inch
RPM	Revolutions Per Minute
Sec	Second
U	Units
V	Volt

Publications and Presentations

Poster Presentations

- LM McEvoy, SA O'Toole, CD Spillane, CM Martin, L Norris, O Sheils, JJ O'Leary. (2012) Novel Hypoxic Biomarkers of Ovarian Cancer. *Poster Presentation at the British Gynaecological Cancer Society Annual Scientific Meeting.*
- LM McEvoy, SA O'Toole, CD Spillane, A McGoldrick, L Norris, CM Martin, O Sheils, JJ O'Leary. (2012) Downregulation of Genes Contributes to Chemoresistance Induced by Hypoxia. *Poster Presentation at the United States and Canadian Academy of Pathology Conference.*
- LM McEvoy, SA O'Toole, CD Spillane, CM Martin, O Sheils, JJ O'Leary. (2012) Novel Hypoxic Biomarkers of Ovarian Cancer. *Poster Presentation at the Irish Association for Cancer Research Annual Meeting.*
- LM McEvoy, SA O'Toole, CD Spillane, CM Martin, O Sheils, JJ O'Leary. (2011) Hypoxia Potentiates the Inverse Relationship Between Resistance to cisplatin and Paclitaxel in Ovarian Cancer Cell Lines. *Poster Presentation at the Irish Association for Cancer Research Annual Meeting.*
- LM McEvoy, SA O'Toole, CD Spillane, CM Martin, O Sheils, JJ O'Leary. (2011) Hypoxia Potentiates the Inverse Relationship Between Resistance to cisplatin and Paclitaxel in Ovarian Cancer Cell Lines. *Poster Presentation at the United States and Canadian Academy of Pathology Conference.*
- LM McEvoy, SA O'Toole, CD Spillane, CM Martin, O Sheils, G Kijanka, JJ O'Leary. (2010). The Role of Hypoxia in the Response of Ovarian Cancer Cells to Chemotherapy. *Poster Presentation at the American Society of Human Genetics Annual Meeting.*
- LM McEvoy, SA O'Toole, CD Spillane, CM Martin, O Sheils, JJ O'Leary. (2009) Hypoxia Induces Chemoresistance in Ovarian Cancer Model. *Poster Presentation at the Centre for Cancer Research and Cell Biology's 2nd International Symposium.*

Table of Contents

I	Developing Novel Therapeutic Approaches in Chemoresistant Ovarian Cancer Patients.....	i
II	Declaration	ii
III	Summary.....	iii
IV	Acknowledgements	v
V	Dedication.....	vii
VI	List of Tables	viii
VII	List of Figures.....	xiii
VIII	Abbreviations.....	xix
IX	List of Units	xxvi
X	Publications and Presentations	xxvii
XI	Table of Contents.....	xxviii
1.	Introduction	1
1.1	Cancer	2
1.1.1	Vogelstein & Kinzler’s Theory.....	2
1.1.2	Hanahan & Weinberg’s Theory	4
1.2	Ovarian Cancer	13
1.2.1	Epidemiology and Risk Factors for Ovarian Cancer.....	13
1.2.2	Histology	15
1.2.2.1	Epithelial Ovarian Cancer	15
1.2.2.2	Borderline Tumours.....	16
1.2.2.3	Serous Ovarian Cancer.....	17
1.2.2.4	Mucinous Ovarian Cancer	17
1.2.2.5	Endometrioid Ovarian Cancer	17
1.2.2.6	Clear Cell Ovarian Cancer	18

1.2.2.7	Stromal Ovarian Cancer	18
1.2.2.8	Germ Cell Tumours	18
1.2.3	Aetiology	19
1.2.4	Diagnosis	22
1.2.5	Tumour Stage	24
1.2.6	Tumour Grade	24
1.2.7	Treatment	26
1.2.8	Chemoresistance in Ovarian Cancer	28
1.3	Tumour Hypoxia	30
1.3.1	Hypoxia and Chemoresistance	37
1.3.2	HIF-1 α and Prognosis	38
1.4	Hypothesis and Aims	40
2.	Materials and Methods	41
2.1	Cell Lines	42
2.1.1	Resuscitation of Stocks from Liquid Nitrogen	42
2.1.2	Cell Culture	42
2.1.3	Subculture of Cell Lines	43
2.1.4	Cell Count	44
2.1.5	Freezing Down Stocks	45
2.1.6	Mycoplasma Testing	45
2.1.6.1	Principle	45
2.1.6.2	Protocol	46
2.2	Hypoxia Chamber	47
2.3	MTT Assay	48
2.4	RNA Extraction	49
2.4.1	Principle	49

2.4.2	Cell Lysis and Homogenization	50
2.4.3	RNA Purification I.....	50
2.4.4	DNase Digestion.....	50
2.4.5	RNA Purification II and Elution	51
2.5	Assessment of RNA Yield using the NanoDrop.....	51
2.6	Bioanalyzer	52
2.6.1	Principle	52
2.6.2	RNA Integrity Number	52
2.6.3	Protocol.....	54
2.6.3.1	Preparation of the Ladder	54
2.6.3.2	Preparation of Reagents.....	55
2.6.3.3	Sample Loading.....	55
2.7	Affymetrix Human Gene 1.0 ST Arrays.....	56
2.7.1	Workflow	59
2.7.2	Preparation of Total RNA and Poly-A Controls.....	62
2.7.3	First Strand cDNA synthesis.....	63
2.7.4	Second Strand cDNA Synthesis.....	63
2.7.5	cRNA Synthesis by In Vitro Transcription	64
2.7.6	cRNA Purification.....	65
2.7.7	Second-Cycle cDNA Synthesis.....	66
2.7.8	RNaseH Hydrolysis.....	67
2.7.9	Second-Cycle cDNA Purification	67
2.7.10	Fragmentation of Single-Stranded DNA.....	69
2.7.11	Labelling of Fragmented Single-Stranded DNA	70
2.7.12	Hybridization.....	71
2.7.13	Set-up of Fluidics Station and Scanner	72

2.7.14	Array Staining.....	72
2.7.15	Array Scanning.....	73
2.8	Taqman® Real-Time PCR.....	73
2.8.1	Principle.....	73
2.8.2	Procedure.....	75
2.8.2.1	cDNA Synthesis.....	75
2.8.2.2	Taqman® PCR.....	76
2.8.2.3	Data Analysis.....	77
2.8.2.3.1	The $2^{-\Delta\Delta CT}$ Method.....	78
2.9	Protein Extraction.....	79
2.9.1	Protein Extraction in Normoxia.....	79
2.9.2	Protein Extraction in Hypoxia.....	80
2.9.3	Protein Quantification with the BCA Assay.....	81
2.9.3.1	Principle.....	81
2.9.3.2	Protocol.....	81
2.9.4	Western Blots.....	82
2.9.4.1	Rig Set-up.....	82
2.9.4.2	Sample Preparation and Loading.....	83
2.9.4.3	Wet Transfer.....	84
2.9.4.4	Blocking and Antibody Staining.....	85
2.9.4.5	Detection.....	86
2.9.4.6	Control Antibody.....	86
3.	Hypoxia Induces Chemoresistance in an Ovarian Cancer Cell Line Model.....	87
3.1	Introduction.....	88
3.1.1	Chemoresistance.....	88

3.1.2	Models of Chemoresistance	88
3.1.3	Cisplatin	89
3.1.4	Cisplatin Resistance	90
3.1.4.1	Reducing Cisplatin Entry	90
3.1.4.2	Reducing Cisplatin Effectiveness Within the Cell	91
3.1.4.3	Increasing Cisplatin Efflux	92
3.1.4.4	Hypoxia and Cisplatin Resistance	92
3.1.4.5	Cisplatin Resistance, Hypoxia and Ovarian Cancer	93
3.1.5	Paclitaxel	95
3.1.6	Paclitaxel Resistance	96
3.1.6.1	Tubulin Modification	96
3.1.6.2	Tau and other Microtubule-Associated Proteins	96
3.1.6.3	P-Glycoprotein	97
3.1.6.4	Hypoxia and Paclitaxel Resistance	97
3.1.7	Aim	98
3.2	Methods	99
3.2.1	Cell Culture	99
3.2.2	Drug and Vehicle Control Formulation	99
3.2.3	MTT Assays	99
3.2.3.1	Optimization of Seeding Density	100
3.2.3.2	Optimization of Drug Treatment Period	101
3.2.3.3	Hypoxia Matrix Experiments	101
3.2.4	Timecourse of HIF-1 α Expression in Hypoxia	105
3.2.5	Statistical Analyses	106
3.3	Results	107

3.3.1	Characteristics of Morphology of A2780 and A2780cis Cell Lines.....	107
3.3.2	Hypoxia and Morphology of A2780 and A2780cis	107
3.3.3	Optimization of Seeding Density	110
3.3.4	Optimization of Treatment Period	112
3.3.5	Hypoxia Matrix Experiments	115
3.3.5.1	Effect of Cisplatin on Morphology of A2780 and A2780cis in Normoxia and Hypoxia	115
3.3.5.2	Comparison of Drug Sensitivity/Resistance in A2780 and A2780cis in Normal Oxygen Conditions	115
3.3.5.3	Acute Hypoxia Increases Resistance to Cisplatin and Paclitaxel in A2780 Cells	115
3.3.5.4	Chronic Hypoxia Increases Resistance to Cisplatin and Paclitaxel in A2780 Cells	123
3.3.5.5	Treating A2780 in Hypoxia Increases Resistance to Cisplatin and Paclitaxel	126
3.3.5.6	Acute Hypoxia Increases Resistance to Cisplatin but not Paclitaxel in A2780cis Cells.....	129
3.3.5.7	Chronic Hypoxia Increases Resistance to Cisplatin but not Paclitaxel in A2780cis Cells	132
3.3.5.8	Treating A2780cis in Hypoxia Increases Resistance to Cisplatin but not Paclitaxel	135
3.3.6	Timecourse of HIF-1 α Expression in A270 and A2780cis.....	138
3.4	Discussion	140
3.5	Summary.....	147
4.	Gene Expression Profiling of Ovarian Cancer Cell Lines in Normoxia and Hypoxia	149
4.1	Introduction	150
4.1.1	Microarrays.....	150

4.1.2	Uses of DNA Microarrays.....	150
4.1.2.1	Gene Profiling	150
4.1.2.2	Diagnostic Biomarker Discovery	151
4.1.2.3	Prognostic Biomarker Discovery.....	153
4.1.2.4	Therapeutic Biomarker Discovery	155
4.1.3	Microarray Analysis of Hypoxia-Induced Changes	156
4.1.4	Aim	158
4.2	Methods.....	159
4.2.1	Sample Selection	159
4.2.2	Sample Preparation	159
4.2.3	Array Quality Control Analysis.....	160
4.2.4	Array Data Analysis	162
4.2.4.1	Data Normalization.....	162
4.2.4.2	Differential Gene Expression Analysis	163
4.2.4.3	Analysis of Target Gene Lists	164
4.3	Results.....	165
4.3.1	Quality Control of Arrays	165
4.3.1.1	Visual Quality Control.....	165
4.3.1.2	Probe Metrics Quality Control.....	167
4.3.2	Differential Gene Expression Analysis	170
4.3.2.1	Summary Characteristic Analysis.....	170
4.3.3	Results: Comparison of A2780 and A2780cis	173
4.3.4	Discussion: Comparison of Gene Profile of A2780cis with A2780.....	177
4.3.5	Results: The Effect of Hypoxia on the Transcription Profile of A2780 and A2780cis.....	182

4.3.5.1	Identification of Common Gene Expression Changes in A2780 and A2780cis in Response to Hypoxia.....	189
4.3.5.2	Evaluation of Common Gene Expression Differences in A2780cis and Hypoxia A2780 Cells.....	191
4.3.6	Discussion: General Gene Expression Response to Hypoxia in A2780 and A2780cis.....	195
4.3.7	Summary.....	207
4.3.8	Results: The Effect of Hypoxia on Response to Cisplatin in A2780 and A2780cis.....	208
4.3.8.1	Comparison of Untreated A2780 Cells with Cisplatin Treated A2780 Cells in Normoxia and Hypoxia	208
4.3.8.2	Comparison of Untreated A2780cis Cells with Cisplatin Treated A270cis Cells in Normoxia and Hypoxia	219
4.3.9	Discussion: The Effect of Hypoxia on Response to Cisplatin in A2780 and A2780cis.....	230
4.3.10	Hypoxic Biomarker Discovery	236
4.3.11	Summary.....	238
5.	Evaluation of Novel Hypoxia Biomarkers of Ovarian Cancer	239
5.1	Introduction	240
5.1.1	Angiopoietin-Like 4	241
5.1.2	Brain-Derived Neurotrophic Factor	242
5.1.3	HER3.....	243
5.1.4	MAD2L1	244
5.1.5	HIF-1 α	245
5.1.6	Aim	246
5.2	Methods.....	247
5.2.1	Samples – Cell Lines.....	247

5.2.2	Samples – Tumour Tissue	247
5.2.3	Sample Grouping and Relative Quantitation.....	249
5.2.4	Kaplan-Meier Survival Analysis.....	250
5.3	Results.....	252
5.3.1	Array Validation	252
5.3.1.1	ANGPTL4	252
5.3.1.2	BDNF	252
5.3.1.3	HER3.....	252
5.3.1.4	MAD2L1	253
5.3.2	Further Evaluation of the Hypoxia Matrix.....	257
5.3.2.1	ANGPTL4	257
5.3.2.2	BDNF	257
5.3.2.3	HER3.....	257
5.3.2.4	MAD2L1	258
5.3.3	Expression of ANGPTL4, BDNF, HER3 and HIF-1 α in Tumour Sample Cohort	261
5.3.3.1	ANGPTL4	261
5.3.3.2	BDNF	261
5.3.3.3	HER3.....	261
5.3.3.4	HIF-1 α	262
5.4	Discussion	267
5.4.1	Biomarker Selection.....	267
5.4.2	Cell Lines	268
5.4.3	Tumour Samples	273
5.4.4	Summary.....	278
6.	General Discussion.....	279

6.1	Introduction	280
6.2	Hypoxia and Ovarian Cancer 2008.....	280
6.3	Additions to Current Knowledge on Hypoxia and Ovarian Cancer Chemoresistance by this Project.....	284
6.4	Hypoxia and Ovarian Cancer 2012; How this Study Compares	291
6.5	Limitations of the Study.....	293
6.6	Future Work.....	294
6.7	Conclusion.....	296
XII	Appendix.....	xxxviii
XIII	References	xi

Chapter 1

Introduction

1.1 Cancer

Cancer is defined by the National Cancer Institute, United States of America, as ‘a term used for diseases in which abnormal cells divide without control and are able to invade others’. A diagnosis of cancer leads to many difficulties both for the patient – physically and emotionally – and for society – economically and socially. While there are thousands of articles chronicling experiments carried out to try and understand why cancer occurs, there have been two main theories of carcinogenesis put forward. This introduction will mainly focus on cancer theory in relation to ovarian cancer.

1.1.1 Vogelstein & Kinzler’s Theory

Vogelstein and Kinzler’s theory is based on the idea that cancer is a genetic disease [1]. They identify three gene types in which alterations result in tumourigenesis – tumour suppressors e.g. p53, p16, oncogenes e.g. KIT, MET and stability genes e.g. BRCA1 (breast cancer associated 1, early onset), BRCA2. They explain that cancer does not occur as a result of a single gene defect, rather it occurs as a result of a number of gene defects which combine to facilitate tumourigenesis.

Defects in tumour suppressor genes have been widely identified in ovarian cancer. Genes may be rendered defective through methylation, loss of heterozygosity (LOH) and mutation. Methylation of p16 has been observed in over 50% of ovarian cancers [2] while a case study of ovarian cancer has identified inactivation of the adenomatous polyposis coli (APC) gene, a gene which, when inactivated, causes predisposition to colorectal cancer [3]. Other tumour suppressor genes have been identified as being inactivated in both ovarian cancer cell lines and tumour tissues such as GPC3 (glypican-3) [4], VHL (von Hippel-Lindau protein) [5], PTEN (phosphatase and tensin homologue) [6]. ARHI (aplasia Ras homolog member 1) and PEG3 (paternally expressed 3) are two imprinted tumour suppressor genes which are regularly lost in ovarian cancer cells and tissues due to LOH and methylation [7].

When mutated, oncogenes can become inappropriately activated, or continuously activated [1]. Many oncogenes have been identified, including KIT, MET, PDGFRA and RET [1]. KIT (CD117) is a receptor tyrosine kinase whose activation results in stimulation of genes related to proliferation, differentiation, migration and survival [8]. KIT expression has been particularly studied in gastrointestinal stromal tumours, and inhibitors of KIT have been employed in their treatment [9]. Expression of KIT has been associated with cancer stem cell characteristics, and ovarian tumour cells expressing KIT have been shown to be highly tumourigenic in mice, and analysis of KIT expression in ovarian tumours has shown that KIT-positive tumours are less likely to respond to first-line chemotherapy and have a shorter progression free survival than KIT-negative tumours [10]. MET is a proto-oncogene and tyrosine kinase receptor for hepatocyte growth factor (HGF) [11]. Binding of HGF to MET results in stimulation of signalling cascades through the Ras/MAPK (mitogen activated protein kinase) and PI3K/Akt pathways which promote cell survival and migration [11]. MET has been shown to be dysregulated in many cancers, including ovarian cancer [12].

Stability genes are those which regulate DNA repair, chromosome segregation, mitosis *etc.* and dysregulation of these genes can lead to a higher frequency of mutation in other genes [1]. The Fanconi's anaemia (FA) is an autosomal recessive chromosomal instability syndrome characterized by an increased risk for development of cancer [13]. There are seven FA complementation groups (FANC), and these genes are essential in DNA repair pathways [13]. Loss of members of the FANC family due to promoter hypermethylation has been observed in cervical cancer cell lines and tumour samples [13]. In ovarian cancer, disruption of the FA pathway has been linked to development of sporadic tumours, and silencing of FANC genes through methylation leads to sensitivity to platinum chemotherapeutics due to interference with cellular DNA repair pathways [14]. Similarly, loss of other DNA repair associated genes such as XPA (xeroderma pigmentosum complementation group A) due to LOH has been

linked to tumourigenesis in a percentage of ovarian, colon and lung tumours [15].

Vogelstein and Kinzler postulate that tumourigenesis hinges on alterations in these gene types and pathways, and is supported by the tumour microenvironment – stroma, angiogenesis etc.

1.1.2 Hanahan & Weinberg's Theory

Hanahan and Weinberg put forward a theory that there are six major alterations in cellular physiology which dictate malignant growth [16] – self-sufficiency in growth signals, insensitivity to growth-inhibitory signals, evasion of apoptosis, limitless replicative potential, sustained angiogenesis and tissue invasion and metastasis (Figure 1.1).

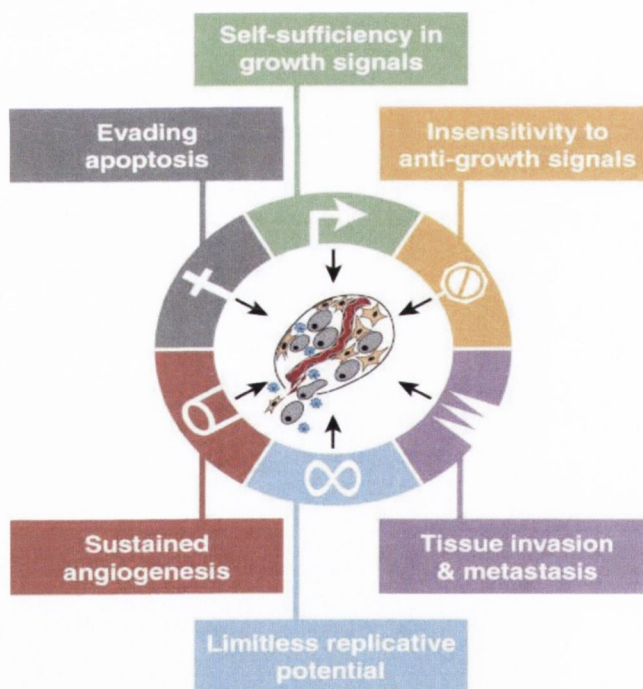


Figure 1.1. Six Hallmarks of Cancer. The six hallmarks of cancer as postulated by Hanahan & Weinberg, who propose that acquisition of these six traits is shared between most/all tumour types. (From Hanahan and Weinberg [16])

It is essential for normal cells to be stimulated by mitogenic signals in order to grow [16]. Tumour cells can synthesise growth factors and their receptors which then act in an autocrine fashion to promote tumour growth [16]. In breast cancer, several growth-stimulating autocrine and paracrine signalling loops have been observed including platelet derived growth factor (PDGF) and the PDGF receptor, transforming growth factor alpha ($TGF\alpha$) and the epidermal growth factor receptor (EGFR), transforming growth factor beta ($TGF\beta$) and the $TGF\beta$ receptor and vascular endothelial growth factor (VEGF) and its receptor [17]. Similarly, neuropeptides such as neurotensin and bombesin have been shown to have growth stimulatory activities in lung cancer [18] and insulin-like growth factor has been shown to be mitogenic in several cancers such as prostate [19] and pancreatic [20]. In ovarian cancer, several autocrine signalling loops including HER3/HRG1 have been observed [21].

In normal cells, anti-proliferative signals maintain tissue homeostasis by forcing cells into a quiescent (G_0) state or by being forced into a post-mitotic state (senescence) [16]. The cell cycle represents the different phases of growth for a cell, and the proteins and enzymes associated with it can act in response to pro- and anti-proliferative signals (Figure 1.2) [16].

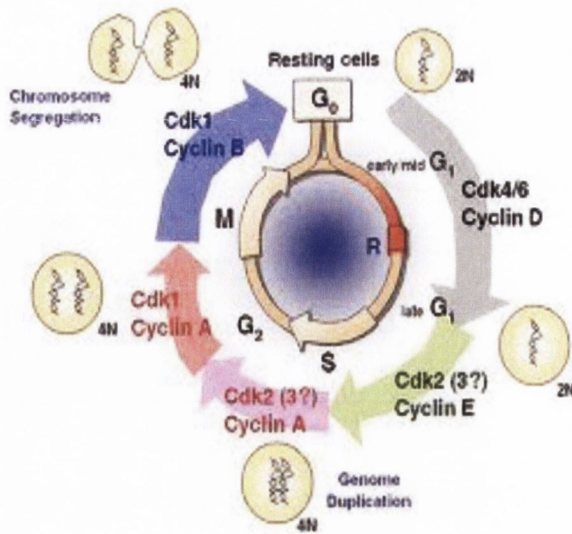


Figure 1.2. The Cell Cycle. The cell cycle represents the five possible replicative states a cell may be in, and its progression is controlled by cyclin-dependent kinases (CDKs) and their cyclin partners as well as cyclin-dependent kinase inhibitors. The phases include G₀ (resting/quiescent), G₁ (gap 1), S (synthesis of DNA), G₂ (gap 2) and M (mitosis). (www.sciencewatch.com)

Cell cycle progression is positively regulated by cyclin-dependent kinases (CDKs) which are phosphorylated and activated by binding of cyclin proteins [22]. Cyclin-dependent kinase inhibitors (CKIs) negatively regulate cell cycle progression by binding to and inactivating CDK-cyclin protein complexes [22]. There are two families of CKI – Ink4 and Cip/Kip. There are four Ink4 proteins – p16, p15, p18 and p19 which inactivate CDK4 and CDK6, thus preventing movement of the cell out of G₁ and into S phase [22]. Three Cip/kip proteins – p21, p27 and p57 are also present – these bind and inactivate all types of CDK [22]. E2F transcriptional activators/repressors can also stimulate progression of the cells into S phase. They are regulated by members of the retinoblastoma protein (pRb) family (pRb, p103 and p107) – these proteins complex with E2F and must be released through phosphorylation by CDKs in order for E2F to carry out its function [22]. Disruption of the pRb family of proteins liberates E2Fs and allows for insensitivity of cancer cells to anti-growth signals [16]. Dysregulation of pRb has been extensively researched in cervical cancer, in which the human

papillomavirus oncogenic protein E7 complexes with and inactivates pRb [23]. In ovarian cancer, reduced pRb expression has been linked with poor survival [24].

Apoptosis can be triggered through extrinsic – Fas/Fas ligand, tumour necrosis factor alpha (TNF α)/TNF receptor – and intrinsic – DNA damage, hypoxia, oncogene – sensors [16]. Cancer cells can evade apoptosis in many ways. Fas signalling (Figure 1.3) consists of binding of Fas ligand (FasL) to its receptor which results in sequential activation of caspase enzymes and cellular death. Resistance to Fas-mediated apoptotic signalling has been observed in oesophageal cancer [25] and colon cancer [26]. A study in lung and colon cancer has demonstrated up-regulation of a Fas decoy receptor, which binds FasL and inhibits apoptosis [27]. In addition, polymorphism analysis of Fas in lymphoma has demonstrated that certain Fas polymorphisms drive apoptosis to a lower extent [28].

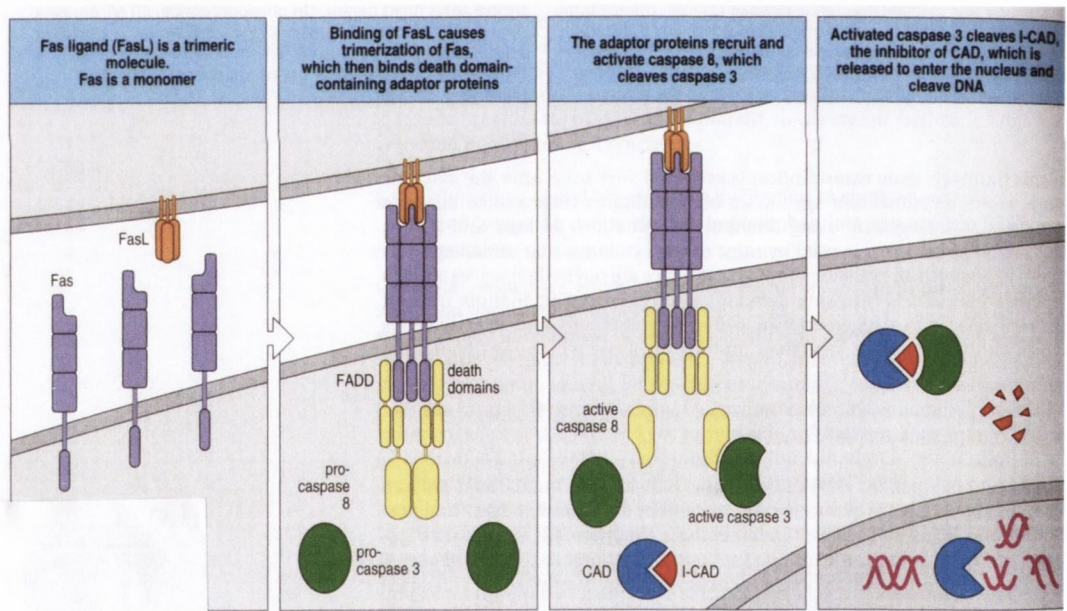


Figure 1.3. Fas Signalling Pathway. Binding of Fas ligand (FasL) to its receptor results in Fas binding to death domain-containing adaptor proteins such as FADD, and leads to sequential activation of caspase enzymes leading to cellular death. (www.bio.davidson.eu)

The tumour suppressor p53 induces apoptosis in response to DNA damage through activation of numerous genes such as p21, GADD45, Noxa and MDM2,

and inactivation of p53 through mutation allows for evasion of apoptosis and cellular senescence [29]. Similarly, aberrant expression of p53-related genes also influences the cell's apoptotic response. Mutation of p53 has been observed in up to three quarters of epithelial ovarian cancer patients and has been correlated with ovarian carcinogenesis [30,31]. KLF6-SV1, an anti-apoptotic protein, targets the p53-inducible protein Noxa for degradation, and inhibition of KLF6-SV1 results in improved survival in *in vivo* models [32]. MDM2 negatively regulates p53 by targeting it for ubiquitin-mediated proteasomal degradation [33], and up-regulation of MDM2 has been linked to tumour progression in breast cancer [34] and poor survival in ovarian cancer [35].

Cultured cells normally have limited potential for replication in culture, and after a certain number of doublings enter senescence [16]. Deactivation of the tumour suppressors p53 and pRb prevents senescence, leading to the growth of cells which can grow without limitation [16]. While most normal cells are capable of approximately 60 – 70 doublings – enough to create a tumour – this is concomitant with widespread apoptosis therefore immortalization of tumour cells is necessary to facilitate substantial tumour growth [16]. Transformation and immortalization of cells can be achieved by viral oncoproteins e.g. the human papillomavirus E6 and E7 proteins which inactivate tumour suppressors p53 and pRb respectively [36], and the Epstein-Barr virus whose viral latent membrane proteins (LMPs) immortalize resting B cells, resulting in several cancers including Hodgkin's lymphoma and Burkitt's lymphoma [37]. Immortalization has also been linked to deregulation of micro RNAs, non-coding short RNA molecules, in mouse embryonic fibroblasts [38] and lymphoblastoid cell lines [39], and to mutation and methylation of tumour suppressor genes [40].

In order to grow, tumours must be able to induce angiogenesis, the formation of new blood vessels [16]. Normally, angiogenesis is controlled by a balance of pro- and anti-angiogenic molecules including vascular endothelial growth factor (VEGF), fibroblast growth factor (FGF), integrins and thrombospondin 1 (THBS1) [16]. Tumour cells must tilt the balance towards pro-angiogenesis in order to

produce new blood vessels to provide them with their on-going nutritional requirements [41]. This is normally achieved by stimulating sprouting of new blood vessels from existing ones, however, it can also involve differentiation of tumour stem cells (Figure 1.4) [41]. The presence of tumour hypoxia and nutrient deprivation stimulates release of many pro-angiogenic molecules including growth factors, enzymes for extracellular matrix remodelling, and cytokines in order to stimulate new blood vessel formation [41]. Angiogenesis is observed in a wide range of solid malignancies including breast [42], prostate [43], colon [44] and ovarian [45] carcinomas.

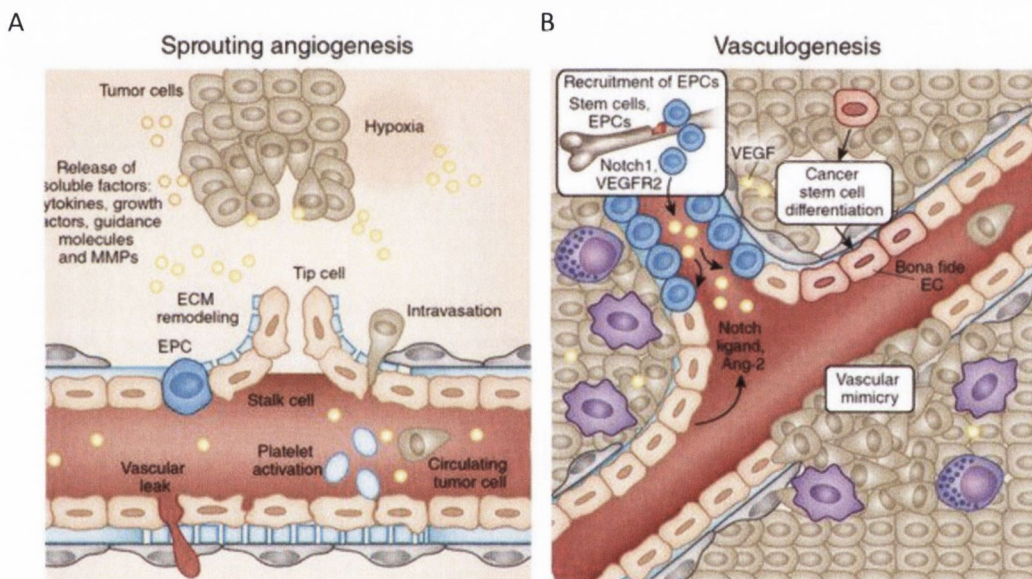


Figure 1.4. Tumour Angiogenesis. The presence of hypoxia, and nutrient deprivation stimulates both sprouting angiogenesis (A) where new blood vessels are encouraged to grow from pre-existing ones, and vasculogenesis (B) which is the *de novo* growth of blood vessels due to differentiation of cancer stem cells. (From Weis *et al.* [41])

Most tumours eventually invade the surrounding tissues and metastasize to other areas in the body – metastases are the main cause of cancer death [16]. Metastasis allows the tumour to spread to new areas where there is a plentiful nutrient and oxygen supply [16]. It is not entirely understood how tumours invade and metastasize, however certain groups of molecules are implicated,

including cell adhesion molecules (CAMs), cadherins, integrins and protease enzymes. Expression of L1-CAM in pancreatic cancer tissue is associated with vascular and peri-neural invasion and lymph node metastasis [46], while activated leukocyte adhesion molecule (ALCAM) expression is associated with invasion in melanoma [47]. Loss of E-cadherin has been shown to promote invasion of colorectal carcinoma cells in cell line studies, and E-cadherin expression on colorectal tumours has been negatively associated with liver metastasis [48]. Similarly, in breast cancer, loss of E-cadherin has also been linked to increased invasion [49]. Culture of cells derived from borderline ovarian tumours (non-invasive) has shown that inactivation of p53 results in loss of E-cadherin and increased invasive capacity [50]. Integrins are glycoproteins which bind to molecules in the extracellular matrix (ECM) such as collagen, laminin and fibrinogen [51]. Integrin signalling is linked to invasion in ovarian cancer [52], breast cancer [53] and colon cancer [54]. Matrix metalloproteases (MMPs) are enzymes secreted by tumour cells to degrade the ECM and facilitate invasion and metastasis [55]. In addition, degradation of the ECM by MMPs releases bioactive molecules which can take part in oncogenic signalling, and MMPs can regulate the local inflammatory process surrounding a tumour [55]. MMP-2 is associated with ovarian cancer invasion and metastasis [56,57], while a recent study by our group identified MMP9 as a potential marker of chemoresistance in ovarian cancer, and found that co-incubation of ovarian cancer cells with an MMP9 inhibitor and cisplatin resulted in enhanced cytotoxicity compared to cisplatin alone (manuscript submitted). Our group has also recently published regarding the utilization of platelets by ovarian cancer cells during metastasis [58]. It showed that ovarian cancer cells can both bind to and activate platelets, and that incubation of ovarian cancer cells with the released products of activated platelets (platelet releasate) resulted in up-regulation of genes associated with prevention of apoptosis, facilitation of angiogenesis and cell adhesion and migration.

While Hanahan and Weinberg outline these six features of cancer, they also note that genetic instability is also necessary, as described by Vogelstein and Kinzler.

In 2011, Hanahan and Weinberg proposed two additional hallmarks of cancer – abnormal metabolism and immune evasion, and described two ‘enabling characteristics’ of cancer (i.e. they facilitate acquisition of the core hallmarks) – chromosomal abnormalities and inflammation (Figure 1.5) [59].

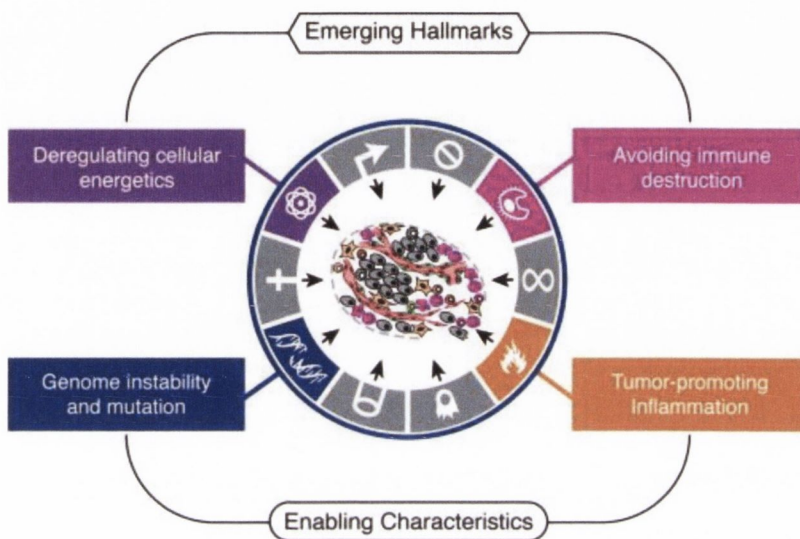


Figure 1.5. Emerging Hallmarks of Cancer. Two additional hallmarks of cancer proposed by Hanahan and Weinberg in 2011 include deregulation of metabolism and immune evasion. In addition, two enabling characteristics of cancer include inflammation and genome instability. (From Hanahan and Weinberg [59])

Hanahan and Weinberg describe tumour progression as a multi-step clonal expansion of cells which acquire mutation at each step, through exposure to mutagens, and inactivation of the surveillance systems which monitor genome integrity e.g. p53 [59]. In addition, genomic instability can be a result of loss of telomeric DNA, resulting in both karyotypic instability and amplification/deletion of gene segments [59]. Indeed, single nucleotide polymorphisms (SNPs) in the TERT gene (encodes telomerase, an enzyme which prevents loss of DNA during replication) result in increased risk of ovarian cancer [60], and a recent study has shown that the majority of high grade serous carcinomas have shorter telomeres than normal epithelium [61]. Comparative genomic hybridization (CGH) is a

method for documenting chromosome copy gain and loss, and has identified aberrations in copy number in many cancers. A study of more than 20 ovarian cancer cell lines revealed frequent abnormalities in chromosome copy number in particular in chromosome 4 and chromosome 20 [62]. Similarly, a study of 26 ovarian carcinomas of mixed histology identified a number of amplified regions, including regions encoding Cyclin E1 and MDM2 [63].

While it has long been recognised that tumours contain an inflammatory infiltrate, it has been recognized that the immune response actually enhances tumourigenesis through supplying growth factors, survival signals, pro-angiogenic factors and ECM-modifying enzymes to the tumour microenvironment [59]. Inflammation has been observed to promote cell survival in ovarian cancer stem cells through activation of the NF κ B pathway, increased production of cytokines and anti-apoptotic proteins and reduced sensitivity to TNF α and Fas-induced cell death [64]. In addition, epidemiologic studies of ovarian cancer have associated pelvic inflammation through talc use, with increased risk of ovarian cancer, and found that use of aspirin and other non-steroidal anti-inflammatory drugs were negatively associated with risk of mucinous carcinomas of low malignant potential [65].

In normal proliferating cells, under aerobic conditions, glucose is converted to pyruvate by glycolysis in the cytosol and is shuttled to the mitochondria where it is converted to energy via the citric acid cycle, while in anaerobic conditions glycolysis alone is the main form of energy production [59]. The Warburg effect refers to the use of glycolysis as the main source of energy production by proliferating cancer cells even in the presence of oxygen, and has been associated with activation of oncogenes and mutation of tumour suppressors [59]. In ovarian cancer, glycolysis has been associated with resistance to cisplatin, and inhibition of glycolysis-related proteins has been shown to increase sensitivity [66]. In addition, increased serum levels of lactate dehydrogenase (LDH), the enzyme responsible for interconversion of lactate and pyruvate, the product of glycolysis, are raised in ovarian cancer patients compared to normal controls [67].

While the immune system normally monitors cells and tissues and eliminates the majority of tumour cells, however solid tumours do seem to be able to avoid destruction through evasion of the immune response [59]. Ovarian carcinoma cells have been shown to evade the immune response through TGF β signalling [68] and expression of modulatory glycoproteins [69], and down-regulation of immune recognition molecules such as human leukocyte antigen (HLA) class I molecules is associated with poorer prognosis [70]. Tumour-associated macrophages isolated from ovarian carcinomas have been shown to express receptors associated with immune suppression when activated by tumour-derived mucins [71]. The use of immune-mediated therapies is being explored in ovarian cancer. A recent phase II trial explored the co-treatment of advanced ovarian cancer patients with cyclophosphamide with dendritic cell loaded with a number of tumour-related peptides [72]. They found promising survival data, with 3-year survival of 90% in patients and 6 of 11 patients showing no recurrence at 36 months.

1.2 Ovarian Cancer

1.2.1 Epidemiology and Risk Factors for Ovarian Cancer

Cancer of the ovary is the fifth most common cause of cancer death in women, and the leading cause of death from gynaecological malignancy in the Western world [73]. According to the National Cancer Registry, Ireland (NCRI), in 2011, there were 315 new cases of ovarian cancer in Ireland (3% of all female invasive cancers, 7th most common) and 269 deaths (7% of all female cancer deaths) [74].

Several risk factors have been associated with development of ovarian cancer, including:

- Age: The strongest risk factor is increasing age – the incidence of ovarian cancer increases with each additional year of life [75]. In addition, age at menarche and menopause have been linked to risk of ovarian cancer –

there may be a link between early menarche (before age 12) and late menopause and ovarian cancer risk [76].

- Ethnicity: Ovarian cancer is more common in Caucasian women than African-American women in the United States, while generally ovarian cancer is more common in Western compared to Eastern countries [75].
- Parity: Women who are nulliparous or have first childbirth after 35 years of age, and those who suffer from infertility all have an increased risk of ovarian cancer [75]. Risk reduction of approximately 40% is observed following first childbirth, and each subsequent childbirth offers added protection [76].
- Lactation: Breastfeeding has been shown to confer protection from ovarian cancer – this may depend on the length of the breastfeeding period [77].
- Hormones: Long term oral contraceptive use has been linked to reduced risk of ovarian cancer, which remains following cessation of use [76,78]. There seems to be an increased risk in women who receive fertility stimulating drugs, although there is no definite link as yet [79].
- Hysterectomy: Bilateral salpingo-oophorectomy almost completely removes risk of ovarian cancer, although it is not carried out routinely [76]. Tubal ligation and hysterectomy are generally shown to reduce risk of ovarian cancer [80]. Recent evidence suggests that the majority of ovarian tumours actually arise in the fallopian tube, and it has been suggested that removal of fallopian tubes post-menopause could be beneficial in terms of reducing risk with virtually no side-effects [81].
- PCOS: Polycystic ovarian syndrome (PCOS) is caused by an imbalance of reproductive hormones, and is linked to increased ovarian cancer risk [82]. Similarly, risk of ovarian cancer is also increased in women suffering from endometriosis [83].

- Family history: Aside from age, family history is the next strongest risk factor for ovarian cancer [75]. Approximately 5 – 10% of ovarian cancers are due to inherited mutations, and three familial ovarian cancer syndromes are identified – site specific ovarian cancer syndrome, hereditary breast/ovarian cancer syndrome and hereditary nonpolyposis colorectal cancer syndrome (HNPCC) [75].

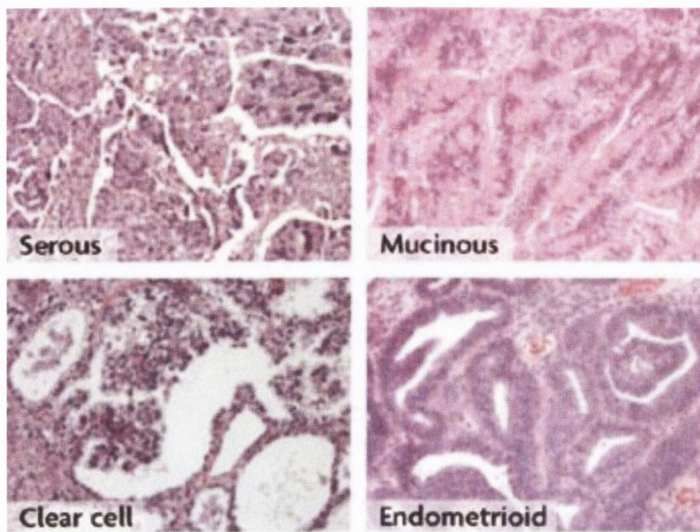
There have also been links made to ovarian cancer risk with talc use, diet, alcohol, smoking and caffeine, although these are not as clear [76].

1.2.2 Histology

There are three main types of ovarian cancer – epithelial, germ cell and stromal cell. As epithelial tumours account for the largest proportion of tumours (>90% [84]), they will be the main focus of this introduction.

1.2.2.1 Epithelial Ovarian Cancer

The vast majority of ovarian cancers are epithelial tumours which are then subdivided into a number of histological categories including serous, mucinous, endometrioid and clear cell (Figure 1.6). Serous tumour cells resemble normal well-differentiated cells of the fallopian tube/ovarian surface, mucinous resemble endocervical cells, endometrioid resemble endometrial cells, while clear cells resemble cells which form nests within the vagina [85]. The different histological subtypes differ in many respects including epidemiology, genetics, responsiveness to chemotherapy and expression of tumour markers [85].



Nature Reviews | Cancer

Figure 1.6. Histology of Epithelial Ovarian Cancer Subtypes. There are four main subtypes of epithelial ovarian cancer including serous, mucinous, clear cell and endometrioid. They differ in many respects including their biology, pathology and responsiveness to therapy. (From Bast *et al.* [85])

1.2.2.2 Borderline Tumours

Borderline tumours are intermediate lesions between cystadenomas and carcinomas and are associated with a favourable prognosis, even when presenting with widespread peritoneal metastases [86]. Borderline tumours can be composed of any histologic subtype of ovarian cancer which displays more proliferation than cystadenoma and nuclear atypia but no invasion [87]. Most borderline tumours can be cured by surgery, and 5-year survival is 95%, however tumours can recur in the abdomen [88]. This is a heterogenous group of tumours, made more complicated by the fact that they often present during a woman's reproductive years, and patients often want to conserve their fertility [86]. There are a number of difficulties arising in the pathological diagnosis of borderline tumours. While most of a tumour may be borderline, occult regions of invasion may persist, therefore adequate sampling is essential [86]. Metastatic lesions associated with borderline lesions can be categorized as invasive, or non-invasive, and non-invasive lesions are associated with a significantly better prognosis [86]. The most common borderline histology is

serous, and is associated with mutation of KRAS and BRAF genes, unlike high-grade serous carcinomas [89]. In fact, borderline lesions may represent a precursor for the development of low-grade serous carcinomas [89].

1.2.2.3 Serous Ovarian Cancer

Serous carcinomas can be divided into high- and low-grade types. Low-grade often contain mutations in KRAS and BRAF and have borderline components, while high-grade often have p53 and BRCA mutations with no borderline components [90]. On histology, high-grade tumours often display nuclei of irregular size and frequent mitotic activity, while low-grade tumours are less common than high-grade, and on histology display nuclei of uniform size and a low mitotic activity rate as measured by Ki-67, a proliferation marker [90].

1.2.2.4 Mucinous Ovarian Cancer

Mucinous carcinomas are usually diagnosed early and have a better prognosis in comparison to other subtypes of ovarian cancer [91]. In addition, patients generally present at a younger age, and with tumours which are confined to the ovary [92]. Mucinous tumours are thought to develop from benign cysts to borderline to invasive tumours, however it is difficult to identify areas of invasion, and it is thought that most mucinous ovarian tumours are in fact metastases from other sites of origin [91]. Mucinous tumours frequently express mutations in KRAS but rarely in p53 [91]. While early stage mucinous tumours generally seem to have a favourable prognosis, late stage mucinous tumours have a very poor prognosis, most likely due to a combination of poor chemoresponsiveness, aggressive tumour biology or perhaps due to misclassification of tumours as primary rather than metastatic [93].

1.2.2.5 Endometrioid Ovarian Cancer

Endometrioid tumours account for approximately 10% of ovarian tumours, are usually found in perimenopausal women and are usually diagnosed at an early stage [90]. They are generally low grade tumours and are associated with endometriotic ovarian cysts [90]. Atypical endometriosis is a precursor for

endometrioid and clear cell carcinomas of the ovary [90]. Studies in mice have identified PTEN as a potentially important gene in carcinogenesis of this tumour, and loss of PTEN is associated with activation of the PI3K/Akt pathway favouring cell survival [90]. Endometrioid carcinoma of the ovary is the most common histological subtype diagnosed in the context of HNPCC, and in up to a fifth of cases, it is diagnosed with a simultaneous uterine carcinoma [90].

1.2.2.6 Clear Cell Ovarian Cancer

Clear cell carcinomas are generally quite different to other types of ovarian tumours – they often present as a large pelvic mass, and are usually diagnosed at an early stage [94]. Early stage clear cell carcinoma is associated with an increased rate of recurrence and a lower survival rate, likely due to its poor sensitivity to platinum/taxane based chemotherapy [94]. Clear cell carcinoma is also associated with a high risk of venous thromboembolism [95]. A recent study has identified a gene signature for clear cell carcinoma which represented certain aspects of its biology including oxidative stress, cytokines, MAPK activity and coagulation [96].

1.2.2.7 Stromal Ovarian Cancer

Stromal tumours are classified as granulosa cell tumours, thecomas, sertoli-stromal cell tumours, sex cord tumours, gyandroblastomas, steroid cell tumours or 'unclassified' and they account for approximately 7% of ovarian tumours [97]. The tumours are usually diagnosed at menopause and have a relatively good prognosis [97]. They are generally treated with surgical removal of the tumour, however the role of chemotherapy in these patients is unclear [97].

1.2.2.8 Germ Cell Tumours

Germ cell tumours account for <5% of ovarian carcinomas in the United States, however in Asian countries they represent up to 15% [97]. They are normally identified in young patients and are histologically similar to embryonic and extraembryonic structures. There are different subtypes of germ cell tumour including dysgerminomas, yolk sac tumours, embryonal tumours and

nongestational choriocarcinomas [97]. Serum tumour markers such as alpha fetoprotein (AFP) and human chorionic gonadotropin (hCG) can be used to distinguish between types of germ cell tumour. Correct staging is essential as this will affect the course of treatment – cure rates for germ cell tumours are higher than epithelial tumours, however a certain group of patients also become resistant to cisplatin [97].

1.2.3 Aetiology

Unlike other epithelial-type cancers, the aetiology of epithelial ovarian cancer is still unclear. The ovary is surrounded by surface epithelium which has the potential to differentiate into a number of different cell types [98]. The recent white paper by Schorge *et al.* [98] describes a number of hypotheses regarding ovarian cancer aetiology, summarized in Table 1.1. All of these hypotheses can be related to the risk factors identified for ovarian cancer e.g. incessant ovulation – early menarche and late menopause confer increased risk. Generally, it is thought that ovarian cancer occurs as a result of transformation of the surface epithelium [99], however, more recent studies of ovarian cancer have postulated that ovarian cancer may not be primary in most cases – it may have developed in the fallopian tube and metastasized [100-102].

Table 1.1. Hypotheses Regarding the Aetiology of Ovarian Cancer. (adapted from Schorge *et al.* [98])

Hypothesis	Mechanism
Incessant Ovulation	Epithelium damaged from repeated cycles of ovulation and repair, leading to increased mutation risk
Gonadotropin Stimulation	Follicle stimulating hormone and luteinizing hormone promote proliferation
Hormonal Stimulation	High levels of androgens promote carcinogenesis, while progestins decrease risk
Inflammation	Damage of the epithelium by ovulation induces inflammation which promotes reconstruction and enhances mutagenic potential

Generally, epithelial ovarian tumours can be broadly categorized into Type I and Type II (Figure 1.7). Type I tumours are slow growing with a stepwise accumulation of genetic defects and are generally less responsive to chemotherapy, while Type II tumours are high-grade, rapidly metastatic, and generally responsive to chemotherapy [98]. Low-grade serous carcinomas (Type I) are thought to arise from borderline tumours in most cases, and have a normal karyotype yet often harbour mutations in KRAS and BRAF genes [103]. Other histological subtypes of Type I tumours include low-grade mucinous and clear cell carcinomas, which are generally not chemosensitive [103]. Type II tumours have an abnormal karyotype, often with amplification of genes involved in the PI3K/Akt signalling pathway, and include hereditary cancers [103]. Type II tumours are often associated with dysfunction of the p53 and pRb tumour suppressor genes [103].

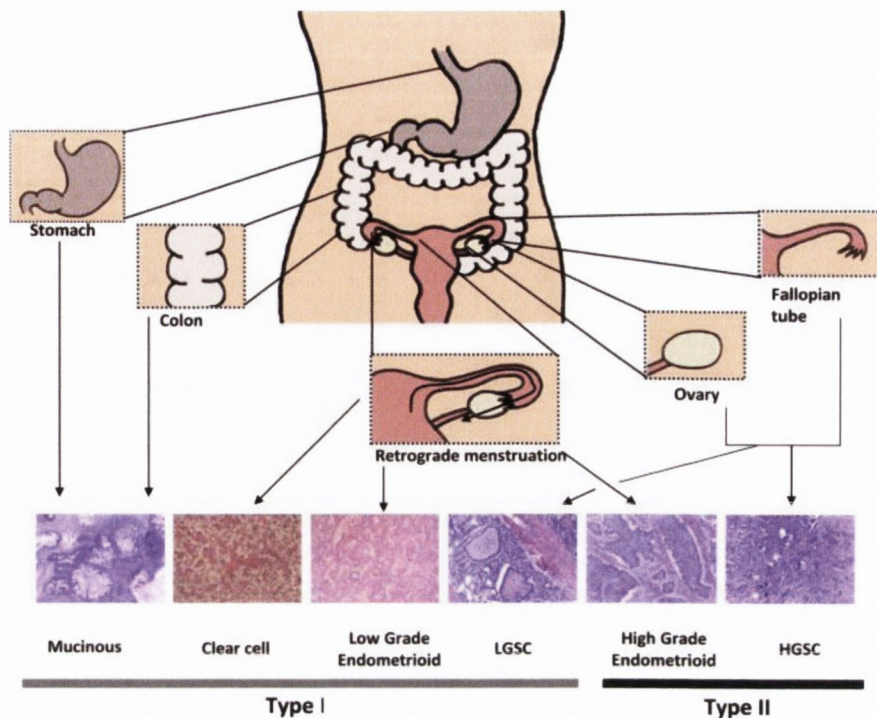


Figure 1.7. Histology of Type I and Type II Ovarian Tumours. The various histologies of ovarian tumours and their categorization into type I and type II tumours. (From Romero & Bast. [103])

Inherited ovarian cancers constitute approximately 10% of all cases, and of these, 90% are due to mutation in the DNA repair proteins BRCA1/BRCA2 [99]. The remaining 10% are due to mutations in the mismatch repair proteins MLH1 and MSH2 [104]. As mentioned previously, there are three types of hereditary cancer syndromes responsible for ovarian cancer – site specific, hereditary breast/ovarian syndrome (HBO) and HNPCC. Site specific ovarian cancer is diagnosed when two first-degree or both first- and second-degree relatives are diagnosed, however is closely related to HBO [104]. Hereditary breast/ovarian syndrome is diagnosed when there is a familial history of early breast cancer, ovarian cancer or both while HNPCC syndrome patients may have a familial history of a number of cancers such as colon cancer, endometrial, ovarian and pancreatic [104].

BRCA1 and BRCA2 are tumour suppressor genes, which when mutated, account for 5% of breast cancers [105]. BRCA1 mutation confers a higher risk of breast

and ovarian cancer than BRCA2 [105]. Normally, when a DNA double-strand break occurs e.g. due to DNA damaging agents, BRCA1 and BRCA2 are recruited to take part in homologous recombination, thus repairing the damage [105]. In addition, BRCA1 is involved in cell cycle checkpoint control, spindle assembly and chromosome separation [105]. In studies of ovarian cancer, BRCA mutated tumours generally respond better to platinum-based chemotherapy [106] and a recent meta-analysis of survival studies of BRCA1/2 mutated ovarian cancer patients showed an improved 5 year survival rate for mutation carriers, particularly for those with BRCA2 mutation [107]. Risk-reducing salpingo-oophorectomy is a prophylactic treatment offered to women known to carry BRCA1/2 mutations, however it is not opted for universally due to the subsequent premature menopause and infertility [108].

1.2.4 Diagnosis

Diagnosis of ovarian cancer is made based on pelvic examination for palpation of abdominal masses and radiological imaging such as transvaginal ultrasound and/or computed tomography (CT) scanning (Figure 1.8) and magnetic resonance imaging (MRI). Ovarian cancer has traditionally been considered a silent killer due to a lack of symptoms, however, most women presenting with ovarian cancer do have symptoms such as bloating, abdominal discomfort, alteration in urinary frequency and bowel movements [75]. Due to the non-specific nature of these symptoms, delays in diagnosis frequently occur, and the majority of cases of ovarian cancer are only discovered once the disease has already spread beyond the ovary [109].

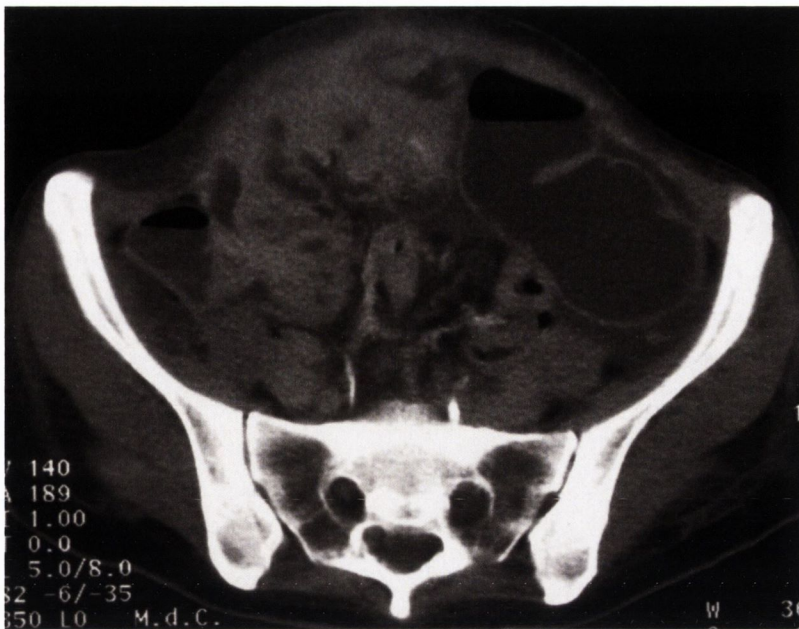


Figure 1.8. Computed Tomography Scan of Advanced Ovarian Cancer.
(www.biomedcentral.com)

As late diagnosis of ovarian cancer contributes to the high mortality rate, many biomarkers have been evaluated for potential usefulness in diagnosis of early ovarian cancer. The Ca125 antigen is expressed on the surface of ovarian tumour cells and can be secreted into the circulation following phosphorylation by epidermal growth factor [110]. Its serum levels are elevated in 90% of patients with late stage ovarian cancer, yet only in approximately 50% of early stage ovarian cancers, thus limiting its use for early diagnosis [111]. An additional limitation of Ca125 is its elevation in a variety of cancers other than ovarian such as pancreatic, breast and lung cancer, and in non-cancerous conditions such as endometriosis, fibroids, and liver disease [111].

Since Ca125, there have been a number of different avenues identified for potential biomarker development. Proteomic profiling of ovarian cancer has identified this as a highly specific and sensitive detector of early stage ovarian cancer although this has certain limitations in terms of instrument reproducibility [112]. In addition, several single protein biomarkers of ovarian cancer have been discovered including osteopontin and HE4, however their positive predictive values are too low for reliable early diagnosis [112]. Non-coding micro RNA molecules (miRNAs) have also been explored as a potential diagnostic tool for

ovarian cancer. miR-148b has been identified as a potential biomarker [113] and profiles of numerous miRNAs are also being evaluated as diagnostic tools by our group (unpublished) and others [114]. In addition, our group have recently published an article which analysed the potential utility of an auto-antibody profile to p53 and other novel auto-antigens in the sera of ovarian cancer patients and identified a potentially useful autoantibody profile to a cytoskeletal protein, adducin, in a subset of early stage patients [115].

1.2.5 Tumour Stage

Ovarian cancer is currently staged using the FIGO (International Federation of Obstetricians and Gynaecologists) classification (Table 1.2). Staging is carried out at surgery and has prognostic implications for patients.

1.2.6 Tumour Grade

Tumours are graded from 1 – 3 depending on the degree of differentiation. Well differentiated tumours retain their glandular features and are grade 1, while in grades 2 – 3 there is progressive loss of glandular features [75]. Grade of tumour is particularly important in early stage tumours, in which it affects prognosis and treatment options [75].

Table 1.2. FIGO Classification of Ovarian Cancer.

Stage	Description	
1A	Tumour in one ovary, capsule intact No tumour on ovarian surface Negative ascites/peritoneal washings	Tumour Confined to the Ovaries
1B	Tumour in both ovaries, capsule intact No tumour on ovarian surface Negative ascites/peritoneal washings	
1C	Tumour in one or both ovaries, capsule ruptured Tumour present on ovarian surface Positive ascites/peritoneal washings	
2A	Tumour extended into uterus and/or fallopian tubes Negative ascites/peritoneal washings	Tumour in One or Both Ovaries and Extends into the Pelvis
2B	Tumour extended to another pelvic organ Negative ascites/peritoneal washings	
2C	Tumour as in 2A/B Positive ascites/peritoneal washings	
3A	Microscopic peritoneal metastases beyond the pelvis	Tumour in One or Both Ovaries with Microscopically Confirmed Micrometastases Outside the Pelvis with/without lymph node involvement, including liver capsule involvement
3B	Microscopic peritoneal metastases beyond the pelvis <2cm in diameter	
3C	Microscopic peritoneal metastases beyond the pelvis >2cm in diameter and/or regional lymph node metastasis	
4		Distant metastasis and liver parenchymal metastasis

1.2.7 Treatment

Treatment of ovarian cancer consists of surgical staging including total abdominal hysterectomy, bilateral salpingo-oophorectomy and location of metastatic disease within the abdominal cavity [75]. Correct staging is essential, as it has implications for both prognosis and adjuvant therapies [116]. Debulking surgery consists of removing as much bulk disease as possible, however, if complete clearance of tumour is not possible, the goal is to reduce the tumour to minimal residual disease [116]. The volume of residual disease following primary cytoreductive surgery is an important prognostic factor [117] for ovarian cancer patients. To achieve a survival benefit, there should be no tumours larger than 2cm remaining following surgery, and the Gynecologic Oncology Group (GOG) describe 'optimal' debulking as residual tumour <1cm, however this is an often unachievable outcome in late stage ovarian cancer patients [118].

Following debulking surgery, patients are generally referred to oncology for adjuvant chemotherapy. Six cycles of carboplatin and paclitaxel are the current standard adjuvant treatment [103]. Early treatment of ovarian cancer consisted of single-agent melphalan, an alkylating agent [119]. This was replaced by combination cyclophosphamide and doxorubicin, and subsequently with an addition of cisplatin, or cisplatin alone [119]. Carboplatin is a platinum agent similar to cisplatin, although not as potent, yet has significantly less associated toxicity and is the platinum agent of choice today [119]. Chemotherapy is delivered intravenously. Intra-peritoneal chemotherapy has been explored as an alternative mode of delivery, and improves outcome yet is associated with increased toxicity [120]. A subsequent advance on this is hyperthermic intra-peritoneal chemotherapy in which chemotherapeutic drugs are warmed before they are infused – this is currently being evaluated in clinical trials [121]. More recently, the addition of bevacizumab to standard chemotherapy has been explored. Bevacizumab is an anti-angiogenic monoclonal antibody targeted against VEGF [122]. In two front-line therapy studies, preliminary data showed that addition of bevacizumab prolonged progression free survival but

not overall survival, while in one study of recurrent ovarian cancer it was found that treatment with bevacizumab in platinum sensitive cancers improved overall survival [123]. Use of bevacizumab in platinum resistant cancers is currently being evaluated.

Although prognosis is relatively good for patients who are optimally debulked, as mentioned previously, this is not possible in a large proportion of late stage ovarian cancer patients. Neoadjuvant chemotherapy – pre-operative chemotherapy to reduce tumour mass before debulking – is a potential solution for these patients [124]. Neoadjuvant chemotherapy can be considered in two settings, before initial cytoreductive surgery, and between an initial suboptimal cytoreductive surgery and interval debulking (induction therapy) [124]. A study by the EORTC (European Organization for Research and Treatment of Cancer) on patients who were initially suboptimally debulked examined the effect of three cycles of cisplatin/cyclophosphamide before subsequent interval debulking surgery [125]. They found that interval debulking significantly improved prognosis, and that this improvement was greater in patients whose tumours had shrunk to <1cm following neoadjuvant chemotherapy. In fact, the majority of studies on neoadjuvant chemotherapy have shown that patients who subsequently have optimal surgical cytoreduction have improved prognosis compared to those who are sub-optimally debulked [124]. Neoadjuvant chemotherapy is also seen to be beneficial to patients who are of general poor health and those with a high load of metastatic disease [117], however a recent meta-analysis of 21 studies has shown that there is little difference in prognosis between patients who undergo primary debulking and those who undergo neoadjuvant chemotherapy [126], thus appropriate patient selection is crucial to provide benefit. More recently, there has been a move towards neoadjuvant treatment of high-grade serous adenocarcinomas, however this is still determined on a case-by-case basis and at multi-disciplinary team meetings.

For patients with chemosensitive tumours, secondary cytoreduction followed by second-line chemotherapy seems to be of benefit for recurrent tumours [75].

Patients considered platinum sensitive (recurrence >6 months after completion of chemotherapy) may be re-challenged with carboplatin/cisplatin with or without paclitaxel, while those who are platinum insensitive (recurrence <6 months after completion of chemotherapy) may be treated with a number of agents including topotecan, liposomal doxorubicin or docetaxel to name a few [75]. Recurrence can be monitored by serum levels of Ca125, and a doubling of Ca125 from baseline has been shown to be a good indicator of recurrence, however, rises in Ca125 can often occur earlier than a patient becomes symptomatic, and it has been recently shown that patients receiving chemotherapy on the basis of Ca125 did not have a better survival than those who did not receive chemotherapy until they were symptomatic [127]. The most important predictors of how well a patient will respond to second-line chemotherapy are the previous response to cisplatin and the treatment/platinum-free interval [127].

1.2.8 Chemoresistance in Ovarian Cancer

While the majority of patients (80%) initially respond well to chemotherapy, a large percentage relapse, and become resistant to chemotherapy [128]. Approximately a fifth of patients do not respond to chemotherapy initially, and are considered to have *de novo* (intrinsic) chemoresistance [129]. The details of mechanisms of platinum and taxane resistance are discussed in detail in Chapter 3, however, in brief, resistance to these drugs is multi-factorial. Several different causes of chemoresistance have been identified, mainly depending on the drug's mechanism of action. For example, cisplatin (platinum) resistance has been associated with up-regulation of DNA repair mechanisms, increased intra-cellular trapping of the drug and increased drug efflux. Paclitaxel (taxane) resistance has been mainly associated with the multi-drug resistance protein, P-glycoprotein. The tumour microenvironment is also recognized as important in the development of chemoresistance, and the influence of tumour hypoxia is discussed below.

The degree of platinum resistance is classified according to the length of time between end of treatment and recurrence (Table 1.3) [127].

Table 1.3. Classification of Platinum Resistance. (Adapted from Hall and Rustin [127])

Title	Interval
Platinum Refractory	Progressive disease during platinum chemotherapy
Platinum Resistant	Progressive disease within 6 months following end of platinum chemotherapy
Platinum partially sensitive	Progressive disease from 6 – 12 months following end of platinum chemotherapy
Platinum sensitive	Progressive disease longer than 12 months following end of platinum chemotherapy

Several strategies are being explored to circumvent platinum resistance. Pharmacokinetic approaches are based on alterations in dosage intensity and in modalities of drug treatment e.g. intra-peritoneal vs. intra-venous; use of platinum analogues which are unsusceptible to known modes of cisplatin resistance; use of alternative microtubule affecting agents; use of novel therapeutics; and combination chemotherapy approaches [129].

1.3 Tumour Hypoxia

Tumour hypoxia is defined as a reduced level of oxygen tension within the tumour. Normal oxygen tension within a tissue is in the range of 4 – 1%, while hypoxia is <1% [130]. This is a common feature of solid tumours such as ovarian cancer and is associated with low pH and nutrient starvation [131]. Hypoxia may be acute or chronic, and is caused in several ways. Firstly, tumours are growing so erratically that they may compress blood vessels and thus eliminate blood flow, and secondly, they may grow such a distance away from blood vessels that they don't receive enough nutrients from the blood.

Tumour hypoxia has several consequences for patients. It switches on genetic pathways which promote tumour aggressiveness, metastasis and chemoresistance, thus patients with hypoxic tumours generally have a poorer prognosis [131]. Tumour hypoxia can be detected and monitored in several different ways. The gold standard for measurement of tumour hypoxia involves the use of invasive polarographic oxygen electrodes, however a number of non-invasive methods have been explored. Tracers which are retained in hypoxic regions such as ¹⁸F-FAZA (fluoro-azomycinarabino-furanoside) [132], and ¹⁸F-HX4 (3-[¹⁸F] fluoro-2-(4-((2-nitro-1H-imidazol-1-yl)methyl)-1H-1,2,3-triazol-1-yl)) [133] can be used for visualization by positron emission tomography (PET) and single photon emission computed tomography [134]. In addition, several magnetic resonance imaging (MRI) methods can be employed – electron paramagnetic resonance (EPR) oximetry, ¹⁹F MRI and blood oxygen level dependent (BOLD) contrast MRI [134]. EPR oximetry is based on the detection of oxygen free radicals within the vicinity of paramagnetic materials, ¹⁹F MRI is based on the detection of perfluorocarbons which can enter the tumour environment through 'leaky' blood vessels, and BOLD imaging reflects changes in oxygenation of the blood and can be used to image acute and chronic blood flow within tumours [134].

Tumour hypoxia results in activation of the Hypoxia-inducible factor 1 (HIF1) pathway. The HIF-1 protein was discovered by Gregg Semenza in 1991. It is composed of two subunits, the hypoxia-regulated α subunit, and the non-hypoxia-regulated β subunit [131]. It belongs to the basic helix-loop-helix Per Arnt Sim (PAS) protein family [135,136]. HIFs bind to hypoxia-regulated elements (HREs) contained within the promoter sequences of many genes [131]. It has recently been estimated that more than 70 genes are regulated by HIF-1 α [135]. HIF-1 controls the expression of genes regulating metabolism, cell survival, angiogenesis and invasion i.e. genes which allow the cells to adapt to hypoxia [131], summarised in Figure 1.9. While the β subunit of HIF is constitutively expressed in many tissues, the α -subunit is normally degraded in oxygen [135]. The HIF-1 α subunit contains an oxygen dependent degradation (ODD) which is a target for proline hydroxylase enzymes. These enzymes hydroxylate HIF-1 α at proline⁴⁰² and proline⁵⁶⁴ thus targeting the protein for proteasomal degradation via the Von Hippel-Lindau (VHL) protein [131,137].

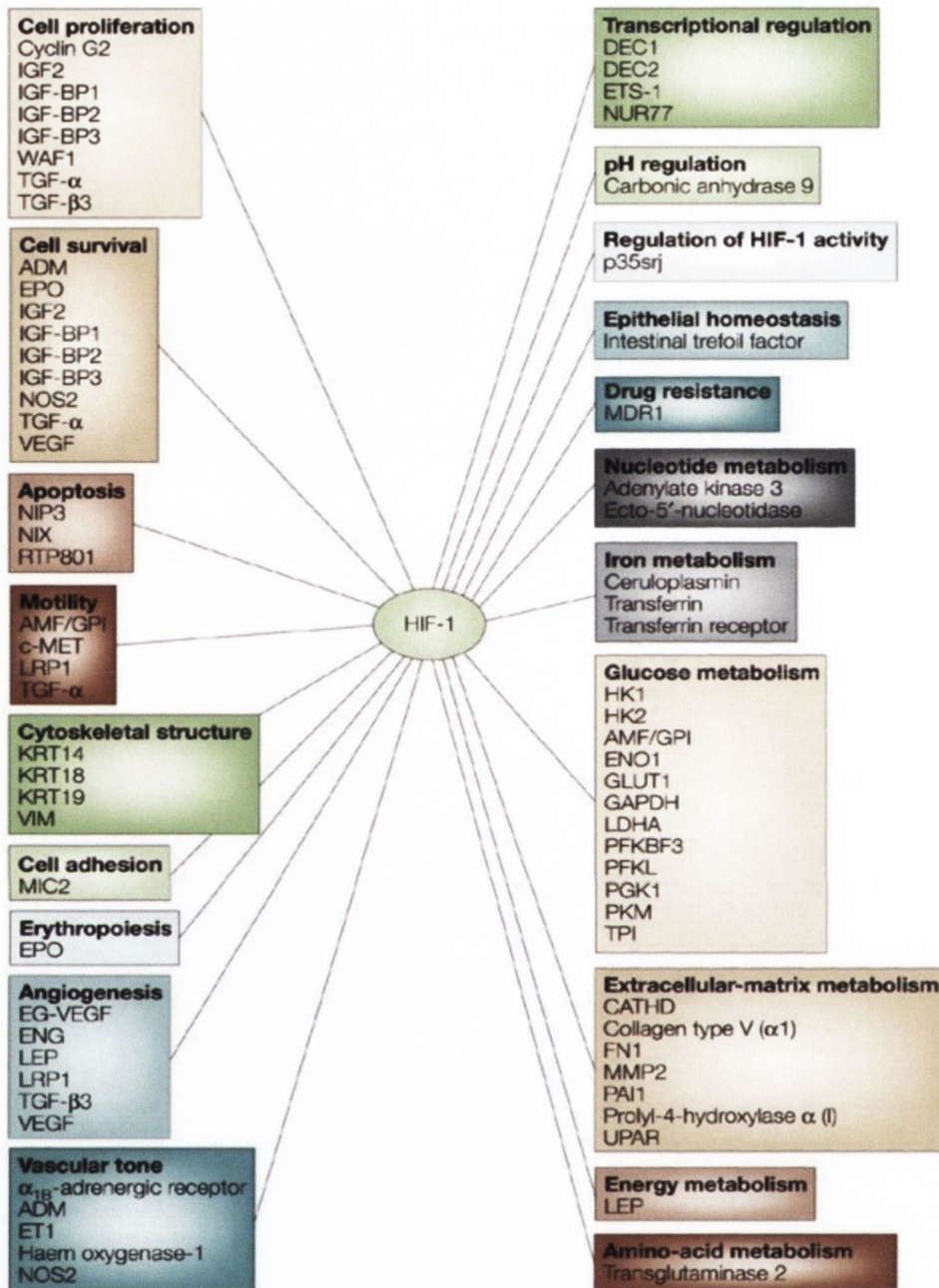


Figure 1.9. Summary of HIF-1-mediated Processes. HIF-1 has been shown to affect many cellular processes such as metabolism, adhesion, and cytoskeletal structure, in addition to stimulation of angiogenesis and proliferation. (From Semenza [137])

HIF-2 α is a closely related protein which also associates with HIF- β , however its expression is restricted to certain tissues [131]. Its activity is best characterized in VHL-dependent renal cell carcinoma, where HIF-2 α is expressed rather than HIF-1 α [138]. HIF-2 α has some similar functions to HIF-1 α , however it also has some specialized functions of its own. It stimulates expression of Oct4, which regulates stem cell maintenance [139]. The two hypoxia-regulated proteins have some opposing roles e.g. while HIF-1 α reduces cell proliferation by targeting c-myc, HIF-2 α increases cell proliferation by activation of c-myc [139]. Studies in HIF-2 α -null mice have shown that it is vital for recruitment of tumour associated macrophages (TAMs) to the tumour microenvironment, a phenomenon which is associated with tumour progression [139]. However, deletion of HIF-2 α has been shown to increase tumour progression in lung cancer models [140].

HIF-3 α , a protein which shares a degree of similarity with HIF-1 α and HIF-2 α , is thought to play a role in negatively regulating the effects of hypoxia [141]. However, little is known about how HIF-3 α is involved in the tumour hypoxic response.

HIF-1 α and HIF-2 α are transcriptionally regulated by a number of different pathways – they can be induced by NF κ B stimulation, and by a number of cytokines [142]. In addition, the c-myc oncogene has recently been shown to induce HIF-1 α transcription in both normal and cancerous cells [143] and KIT ligand (stem cell factor) has been shown to induce HIF-1 α protein accumulation in myeloid leukaemia cells [144]. The Toll-like receptor pathway can also stimulate HIF-1 α expression under normoxic conditions [145]. HIF-1 α protein expression and activity are tightly regulated under normal oxygen conditions. In hypoxia, the exact stimulus for HIF-1 α transcription is not entirely clear, however it is likely that it is due to mitochondrial generation of superoxide, and the redox status of certain regions of HIF-1 α affects its interaction with cofactors [146].

While proline hydroxylases reduce the protein's stability, another protein, Factor Inhibiting HIF-1 (FIH), hydroxylates Asparagine⁸⁰³. This reduces HIF-1 transcriptional activity as it inhibits association of HIF-1 α to its coactivators, CREB-binding protein (CBP) and p300 [135]. Furthermore, another protein, CITED2, represses HIF-1 activity by competing for the CBP/p300 binding site [135]. HIF-1 α is normally stabilized at oxygen levels from 0 – 2%, while HIF-2 α is stabilized at slightly higher oxygen concentrations, 2 – 5%, and its expression is maintained for a longer time period than HIF-1 α [142].

Hypoxia is thought to affect cellular proliferation by inducing growth arrest and through apoptosis [136]. Evidence has shown that cells within tumours may be non-proliferating, although viable [147]. Movement of the cell cycle from G₁ (rest) to S (DNA synthesis) is modulated via cyclin-dependent kinases (CDKs) and cyclin-dependent kinase inhibitors (CKIs). CDKs phosphorylate the retinoblastoma protein, pRb, and growth arrest in hypoxic cells has been linked to hypophosphorylation of this protein. A study using a fibroblast cell line has shown that hypoxia can induce cell cycle arrest via the CKI p27 [147]. This has been shown to be dependent on the presence of HIF-1 α [136]. HIF-1 α has also been observed to promote cell proliferation in ovarian cancer cells through dysregulation of cell cycle protein cyclin D1 [148], while in neural stem cells, mild hypoxia has been shown to increase proliferation [149]. Hypoxia has also been shown to inhibit cellular senescence, a safeguard against tumourigenesis [150].

HIF-1 α is also known to prevent apoptosis. In an *in vivo* model of colon cancer, HIF-1 α was shown to induce expression of the anti-apoptotic protein, survivin, and siRNA-mediated inhibition of HIF- α resulted in decreased survivin expression and reduced tumour load [151]. Additional studies in colon cancer revealed that HIF-1 α activates KRAS, inhibiting apoptosis [152]. HIF-1 α has been shown to induce expression of anti-apoptotic proteins such as Bcl-2 [153] and XIAP (x-linked inhibitor of apoptosis) [154] while it suppresses expression of pro-apoptotic molecules such as Bax [155].

HIF-1 α has several different functions in regulating metabolism including down-regulation of oxygen consumption, regulating expression of enzymes involved in metabolism and inducing mitochondrial autophagy [156]. Cellular hypoxia encourages increased glucose uptake and increased conversion of glucose to pyruvate and anaerobic metabolism [157]. In addition, a number of glycolytic enzymes are altered [158]. HIF-1 α has been shown to stimulate glycogen accumulation in breast cancer cells through regulation of the protein phosphatase 1, regulatory subunit 3C (PPP1R3C) [159]. The 'Warburg effect' refers to the dependence on glycolytic metabolism which is exhibited by cancer cells, and is thought to confer a selective advantage [160]. This seemingly unusual biology for actively growing cells may be explained by the fact that tumour cells are not lacking in nutrients, due to their ability to stimulate increased blood flow, or because it is not efficient for tumour cells to convert all glucose to CO₂ via oxidative metabolism – some must be converted to other macromolecular precursors such as those for amino acid synthesis [160]. The shift from oxidative metabolism to anaerobic glycolysis is mediated through HIF-1 α [161].

Hypoxia is associated with the growth of new blood vessels. In lung carcinoma, HIF-1 α enhanced expression of angiogenic genes including VEGFA and PDGFC (platelet derived growth factor C) [162], while in oral squamous cell carcinoma, HIF-1 α -mediated expression of VEGFA is elicited through the mTOR (mammalian target of rapamycin) pathway [163]. In ovarian cancer, siRNA-mediated knockdown of HIF-1 α reduces the cells' expression of VEGF and angiogenic potential [164]. However, VEGF alone does not seem to be sufficient for successful angiogenesis – mouse studies have shown that blood vessels produced by VEGF are 'leaky', and that co-expression of VEGF and angiopoietin 1 (ANGPT1) produce blood vessels that are not excessively permeable [165]. Expression of other angiogenic molecules in response to hypoxia contribute to blood vessel development including placental growth factor (PGF), PDGF, and fibroblast growth factor 2 (FGF2) [165].

One important role of hypoxia in tumour pathogenesis is its link with cancer stem cells (CSCs). CSCs are a population of tumour cells which are capable of self-renewal and multipotency, and are thought to be influenced by the presence of tumour hypoxia [131]. Indeed, hypoxia has been shown to enhance stem-like characteristics and prevent differentiation of cultured neuroblastoma cells [166] and studies of prostate cancer and lung cancer cell lines have demonstrated up-regulation of stemness markers such as OCT4 and SOX2 in cells exposed to hypoxia [167,168]. Neural stem cells are known to express HIF-1 α [169] and stem cell factor has been shown to induce HIF-1 α in normoxia in haematopoietic cell lines [170,171]. In addition, HIF-1 α has been shown to stimulate expression of the Wnt/ β -catenin signalling pathway, thus maintaining stem-like properties [172]. HIF-2 α has been identified as a potential player in hypoxia-mediated stemness, and in glioblastoma it has been shown to be preferentially expressed by stem-like cells, and localises with cancer stem markers such as CD133 [173]. Interestingly, the use of anti-angiogenic agents has been shown to increase the population of stem-like cells in *in vivo* breast tumour models due to generation of hypoxia – this is particularly important in the context of ovarian cancer, for which the anti-angiogenic monoclonal antibody, bevacizumab, is being trialled [174].

A number of compounds have been shown to have anti-angiogenic properties through inhibition of HIF-1 α such as betulinic acid in prostate cancer cell lines [175] and acacetin in ovarian cancer cell lines [176]. Knockdown of HIF-1 α has been shown to increase sensitivity to chemotherapy in breast cancer, fibrosarcoma and colon cancer [177-179] and reduce invasiveness in glioma cells [180]. Indeed, HIF-1 has been identified as a strong candidate for tumour therapy. Small molecule inhibitors of HIF-1 α have been shown to reduce tumour burden in *in vivo* models through interference with the binding of HIF-1 to its cofactors [181] and in prostate cancer models where they reduce HIF-1 α protein accumulation and prevent metastasis and angiogenesis [182]. Since HIF-1 α has been shown to mediate some of its actions through the PI3K pathway, PI3K inhibitors have been evaluated in

thyroid cancer models, where they have been shown to reduce cell proliferation and metastasis [183]. The concept of bioreductive drugs, where pro-drugs are administered and subsequently activated in hypoxic tumour regions is currently being studied in a number of clinical trials [184].

1.3.1 Hypoxia and Chemoresistance

It has been long noted that hypoxia plays a role in resistance to radiation therapy. However, it can also play an important role in resistance to chemotherapy. It is known to affect resistance to chemotherapy both directly and indirectly, summarized in Table 1.4.

Table 1.4. Effects of Hypoxia on Chemoresistance. (adapted from Wilson & Hay [184])

Hypoxia Effect	Mechanism of Chemoresistance	Type of Drug Affected
Lack of oxygenation of DNA free radicals	Failure to induce DNA breaks	Antibiotics which induce DNA breaks
Cell cycle arrest in G ₁ or G ₂	Repair before progression to S or M phases	Cell cycle-selective drugs. e.g. 5-FU
Distance from vasculature (indirect)	Decreased drug exposure	Taxanes
Extracellular acidification (indirect)	Decreased drug uptake	Basic Drugs e.g. Doxorubicin
Apoptosis resistance	Down-regulation of pro-apoptotic molecules, selection of p53 mutants	Multiple drugs
Genomic Instability	Mutagenesis	Multiple drugs
Suppression of DNA repair	Down-regulation of mismatch repair	DNA methylating agents
HIF-1 stabilization	Several	Multiple

Hypoxia has been observed to induce chemoresistance to a wide range of cytotoxic agents. Hypoxia has been shown to induce resistance to DNA-damaging cisplatin through HIF-1 α activity in a range of cancers such as lung cancer [185], glioma [186], colon carcinoma [187], oral squamous cell carcinoma [188], ovarian cancer [189] and also in normal tissues [190]. In addition, carboplatin is also less active under hypoxic conditions in testicular carcinoma [191]. In neuroblastoma, hypoxia increases resistance to the vinca alkaloid microtubule acting agent, vincristine, and the topoisomerase II inhibitor, etoposide [192], while in colon cancer, hypoxia increases resistance to the antimetabolite, 5-fluorouracil [193]. In pancreatic cancer, HIF-1 α expression was associated with resistance of tumour cells to gemcitabine, a nucleoside analogue, and patients whose tumours were positive for HIF-1 α protein staining had shorter progression-free and overall survival times [194]. A study of lung cancer found that HIF-1 α prevented apoptosis induced by the chemotherapeutic 5-fluorouracil (5-FU) through suppression of cyclin D1 [195]. However, it should be noted that in some instances, the effects of hypoxia can cause sensitivity to certain therapeutic agents [184]. For example, as hypoxia can induce cell cycle arrest in S phase of the cell cycle, it can increase sensitivity to PARP (Poly-ADP ribose polymerase) inhibitors through stalling and collapse of replication forks, and in addition, through acidification of the extracellular matrix, hypoxia can increase uptake of certain acidic drugs such as Chlorambucil [184].

1.3.2 HIF-1 α and Prognosis

Since HIF-1 α is associated with resistance to a number of chemotherapeutic agents, in addition to its general effects on tumour biology, it is likely to impact on progression-free (PFS) and overall survival (OS) of cancer patients. Indeed, head and neck squamous cell carcinomas expressing high levels of HIF-1 α and HIF-2 α are associated with poor PFS and OS [67]. In fact, serum levels of HIF-1 α -regulated molecule VEGF are indicative of progressive disease in head and neck cancer patients, indicating a use for VEGF as a prognostic biomarker [196]. Similarly, in a study of over 700 colorectal cancer patients, tumours over-expressing HIF-1 α were

significantly more likely to suffer colorectal cancer-related death [197], and oral squamous cell carcinomas co-expressing high levels of HIF-1 α and the glucose transporter GLUT-1 are associated with reduced survival [198].

Ovarian tumours expressing high amounts of HIF-1 α have been shown to result in poorer overall survival for patients [199,200], although interestingly, one study of ovarian cancer demonstrated improved survival for ovarian cancer patients with HIF-1 α -expressing tumours [201]. Expression of other downstream effectors of HIF-1 α such as VEGF have also been shown to have prognostic significance [202]. Strong expression of HIF-1 α has been shown to be more frequent in serous adenocarcinomas and endometrioid adenocarcinomas, with fewer positive cases for clear cell carcinoma and mucinous adenocarcinoma [203]. Similar patterns have been observed for GLUT-1, a downstream effector of HIF-1 α [203]. Also, the expression of HIF-1 α and GLUT-1 mRNA and protein has been shown to increase with increasing malignant potential in ovarian serous and mucinous tumours [204]. Activity of HIF-1 α has been shown to be higher in serous adenocarcinomas than mucinous, and in general the expression was stronger in serous tumours compared to mucinous [204]. The authors, [204], suggest that this may be due to the papillary structure of serous tumours, which is more conducive to a hypoxic environment. Also, the hormones oestrogen and progestin have been shown to induce HIF-1 α expression in cell line models [205].

1.4 Hypothesis and Aims

The hypothesis of this study is three-fold:

- i) Hypoxia is responsible for chemoresistance in ovarian carcinoma
- ii) The length of hypoxic exposure is an important determining factor in chemoresistance
- iii) Identification of genes involved in the generation of chemoresistance may provide novel therapeutic/prognostic biomarkers of ovarian cancer

In order to test this hypothesis, the study aims were:

- i) To confirm that hypoxia induces chemoresistance in an ovarian cancer cell line model by monitoring changes in response to chemotherapy, and to evaluate the effect of different lengths of hypoxic exposure on chemoresistance development.
- ii) To determine which genes are influential in the development of chemoresistance by whole-genome profiling cells which are exposed to hypoxia and/or drug treatments.
- iii) To evaluate potential novel hypoxia-related biomarkers of ovarian cancer in tissue samples from ovarian cancer patients.

Chapter 2

Materials and Methods

2.1 **Cell Lines**

The human epithelial (serous) ovarian cancer cell lines A2780 (cisplatin-sensitive) and A2780cis (cisplatin resistant) were purchased from the European Collection of Cell Cultures (ECACC, UK) and stored in cryovials (Sarstedt, Germany) in liquid nitrogen. A2780 express wild-type BRCA1/2 and have a known mutation in Pten (c.383_391del9) [206].

2.1.1 **Resuscitation of Stocks from Liquid Nitrogen**

Cryovials were removed carefully from the liquid nitrogen tank (RS Series, Taylor-Wharton, Germany) and allowed to sit at room temperature for one minute. They were then brought quickly to 37°C in a water bath (Clifton, Bennett Scientific, UK) and brought to the laminar flow hood (Danlafo-matic VFR 1206 BSD, Germany). They were then added to 3 mL of pre-warmed medium (37°C) in a T25 culture flask (Corning, UK) and incubated overnight at 37°C in a humidified atmosphere. Cells were checked for morphological abnormalities under the microscope (Leica Leitz DMIC, Ireland) before incubation.

2.1.2 **Cell Culture**

Cells were cultured according to the conditions set out by the ECACC. Both cell lines were cultured in RPMI 1640 medium (Lonza, UK) supplemented with foetal bovine serum (FBS, Lonza, UK), penicillin/streptomycin mixture (Lonza, UK) and Glutamax (Gibco, Biosciences, Ireland) to the final concentrations outlined in Table 2.1. Additionally, 1 µM cisplatin was added to the A2780cis culture medium every second passage to maintain resistance as per the ECACC's recommendation. All cell culture was carried out in the laminar flow hood. Cells were checked regularly for bacterial, mycoplasma and fungal contamination.

Table 2.1. Concentrations of Supplements Added to RPMI 1640 media for Culture of A2780 and A2780cis Cell Lines.

Supplement	Final Concentration
FBS	10%
Penicillin/Streptomycin	1%
Glutamax	2 mM

2.1.3 Subculture of Cell Lines

A2780 and A2780cis are both adherent cell lines. Cells were cultured in T75 culture flasks (Sarstedt, Germany) containing 15 mL of pre-warmed media (37°C). When cells were approximately 80% (A2780) or 70% (A2780cis) confluent, they were subcultured to provide more space for cell growth. Spent media was removed from the cells. The flasks were rinsed twice with pre-warmed (37°C) phosphate buffered saline (PBS, Lonza, UK). Five mL of pre-warmed 0.25% Trypsin-EDTA solution (Gibco, Biosciences, Ireland) was added to the flasks and they were incubated at 37°C for approximately 7 minutes. Following incubation, the cells were tapped firmly to ensure complete detachment of cells and the flasks were checked under the microscope to confirm this. The trypsin solution was neutralized by addition of an excess of media, and the cell/media solution was transferred to a 50 mL sterile centrifuge tube (Sarstedt, Germany). The solution was centrifuged (ALC PK121R, DJB Labcare, UK) at 2000 rpm for 10 minutes to sufficiently pellet the cells. The supernatant was discarded and 1 mL of fresh media was used to resuspend the cells. The cells were then reseeded at an appropriate cell density for the cell line (Table 2.2) into new T75 culture flasks containing pre-warmed medium. The cells were then incubated at 37°C.

Table 2.2. Cell Densities for A2780 and A2780cis Cell Lines as set out by the ECACC Guidelines.

A2780	A2780cis
$3 - 6 \times 10^4/\text{cm}^2$	$1 \times 10^3 - 1 \times 10^4/\text{cm}^2$

2.1.4 Cell Count

Trypan blue is a vital dye which is excluded from live cells which have an intact plasma membrane, thus the cells appear colourless under light microscopy. Dead cells whose plasma membranes are compromised will take up the blue dye and appear blue under light microscopy. Dead cells were not included in the cell count. To perform a cell count, the cells were trypsinized, centrifuged and resuspended in 1 mL of medium as described above. The cells were then diluted appropriately in filter sterilized trypan blue solution (0.4%, Sigma, UK) and mixed thoroughly. A haemocytometer is a tool used to count cells. It has two chambers, each divided into grids of known size and depth. A sample of the cells to be counted is diluted in trypan blue solution. Using a formula, it is possible to work out the number of cells in a fixed volume. The following formula is used:

Cell count = Average number of cells counted x dilution factor x correction factor

Example: $935 \times 10^4/\text{mL} = 93.5 \times 10 \times 10^4$

Ten μL of the cell/trypan blue solution was added to each chamber of a haemocytometer (Blu Brand, Germany) and the cells were counted under the microscope. The cells within the inner square of the haemocytometer were counted, taking care not to count cells twice. This was achieved by using a mechanical counter, and by not counting cells lying on the top or left hand lines. Both the top and bottom chambers were counted and the scores averaged. This was then multiplied by the dilution factor. Dilutions of 1:2 or 1:10 were carried out, thus the cell count was multiplied by 2 or 10 respectively. This score gave a cell

number $\times 10^4$ /mL. This could then be diluted or combined with other flasks to reduce or increase the cell concentration.

2.1.5 Freezing Down Stocks

Flasks could be frozen down and stored in liquid nitrogen to create stocks of each cell line. Flasks were trypsinized and centrifuged. The supernatant was discarded. One mL of cell freezing medium containing dimethylsulfoxide (DMSO, Gibco, Biosciences, Ireland) was added very slowly to the cell pellet. This was then transferred to a cryovial (Sarstedt, Germany). The cryovial was wrapped in cotton wool, placed in a polystyrene box and stored overnight at -80°C (Hetofrig CL410, Richmond Scientific, UK). The following day it was transferred to liquid nitrogen for long term storage.

2.1.6 Mycoplasma Testing

Infection of cells with mycoplasma is difficult to detect visually in cell cultures, as unlike bacterial or fungal contamination, the cells often do not display any obvious signs of infection. They may, however, display altered growth patterns. The MycoAlert[®] Mycoplasma Detection Kit (Lonza, UK) was used to detect the presence of mycoplasma in cell culture specimens.

2.1.6.1 Principle

This assay is based on the ability of mycoplasmal enzymes to catalyse the reaction where ADP is converted to ATP. Viable mycoplasma present in the media bathing the cells are lysed. They then react with a substrate to catalyse an ADP/ATP reaction. The level of ATP in a sample is measured before and after addition of the substrate. When mycoplasmal enzymes are absent, the second reading will show no increase over the first. When present, the enzymes activity leads to increased levels of ATP. The following reaction illustrates:



Emitted light intensity is linearly related to the concentration of ATP.

2.1.6.2 Protocol

Media surrounding cultured cells was removed and centrifuged to remove cells and debris and 100 μL was then added to a well of a 96 well ELISA plate (Nunc, Fisher Scientific, Ireland). One well was used for each sample tested. MycoAlert[®] Reagent (100 μL) was added to the media and incubated at room temperature for 5 minutes. A one-second integrated reading was then obtained on a luminometer (Wallac, Perkin Elmer, Ireland: Reading A). Following this, 100 μL of MycoAlert[®] Substrate was added to the well and incubated at room temperature for 10 minutes. A second reading was obtained (Reading B). The presence of mycoplasma could be determined by taking a ratio of Reading B/Reading A. A ratio ≤ 1 indicated that the sample was negative for mycoplasma. A ratio >1 indicated contamination with mycoplasma. Positive and negative controls were tested with each sample run (Table 2.3).

Table 2.3. Controls for MycoAlert[®] Assay for Mycoplasma Contamination of Cell Culture.

Positive Control	MycoAlert [®] Assay Control Set (Lonza, UK)
Negative Control 1	Fresh RPMI 1640 media (Lonza, UK)
Negative Control 2	Mycoalert [®] Assay Buffer (Lonza, UK)

2.2 Hypoxia Chamber

The hypoxic conditions used in this project were achieved using the INVIVO₂ 400 hypoxia workstation (Ruskin, UK, Figure 2.1). This benchtop hypoxia chamber is connected to a gas mixer which controls the oxygen and carbon dioxide components of the gas mix entering the chamber, and which can maintain the level of oxygen set by the user. In this study, the oxygen level was maintained at 0.5% O₂. The CO₂ level was set at 5% with the remainder made up with N₂. The interior of the chamber is set to 37°C. A humidistat controls a de-humidification system which removes excess moisture from the chamber and maintains relative humidity within the chamber at 85%. An internal microprocessor within the gas mixer monitors gas levels and gas pressures. If gas pressure falls below the recommended level of 50 – 70 pounds per square inch (PSI), the gas mixing is stopped. A liquid crystal display (LCD) screen on the gas mixer provides information on the chamber's gas demand and the gas levels which have been set by the user.

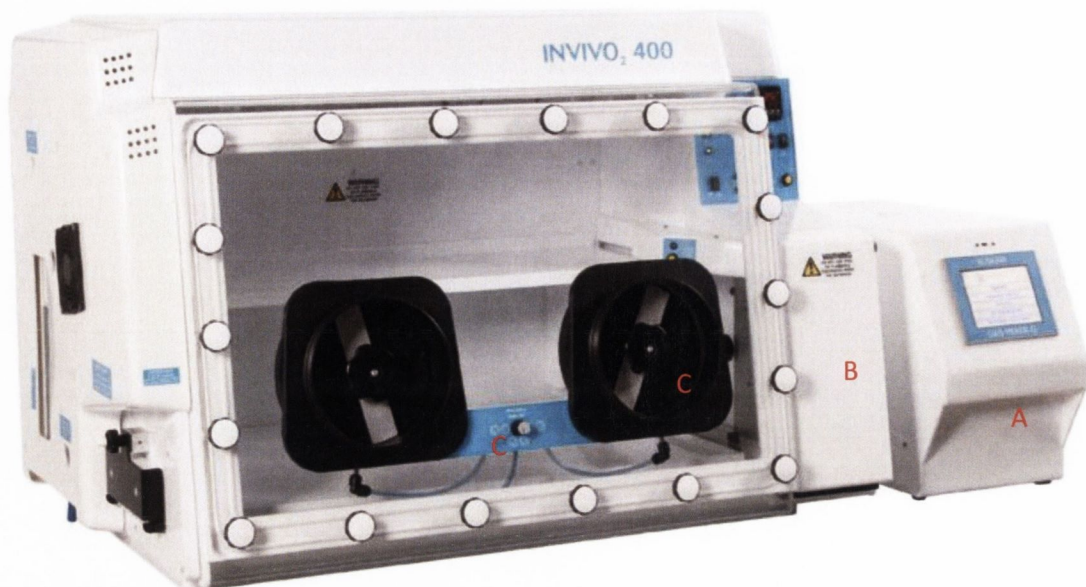


Figure 2.1. INVIVO2 400 Hypoxia Workstation. This workstation was used throughout this study to provide hypoxic conditions. The interior of the chamber was maintained at 0.5% O₂ by a gas mixer (A). The chamber was used by placing the items to enter the chamber in the interlock (B) and by putting one's hands through the ports (C).

To use the chamber, all items to be placed in the chamber/removed were put in the interlock. Air was removed from the interlock before transferring the items to the chamber. The user's arms were put in plastic sleeves connected to the ports on the front of the chamber and the air was removed from the sleeves using a vacuum pump. The ports could then be opened and the user could work comfortably inside the chamber.

2.3 MTT Assay

All cytotoxicity and cell proliferation assays were carried out using a standard MTT assay (Roche, UK). The MTT assay works on the basis that proliferating cells can cleave the yellow MTT (3-(4,5-Dimethylthiazol-2-yl)-2,5-diphenyltetrazolium bromide) reagent, a tetrazolium salt, to create formazan crystals (purple). Only viable cells can act on the MTT dye, therefore the number of crystals present is

proportional to the number of viable cells present (Figure 2.2). Ten μL of MTT reagent at a concentration of 0.5 mg/mL was added to a final volume of 100 μL per well, and left to incubate at 37°C for four hours. During this time, any proliferating cells oxidized the MTT reagent to create formazan crystals. Solubilization buffer (100 μL) (Roche, UK) was then added to dissolve any crystals present and the plates were incubated overnight at 37°C. Following this incubation, the plates were read on an optical plate reader (Dy nex Technologies, US) at 570 nm.

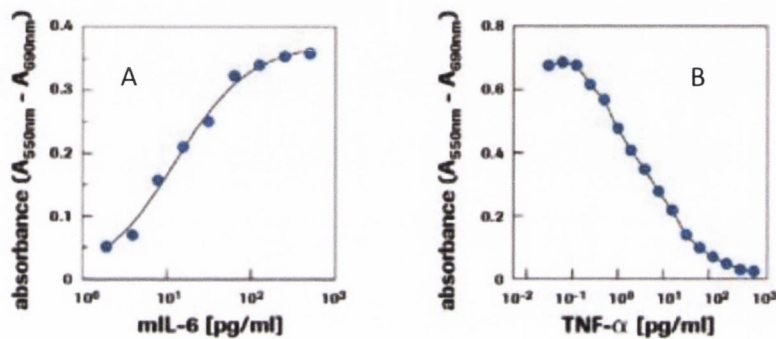


Figure 2.2. Sample Graphs Obtained Using MTT Assay. The MTT assay can be used to evaluate cell proliferation following stimulation (A) or cell viability following addition of cytotoxic agent (B). (From www.roche-applied-science.com)

2.4 RNA Extraction

2.4.1 Principle

Total RNA was extracted from cells using the Qiagen RNeasy mini kit. This kit can extract up to 100 μg of RNA from cells, tissues and yeast using a silica-based membrane system. Samples are lysed using a guanidine-thiocyanate buffer and homogenized using a QIASHredder column. Addition of ethanol promotes binding of RNA to the silica-based spin column, and a series of washes are carried out, along with DNase digestion to remove any contaminating genomic DNA. Finally the RNA is

eluted in RNase-free water. All centrifugations were carried out at 15,000 rpm and at room temperature.

2.4.2 Cell Lysis and Homogenization

Spent media was removed from the cell culture flasks, and the flasks were washed twice in PBS at room temperature. Buffer RLT (600 μ L) was added directly to the flask and the cells were scraped into the buffer using a sterile cell scraper. The buffer containing the lysed cells was transferred to a QIAshredder spin column for homogenization, and centrifuged for 15 seconds. Homogenization was carried out to shear any high molecular weight cellular components present such as genomic DNA. It also increased the efficiency of RNA binding to the spin column in the subsequent extraction and purification.

2.4.3 RNA Purification I

One volume of filtered 70% ethanol was added to the lysate after homogenization and the solution was transferred to an RNeasy spin column and centrifuged for 15 seconds. The flow-through was discarded and the spin column was placed in a new collection tube to reduce any carry-over. Buffer RW1 (350 μ L) was added to the column and centrifuged for 15 seconds.

2.4.4 DNase Digestion

In order to ensure that all genomic DNA was removed, all samples underwent an on-column DNase digestion. DNase I (80 μ L) was added to the spin column membrane and incubated for 15 minutes at room temperature. The column was then washed with 350 μ L of Buffer RW1 for 15 seconds.

2.4.5 RNA Purification II and Elution

The column was placed in a new collection tube to reduce any carry over from the previous steps. Buffer RPE (500 μL) was added to the column and centrifuged for 15 seconds. The flow-through was discarded and an additional 500 μL of RPE was added to the column. The column was centrifuged for 2 minutes. The column was placed in a new collecting tube and centrifuged for one minute. The column was then placed into an RNase-free snap-cap collecting tube and 34 μL of RNase-free water was applied to the column membrane. The column was centrifuged for one minute to elute the RNA. The eluate was then reapplied to the membrane and centrifuged again. The eluted RNA was stored at -80°C .

2.5 Assessment of RNA Yield using the NanoDrop

The quantity and quality of RNA from the extractions was assessed using the Thermofisher NanoDrop 2000. The NanoDrop allows for analysis of small sample volumes without a need to dilute the samples. The sample (1.5 μL) was loaded onto the pedestal. The arm of the NanoDrop was closed, and a sample column was formed. The NanoDrop then adjusted the path length and measured the absorbance at 230 nm, 260 nm and 280 nm to provide the RNA concentration ($\text{ng}/\mu\text{L}$) and two ratios, $A_{260}/280$ and $A_{260}/230$. $A_{260}/280$ is a measure of RNA purity, and should be approximately 2.0 for pure RNA. A lower ratio indicates the presence of protein or phenol. $A_{260}/230$ is a secondary measure of RNA purity, and should be approx. 2.0 – 2.2 for pure RNA.

2.6 Bioanalyzer

2.6.1 Principle

The Agilent 2100 Bioanalyzer is a microfluidics platform which allows for sizing, quantification and quality control of RNA, DNA, protein and cells. It has several advantages over larger scale platforms including better precision and reproducibility, minimal sample consumption and shorter analysis times. Electrophoretic separation of samples occurs on-chip and samples are subsequently detected by laser-induced fluorescence [207]. The software then provides an electropherogram for each sample, as well as a gel-like image. RNA is rapidly degraded by RNase enzymes, compromising its usefulness in downstream applications [208]. Therefore it is vital to ensure that RNA is of sufficient quality to be used in certain experiments such as microarrays.

2.6.2 RNA Integrity Number

The RNA Integrity Number (RIN) is a measure of the integrity of an RNA sample which does not require subjective analysis by the researcher. Previously, researchers used the ribosomal ratio obtained from slab gel analysis to determine RNA quality [207], however this method can be quite inaccurate [209]. RIN is an algorithm which classifies eukaryotic RNA using a numbering system from 1 – 10, 1 being the most degraded and 10 the most intact (Figure 2.3) [207]. Samples are analysed on-chip and an electropherogram is produced which is analysed by the Bioanalyzer Expert software. Rather than just the ratio of the ribosomal RNA bands being analysed, the software analyses the entire electropherogram (Figure 2.4). A RIN may not be calculated if the software detects a peak in an unexpected area of the electropherogram. The RIN cannot determine the usefulness of a sample for downstream experimentation without prior validation – a sample may not be useful for microarray experiments as it is too degraded but may be quite suitable for RT-PCR analysis [207].

In this study, the Bioanalyzer was used to confirm that extracted RNA was of sufficient quality to be utilized on the Affymetrix GeneChip arrays. RNA Nano 6000 chips were used to analyse RNA quality. The Nano chips have a qualitative range of 5 – 500 ng/ μ L for total RNA.

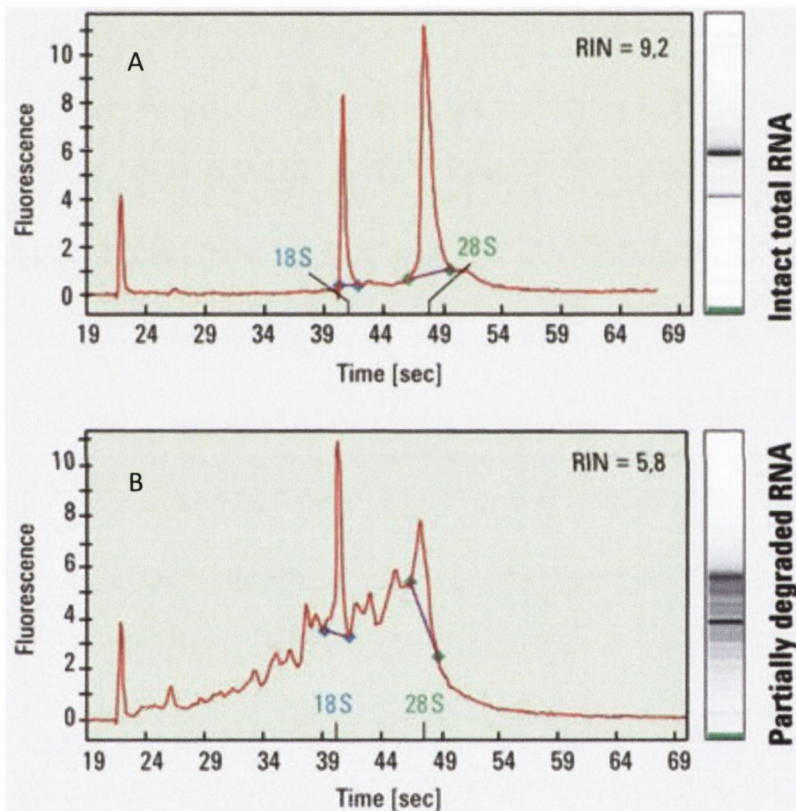


Figure 2.3. Electropherograms Produced from Analysis of RNA Samples by the Bioanalyzer Expert Software. Sample A is intact RNA with a corresponding RIN value of 9.2. Sample B is partially degraded, with multiple peaks in the various regions of the electropherogram.

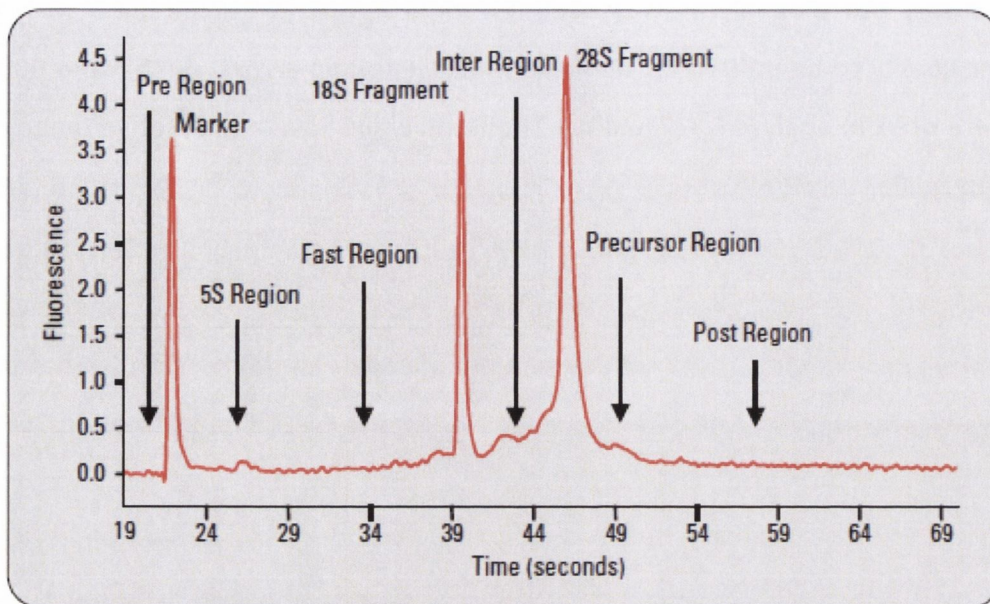


Figure 2.4. Regions of the Electropherogram Analysed by the Bionalyzer Expert Software to Generate a RIN value for RNA Samples. Rather than just analysing the 18S and 28S ratio, the software uses the entire electropherogram to calculate RIN.

2.6.3 Protocol

All reagents were brought to room temperature (dye was kept in the dark as it is light sensitive). The Bioanalyzer was switched on and the Expert software was loaded. The electrodes on the Bioanalyzer were cleaned using the electrode cleaning chips. One chip was filled with 350 μ L of RNase Zap (Ambion, US) and placed in the chip holder within the Bioanalyzer for 1 minute. The second chip was filled with 350 μ L of RNase free water and placed in the chip holder for 1 minute. The lid was opened for a few seconds to allow the water to evaporate from the electrodes and the chip was removed.

2.6.3.1 Preparation of the Ladder

The RNA ladder was transferred to an RNase-free vial and heat denatured for 2 mins at 70°C. Immediately afterwards the vial was cooled on ice and the ladder was aliquoted and stored at -70°C.

2.6.3.2 Preparation of Reagents

Nano Gel Matrix (550 μL) was filtered using spin filters centrifuged at 1500 g for 10 mins. This was then aliquoted into 65 μL aliquots and used within four weeks. The dye concentrate was vortexed thoroughly, spun down and 1 μL was added to 65 μL of filtered gel. This was then vortexed vigorously and centrifuged at 13,000 g for 10 mins.

2.6.3.3 Sample Loading

A new RNA 6000 Nanochip was placed in the chip priming station (Figure 2.5). Gel-dye mix (9 μL) was pipetted into the well marked **G**. The plunger was positioned at 1 mL and the chip priming station was closed. The plunger was pressed down until it was held by the clip. After 30 seconds, the clip was released and the plunger was pulled back to the 1 mL position. Gel-dye mix (9 μL) was added to the wells marked G. Five μL of the Nano marker was placed in all sample wells and the ladder well. One μL of the prepared ladder was added to the ladder well, while 1 μL of RNA sample was added to all the sample wells. The chip was vortexed for 1 minute at 2400 rpm and immediately run in the Bioanalyzer.

After use, the electrodes were cleaned as outlined above. The RNase Zap and water were removed from the electrode cleaning chips and the chips were stored for re-use.



Figure 2.5. Bioanalyzer Chip Priming Station. Chips are placed within the priming station and 9 μL of gel matrix is added to the specified wells. The chip is then primed and samples are loaded for running on the Bioanalyzer. (*from www.genomics.agilent.com*)

2.7 Affymetrix Human Gene 1.0 ST Arrays

Affymetrix Human Gene Arrays provide whole-transcript coverage of the genome. There are 128,869 genes represented, each covered by 26 probes which are spread over the length of the transcript. This is a significant advance over previous 3' oligo (dT)-based priming and labelling assays, as these only interrogate the base pairs closest to the 3' end of the gene. The 3' assays do not take into account splice variants, a phenomenon which is prominent in cancer biology [210]. This means that splice variants with identical poly-A tails and splice variants which lack a poly A tail will either be not differentiated or not detected at all (Figure 2.6).










Genomic locus		Classical 3' Assay	WT Assay
Presumed standard transcript		●	●
Transcripts with undefined 3' end			●
Non-polyadenylated messages			●
Truncated transcripts			●
Alternative polyadenylation sites			●
Degraded samples			●
Genomic deletions			●
Alternative splicing			●
Alternative 5' start sites			●

Figure 2.6. Differences in Gene Change Capture Between 3' Assay and WT Assays. The classical 3' assays can only detect changes in genes with a standard transcript and intact poly-A tail. It cannot detect transcripts lacking a poly-A tail or discriminate between alternative splice variants with identical poly-A tails.

The Affymetrix system uses a perfect match (PM) design with probes which bind to sense targets. Background is determined using 17,000 background probes [211]. The array design is based on the March 2006 human genome sequence assembly and has comprehensive coverage of the RefSeq and Ensembl transcripts [211]. The Human Gene Array used in this study has been shown to be in concordance with the Human Genome U133 Plus 2.0 and Human Exon arrays based on evaluation of true positive and false positive rates (Figure 2.7) [212]. This was examined using a Latin Square spike-in experiment, and a tissue mixture experiment. They showed high repeatability using Pearson's correlations and coefficient of variation. Pearson's correlations of 0.995 or higher were observed between the three array types [212].

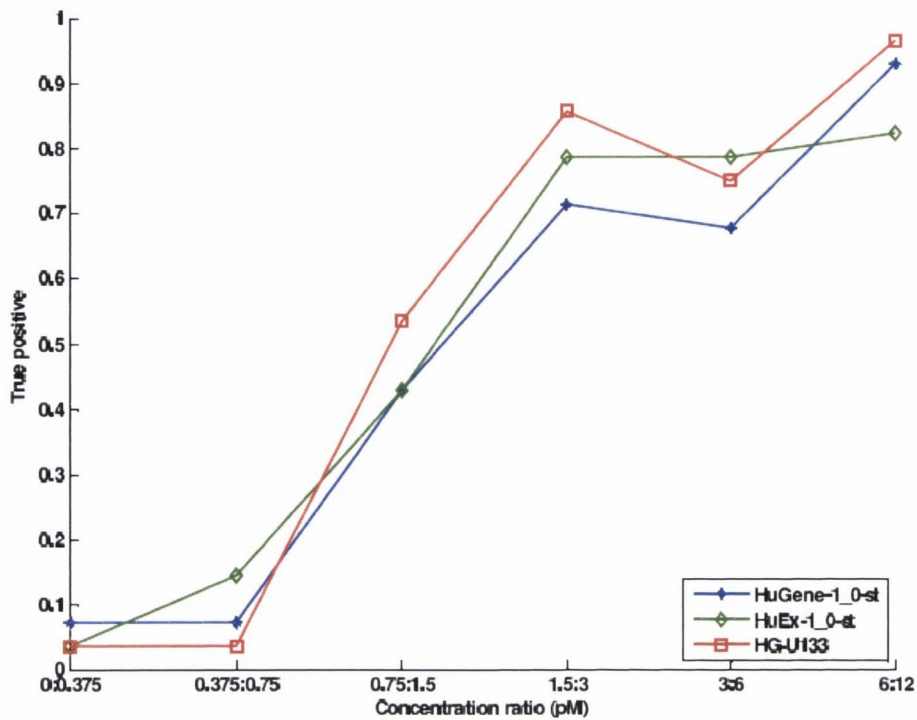


Figure 2.7. Comparison of Detection of Fold Changes of Gene Expression across Varying Concentrations of RNA. The three array types showed quite similar ability to detect changes in gene expression across a variety of starting RNA concentrations.

Synthesis of the GeneChip Arrays is based on a photolithographic method outlined by Pease *et al.* [213]. Synthetic linkers with photo-modifiable protected groups are attached to a glass substrate [214]. Light is then directed at a specific region of the substrate through a photolithic mask, resulting of deprotection of that area (Figure 2.8). Hydroxyl protected deoxynucleosides are incubated with the substrate which chemically couple with the area that has been deprotected. This is then repeated for other areas of the substrate.

the chip, washed, stained and finally scanned. Master mixes were prepared for each step of the protocol to improve reproducibility, enzyme solutions were flick-mixed and tubes were spun down before each PCR step.

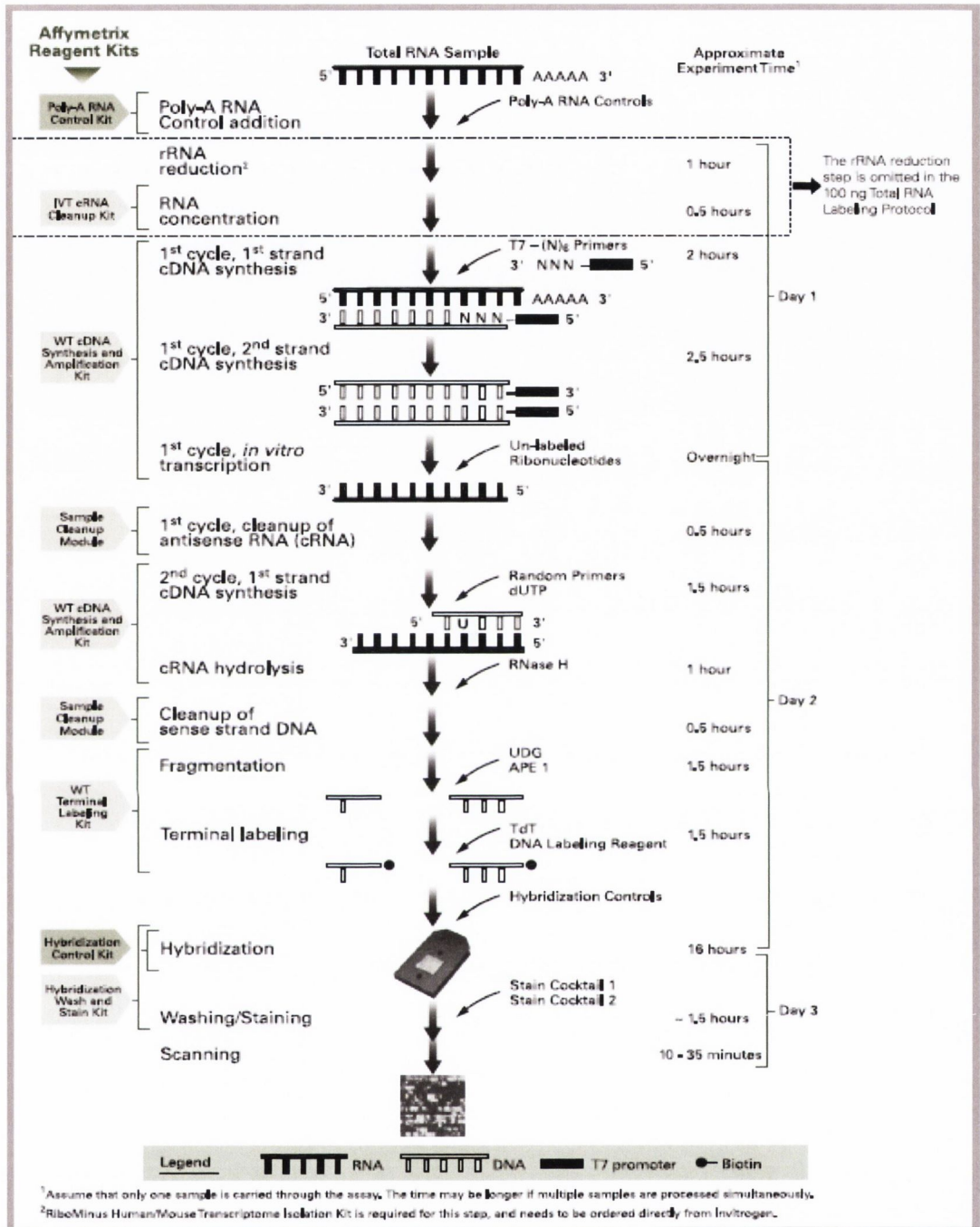


Figure 2.9. Outline of the Three Day Protocol for Array Analysis. The entire procedure is carried out over three days. On the first day, first and second strand cDNA are prepared followed by preparation of cRNA. On the second day, cRNA is purified and used to prepare second cycle cDNA which is then hydrolysed and purified. The cDNA is then fragmented and labelled. On the third day of the protocol, the cDNA is hybridised to the chip, washed and stained and finally scanned.

2.7.2 Preparation of Total RNA and Poly-A Controls

Affymetrix recommends using between 50 – 500 ng of RNA for each sample. For this study 300 ng of total RNA was used for each sample. Samples were quantified and Bioanalyzed before use. The Ambion WT Expression kit (Ambion, US) was used to prepare all samples used in this study. Poly-A RNA spikes were used as exogenous positive controls to monitor the target labelling process. The array chips contain probe sets for several *B. subtilis* genes which are absent in the eukaryotic genome – lys, phe, thr and dap. These controls are in vitro synthesised and premixed at staggered concentrations. The controls are amplified and labelled with the total RNA samples and the hybridization intensities of these controls on the arrays help to monitor the labelling process.

The Poly-A stock was serially diluted to provide the final concentrations listed in Table 2.4. The dilution factors for the control necessary to provide the final concentrations in Table 2.4 were calculated appropriately to the starting RNA concentration in this study. Poly-A control dilution buffer was used to dilute the stock. Two μL of the final dilution was added to each total RNA sample.

Table 2.4. List of Concentrations of Poly-A Controls. When diluted appropriately and added to the RNA samples, the Poly-A spikes have set final concentrations. The spikes are used as an exogenous control to the target labelling process.

Poly-A RNA Spike	Final Concentration (ratio of copy number)
Lys	1:100,000
Phe	1:50,000
Thr	1:25,000
Dap	1:6,667

2.7.3 First Strand cDNA Synthesis

Total RNA samples were primed using reverse transcription with primers containing a T7 promoter sequence. When prepared, the synthesised cDNA contains a T7 promoter sequence. Reagents were thawed at room temperature and the first strand master mix was prepared (Table 2.5). Each component of the master mix was added in sequence.

Table 2.5. First Strand cDNA Master Mix Components. Each component was added in sequence, with a 5% excess prepared to account for pipetting error.

First-Strand Master Mix Component	Volume for One Reaction (µL)
First-Strand Buffer Mix	4
First-Strand Enzyme Mix	1
Total Volume	5

The master mix was vortexed and spun down. Five µL of master mix was added to nuclease free sample tubes and 5 µL of RNA was added to the master mix. Total RNA (300 ng) was used for each sample. Poly-A controls accounted for 2 µL of the sample volume, therefore each total RNA sample was contained in 3 µL. If necessary, total RNA samples were diluted in nuclease free water to bring the final volume to 5 µL. Tubes were vortexed and spun down. They were incubated for 1 hour at 25°C, 1 hour at 42°C and 2 mins at 4°C in a thermal cycler with a heated lid. Following incubation, samples were centrifuged briefly and placed on ice for 2 mins.

2.7.4 Second Strand cDNA Synthesis

Single strand cDNA made in the first step was converted to double stranded cDNA and subsequently used as the template for transcription. DNA polymerase and

RNase H degraded RNA and synthesised second strand cDNA. Reagents were thawed on ice and the second-strand master mix was prepared (Table 2.6).

Table 2.6. Second-Strand Master Mix Components. Each component was added in sequence and a 5% excess was allowed for pipetting errors.

Second-Strand Master Mix Component	Volume for One Reaction (μL)
Nuclease-free Water	32.5
Second-Strand Buffer Mix	12.5
Second-Strand Enzyme Mix	5
Total Volume	50

The master mix was vortexed, centrifuged and placed on ice. Fifty μL of master mix was added to each first-strand cDNA sample and the tubes were flick mixed. The samples were spun down and incubated for 1 hour at 16°C, 10 mins at 65°C and 2 mins at 4°C in a thermal cycler with the lid off. Following incubation, the samples were spun down and placed on ice.

2.7.5 cRNA Synthesis by In Vitro Transcription

Antisense cRNA was synthesised and amplified using in vitro transcription (IVT) of the second strand cDNA template made in the previous step. T7 RNA polymerase is used to carry this out, based on the Eberwine method [215]. Reagents were thawed at room temperature and the IVT master mix was prepared in a nuclease free tube (Table 2.7).

Table 2.7. IVT Master Mix Components. Each component was added in sequence and 5% excess was allowed for pipetting error.

IVT Master Mix Component	Volume for One Reaction (μL)
IVT Buffer Mix	24
IVT Enzyme Mix	6
Total Volume	30

The master mix was vortexed, spun down and 30 μL was added to each second strand cDNA sample. These were mixed by gently vortexing, spun down and incubated for 16 hours at 40°C then overnight at 4°C in a thermal cycler with a heated lid. After the incubation the samples were spun down and placed on ice.

2.7.6 cRNA Purification

Purification was carried out to remove elements present which may have compromised RNA stability, such as salts, unincorporated nucleotides, and enzymes. Elution solution was preheated to 58°C for 10 mins. Ethanol (100%) was added to the nucleic acid wash solution concentrate. The nucleic acid binding beads were vigorously vortexed to ensure full dispersal. The cRNA binding mix was prepared for all samples (Table 2.8).

Table 2.8. cRNA Binding Mix Components. The components were added directly before the experiment, allowing 10% excess for pipetting error. Beads were vigorously vortexed before preparation.

cRNA Binding Mix Component	Volume for One Reaction (μL)
Nucleic Acid Binding Beads	10
Nucleic Acid Binding Buffer Concentrate	50
Total Volume	60

The cRNA Binding Mix was vigorously mixed and 60 μL was added to each sample. Each sample was transferred to a well of a U-bottom plate, and 60 μL of 100% isopropanol was added to each sample and pipetted up and down to mix. The plate was gently shaken for 2 mins on a plate shaker, to allow cRNA to bind to the nucleic acid binding beads. In addition, the samples were manually mixed by pipette for 3 mins to ensure thorough mixing of the beads and sample.

The plate was placed on a magnetic stand for 5 mins to capture the magnetic nucleic acid binding beads. The beads formed pellets against the magnets on the stands and the supernatant was discarded without disturbing the pellets. Nucleic acid wash solution (100 μ L) was added to each sample and the plate was placed on a plate shaker for 1 min. The beads were captured on the magnetic stand as previous. The supernatant was discarded and the beads were washed a second time in nucleic acid wash solution. The plate was placed on a plate shaker and shaken vigorously for 1 min or until all the liquid had evaporated, however care was taken not to over-dry the beads.

The prewarmed elution solution (40 μ L) was added to the purified cRNA and incubated at room temperature for 2 mins. The plate was vigorously shaken for 3 mins to disperse the nucleic acid binding beads and they were also manually pipetted to disperse. The beads were captured on the magnetic stand and the supernatant, which contained the eluted cRNA, was carefully removed and transferred to nuclease-free tubes which were placed on ice.

The cRNA yield was determined using a NanoDrop spectrophotometer before moving on to the next stage.

2.7.7 Second-Cycle cDNA Synthesis

The cRNA was reverse-transcribed to make sense-strand cDNA using random primers. This sense strand cDNA contains dUTP at a fixed ration relative to dTTP. The cRNA from the previous step was prepared to a final concentration of 10 μ g cRNA in 22 μ L of nuclease free water. Second cycle synthesis reagents were thawed and placed on ice.

In nuclease free tubes, 22 μ L of cRNA (containing 10 μ g) was combined with 2 μ L of random primers and mixed by gently vortexing. The sample was spun down and incubated for 5 mins at 70°C, 5 mins at 25°C and 2 mins at 4°C in a thermal cycler

with a heated lid. Following incubation the tubes were spun down and second cycle master mix was prepared (Table 2.9).

Table 2.9. Second-Cycle Master Mix Components. Each component was added in sequence and 5% excess was allowed for pipetting error.

Second-Cycle Master Mix Component	Volume for One Reaction (μl)
2 nd -Cycle Buffer Mix	8
2 nd -Cycle Enzyme Mix	8
Total Volume	16

The master mix was vortexed and spun down. Sixteen μL of master mix was added to each cRNA/random primers sample and mixed by gently vortexing. The sample was spun down and incubated in a thermal cycler for 10 mins at 25°C, 90 mins at 42°C, 10 mins at 80°C and for 2 mins at 4°C. Following the incubation, samples were centrifuged briefly and placed on ice.

2.7.8 RNase H Hydrolysis

The cRNA template is degraded by RNase H to leave single stranded cDNA.

RNase H (2 μL) was added to the second-cycle cDNA samples and they were mixed by pipetting and gently vortexing. The samples were centrifuged briefly and incubated in a thermal cycler with a heated lid for 45 mins at 37°C, 5 mins at 95°C and 2 mins at 4°C. Following the incubation, samples were spun down and placed on ice.

2.7.9 Second-Cycle cDNA Purification

This stage prepared the cDNA for fragmentation and labelling by removing enzymes, salts and any unincorporated dNTPs. Elution solution was heated to 58°C for 10

mins and the nucleic acid binding beads were vortexed vigorously before use to ensure they were fully dispersed.

The cDNA binding mix was prepared at room temperature (Table 2.10).

Table 2.10. cDNA Binding Mix Components. The components were added directly before the experiment, allowing 10% excess for pipetting error. Beads were vigorously vortexed before preparation.

cDNA Binding Mix Component	Volume for One Reaction (μL)
Nucleic Acid Binding Beads	10
Nucleic Acid Binding Buffer Concentrate	50
Total Volume	60

Nuclease-free water (18 μL) was added to each second-cycle cDNA sample. The cDNA binding mix was vigorously vortexed before adding 60 μL to each sample. Samples were pipetted up and down to mix and transferred to a well of a U-bottom plate. To each sample 120 μL of 100% ethanol was added and mixed by pipetting. The plate was gently shaken on a plate shaker for 2 mins to allow the cDNA to bind to the nucleic acid binding beads. In addition, the samples were mixed by pipetting for 3 mins to ensure thorough mixing of the sample and binding mix. The plate was placed on a magnetic stand to capture the beads for 5 mins. The supernatant was carefully discarded and 100 μL of nucleic acid solution was added to the beads. The plate was shaken for 1 minute and placed back on the magnetic stand to recapture the beads. The supernatant was discarded and the beads were washed a second time. The plate was shaken vigorously for 1 minute to evaporate residual ethanol from the beads without over drying the pellets. The cDNA was eluted using 30 μL of the prewarmed elution solution. The bead/elution solution mix was pipetted up and down to ensure thorough mixing and shaken for 3 mins. The beads

were captured on the magnetic stand and the supernatant was carefully transferred to nuclease free tubes and placed on ice.

The cDNA yield was determined using a NanoDrop spectrophotometer before moving on to fragmentation and labelling.

2.7.10 Fragmentation of Single-Stranded DNA

The Affymetrix GeneChip WT Terminal Labelling Kit was used for fragmentation and labelling of single-stranded DNA. The fragmentation reaction was set up in 0.2 mL strip tubes (Table 2.11) and the fragmentation master mix was prepared for all samples (Table 2.12).

Table 2.11. Fragmentation Reaction Components. Single-stranded DNA at a concentration of 5.5 μg was used for each sample, brought up to 31.2 μL with nuclease-free water.

Fragmentation Reaction Component	Volume for One Reaction
Single-stranded DNA	5.5 μg
RNase-free Water	Up to 31.2 μL
Total Volume	31.2 μL

Table 2.12. Fragmentation Master Mix Components. Fragmentation master mix was prepared for each sample.

Fragmentation Master Mix Component	Volume for One Reaction (µL)
RNase-free Water	10
10X cDNA Fragmentation Buffer	4.8
UDG, 10 U/µL	1.0
APE 1, 1,000 U/µL	1.0
Total Volume	16.8

The fragmentation master mix was added to each fragmentation reaction, flick mixed and spun down. The reactions were incubated at 37°C for 60 mins, 93°C for 2 mins and 4°C for 2 mins. Following incubation, the tubes were flick-mixed, spun down and 45 µL of sample was transferred to a new nuclease free tube.

2.7.11 Labelling of Fragmented Single-Stranded DNA

The labelling master mix (Table 2.13) was prepared before adding 15 µL to each of the fragmented DNA samples.

Table 2.13. Labelling Master Mix Components. The components were prepared in a master mix before adding 15 µL to the fragmented DNA samples.

Labelling Master Mix Component	Volume for One Reaction (µL)
5X Tdt Buffer	12
TdT	2
DNA Labelling Reagent, 5 mM	1
Total Volume	15

The samples were flick mixed, spun down and incubated for 60 mins at 37°C, 10 mins at 70°C and 2 mins at 4°C.

2.7.12 Hybridization

The Affymetrix GeneChip Hybridization, Wash and Stain Kit was used for this step. A hybridization cocktail master mix was prepared for each sample in a 1.5 mL RNase-free tube (Table 2.14). The stocks of the eukaryotic hybridization controls were heated to 65°C for 5 mins to ensure they were completely resuspended before aliquoting. Once prepared, 73 µL of the master mix was added to 27 µL of the fragmented and labelled DNA (~25 ng/µL).

Table 2.14. Hybridization Cocktail Master Mix. The master mix was prepared for all samples and added to the fragmented labelled DNA.

Hybridization Cocktail Master Mix Component	Volume for 169 Format Array (µL)	Final Concentration
Control Oligonucleotide B2 (3 nM)	1.7	50 pM
20X Eukaryotic Hybridization Controls (bioB, bioC, bioD, cre)	5	1.5, 5, 25 and 100 pM, respectively
2X Hybridization Mix	50	1X
DMSO	7	7%
Nuclease-free Water	up to 73	
Total Volume	73	

The tubes were flick-mixed and spun down. The hybridization cocktail containing the samples were heated to 99°C for 5 mins, cooled to 45°C for 5 mins and centrifuged at maximum speed for 1 minute. Arrays were equilibrated to room temperature immediately before use and labelled with the name of the sample.

The array format used in this study was '169', therefore 80 μ L of the fragmentation mix was injected into the septa on each GeneChip (Figure 2.10). A pipette tip was used to vent air from the hybridization chamber and care was taken to ensure the bubble in the hybridization chamber floated freely upon rotation – this was to allow the hybridization cocktail to make contact with all portions of the array. The array was placed in 45°C in a hybridization oven at 60 rpm for 17 hours.

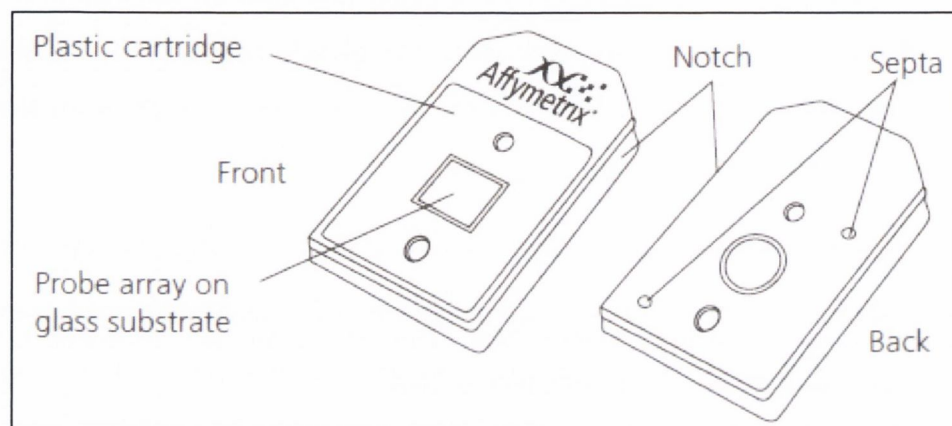


Figure 2.10. Affymetrix GeneChip Array. The sample is introduced to the probe array by pipetting through one of the septa on the back of the chip. Air is vented by placing a pipette tip in the other septum on the back of the chip. A bubble should be seen to float freely in the glass panel on the front of the chip to ensure that the hybridization cocktail can contact the entire hybridization surface.

2.7.13 Set-up of Fluidics Station and Scanner

Sample files were created using the Affymetrix GeneChip Command Console (AGCC) software for all samples to be run. The fluidics station was then set up using the AGCC software and primed to ensure all lines contained the correct fluids before beginning the staining process.

2.7.14 Array Staining

The arrays were removed from the hybridization oven and the hybridization cocktail was removed through one of the septa on the chip, while venting air through the

other septum as previous. The hybridization cocktail was stored at -20°C so that in the event that the hybridization did not occur correctly, the hybridization cocktail could be re-hybridized to a new array. The array was filled with 100 µL of Wash Buffer A and kept at room temperature. The fluidics station is capable of staining four arrays at one time. Additional arrays were kept in 4°C for up to four hours, and re-equilibrated to room temperature before staining. The staining reagents were prepared for the four arrays, taking care not to expose Stain Cocktail A to light as it is light-sensitive. All vials were spun down to remove air bubbles which may interfere with the staining process. The AGCC fluidics control software was used to program the wash stations within the fluidics station. The arrays were inserted into the wash blocks in each wash station and the on-screen instructions for loading the staining solutions were followed.

2.7.15 Array Scanning

Following staining, the arrays were removed from the wash stations and checked for air bubbles. If no bubbles were present they were moved directly to the scanner. If air bubbles were present, they were replaced in the wash blocks and the on-screen instructions were followed to remove the bubbles. The scanner was switched on and allowed to warm up for 10 minutes. If any dust or dirt was present on the glass surface of the array it was gently removed using tissue, and the septa were covered using small 'tough-spot' stickers. The arrays were placed in the scanner and the AGCC scanner control software was used to begin the scanning process. Following scanning, the arrays were removed from the scanner and stored.

2.8 Taqman® Real-Time PCR

2.8.1 Principle

Polymerase chain reaction (PCR) is a technique in which a small amount of nucleic acid can be amplified. It was initially described in the 1980's [216], [217] and is used almost worldwide today. Amplification is achieved by use of two primers – short

sequences of nucleic acid complimentary to the regions surrounding the sequence of interest – and enzymatic activity. The two primers first anneal to the nucleic acid, and an enzyme then synthesises a new nucleic acid strand complimentary to the sequence of interest [216]. This is then repeated many times, resulting in huge amplification of relatively small amounts of nucleic acid. The Klenow fragment of *Escherichia coli* DNA polymerase I was the initial enzyme used, however it was not ideal as it needed to be replenished after each cycle of amplification [218]. Use of DNA polymerase from *Thermus aquaticus* (*Taq*) was a marked improvement over *E coli* [218]. Holland *et al.* were able to improve again on the technique of PCR by utilising the intrinsic exonuclease activity of *Taq* polymerase to cleave a fluorescent probe bound to the amplified sequence, thus providing a signal for detection of the product [218].

The probe is made up of an oligonucleotide with a fluorescent reporter molecule at the 5' end and an internal quencher molecule [219]. Taqman probes contain Minor Groove Molecules which ensure the probe melting temperature (T_m) is at least 10°C higher than the primers to ensure that the probe hybridizes before the primers and remains hybridized during annealing. When excited by irradiation, the reporter molecule will fluoresce, however, when the probe is intact, the reporter is suppressed by the quencher via fluorescent energy transfer (FET) [219]. During PCR, the exonuclease activity of *Taq* polymerase releases the reporter molecule from the probe. It is now able to fluoresce and serves as an indicator that amplification of the target sequence has occurred (Figure 2.11) [219].

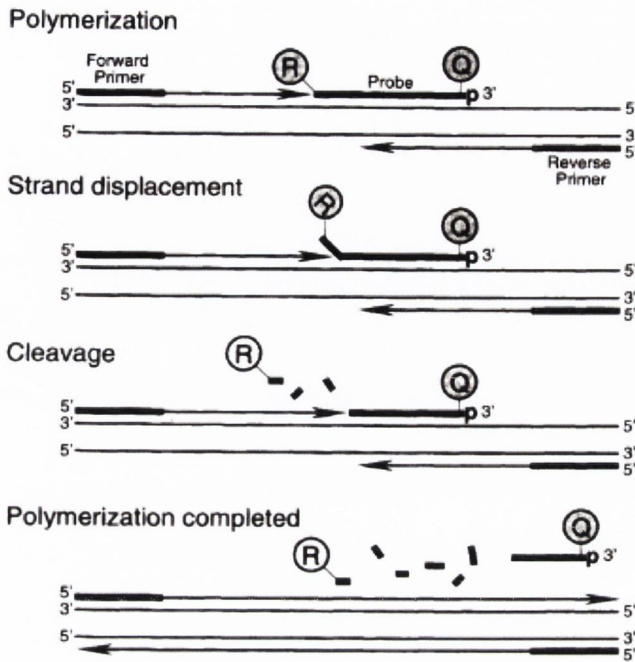


Figure 2.11. Overview of the Taqman® PCR Process. A fluorescent reporter and quencher dye are present on the Taqman® probe. The reporter dye is quenched due to the proximity of the dyes. During PCR, Taq polymerase cleaves the reporter dye from the probe. It can now fluoresce, and serves as a measure of PCR product accumulation.

2.8.2 Procedure

2.8.2.1 cDNA Synthesis

cDNA was made from the extracted RNA using the High Capacity RNA-to-cDNA kit (ABI, USA). A master mix was made up for all samples (Table 2.15) and 11 μL aliquoted into 0.2 mL PCR tubes (Fisher Scientific, Ireland). The desired concentration of RNA was added in a volume of 9 μL , diluted in nuclease free H_2O (Fisher Scientific, Ireland) as necessary.

Table 2.15. Components of Reverse Transcription Master Mix.

RT Master Mix Component	Volume for One Reaction (μL)
Reaction Buffer	10
Enzyme	1

The samples and master mix were placed on ice until placed in a thermocycler (9700, ABI, USA) at 37°C for 60 mins, 95°C for 5 mins and a 4°C hold. The cDNA was then stored at -20°C until use.

2.8.2.2 Taqman® PCR

Taqman® PCR was carried out using Applied Biosystems Universal Master Mix II (without UNG, uracil-DNA glycosylase) and Gene Expression Assays. The master mix contains the DNA polymerase necessary for amplification. Applied Biosystems Gene Expression Assays contain both the primers and the MGB probe.

A master mix for all samples was prepared for each assay and 9 μl aliquoted onto 96-well fast plates (Table 2.16, ABI, USA).

Table 2.16. Components of Taqman® Master Mix

Taqman Master Mix Component	Volume for One Reaction (μL)
Universal Master Mix II	5
Gene Expression Assay	0.5
Nuclease-free H ₂ O	3.5

One μL of cDNA was added to each reaction. An endogenous control and a no template control (NTC) for each assay were run on every plate. All samples and controls were run in triplicate for each assay. The plates were sealed using optical adhesive film (ABI, USA) and centrifuged briefly to remove bubbles and ensure the reaction mixture was at the bottom of the plate. The plates were run on an ABI Fast

7500 at the following conditions – hold 95°C for 10 mins and 40 cycles x 95°C for 15 sec followed by 60°C for one minute. Following the run, the data was analysed using Data Assist software (v.3.0, ABI, USA) and Microsoft Excel.

2.8.2.3 Data Analysis

There are two main analytical methods employed for quantifying gene expression – absolute quantification, in which a gene’s expression level can be extrapolated by comparing it to a known quantity from a standard curve, or through digital PCR; or relative quantification, in which a gene’s expression level is calculated relative to that of a reference sample, or calibrator. For this study, relative quantification was used to calculate all gene expression levels, by the $2^{-\Delta\Delta CT}$ method.

During PCR, repeated cycles of primer/probe annealing and enzymatic activity result in amplification of the gene product of interest. There are three stages to any PCR reaction [220]. Stage 1 is the exponential phase, where product occurs rapidly and there are unlimited reagents. Stage 2 is the linear phase, where product accumulates, and reagents are starting to become limited, while stage 3 is the plateau, where new product is no longer formed due to depletion of the necessary reagents. A sample’s C_T is the threshold cycle value, the intersection between the sample’s amplification plot and the threshold, which is set as a significant level of fluorescence above baseline. The threshold should be set within the exponential phase of all amplification plots in the study (Figure 2.12) [221].

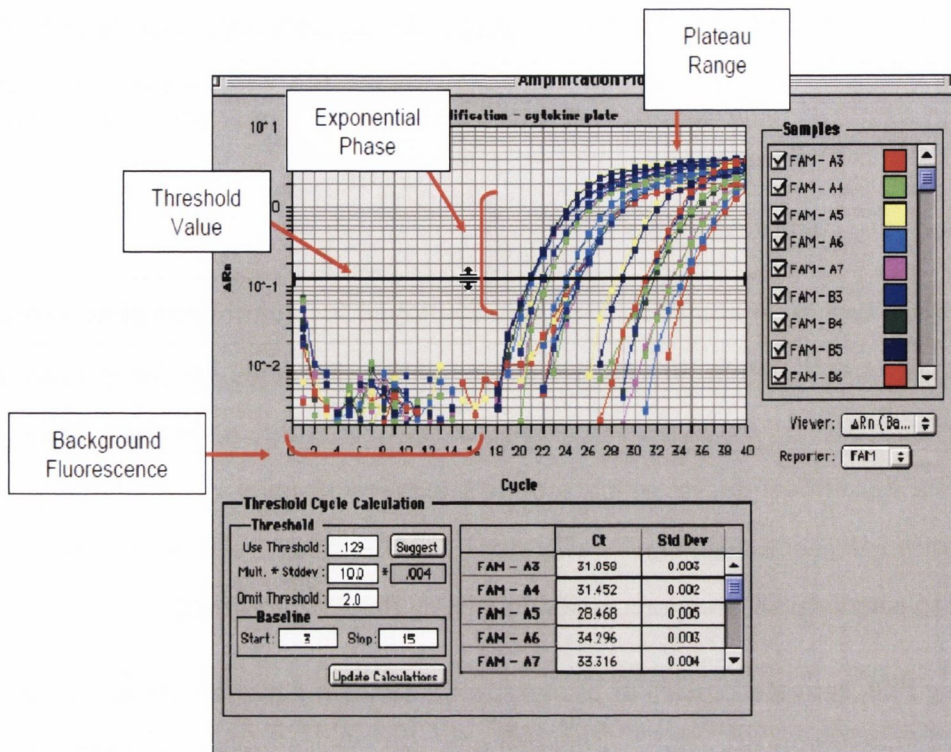


Figure 2.12. Setting the Threshold for PCR Reactions. The threshold should be set within the exponential phase of the amplification plots, while clearing any background fluorescence. This is the point at which a sample’s fluorescence is determined to be significantly different from background (From Applied Biosystems [221]).

2.8.2.3.1 The $2^{-\Delta\Delta CT}$ Method

The $2^{-\Delta\Delta CT}$ method (Comparative C_T method) of relative quantitation was described by Livak *et al.* in 2001 [222]. This method is based on the assumption that the amplification efficiencies of the target gene and the endogenous control should be almost equal.

For each sample in the study, the C_T values of the three replicates were obtained for both the target gene and the endogenous control gene. Any replicate which was an obvious outlier was removed from analysis, and a minimum of two replicates were averaged for each sample.

For each sample:

$$\Delta C_T = C_{T_test} - C_{T_endogenous\ control}$$

The calibrator was determined as the sample/sample group that other samples were compared to. For a group of samples, the ΔC_T value for each sample was averaged to provide the calibrator value ($\Delta C_{T_calibrator}$). A $\Delta\Delta C_T$ value was determined for each sample whose gene expression was to be quantified (test).

$$\Delta\Delta C_T = \Delta C_{T_test} - \Delta C_{T_calibrator}$$

This was then fitted into the following equation in order to calculate a fold-change in gene expression relative to the calibrator:

$$\text{Relative quantity} = 2^{-\Delta\Delta C_T}$$

2.9 Protein Extraction

2.9.1 Protein Extraction in Normoxia

Protein was extracted from both cell lines using a modified RIPA (radioimmunoprecipitation) buffer which was supplemented with protease and phosphatase inhibitors and phenylmethanesulfonylfluoride, PMSF, a serine protease inhibitor (Table 2.17). Spent media was removed and cells were washed twice using ice-cold PBS. Cells were scraped into 5 mL ice-cold PBS and transferred to a cold 50 mL centrifuge tube. The flasks were rinsed in ice-cold PBS and this was transferred to the centrifuge tube. The cells were collected by centrifuging at 4000 rpm for 10 mins at 4°C after which the PBS was decanted and the cells were lysed using ice-cold lysis buffer (Table 2.17). Only sufficient lysis buffer to lyse the cells was added to the pellets to ensure full cell lysis but not diluting the protein too much. The lysate was kept on ice and vortexed every 5 mins for 20 mins. The lysate

was then centrifuged at 14,000 rpm for 15 mins. The supernatant was transferred to ice cold eppendorfs and stored at -20°C.

Table 2.17. Modified RIPA used for Protein Extractions.

Component	Source	Volume for 1 mL total Volume (μL)
RIPA IX	Sigma-Aldrich, UK	975
Protease Inhibitor 1%	Sigma-Aldrich, UK	10
Phosphatase Inhibitor 1%	Sigma-Aldrich, UK	10
PMSF 2 mM	Sigma-Aldrich, UK	5

2.9.2 Protein Extraction in Hypoxia

The protocol was identical to the protocol for protein extraction in normoxia with a couple of exceptions. The PBS used to scrape and collect cells was kept in the hypoxia chamber overnight prior to the extraction to allow it to equilibrate. Approximately one hour before extracting protein, an aliquot of PBS was removed from the chamber and placed on ice. Lysis buffer was also allowed to equilibrate in the chamber for at least two hours prior to the extraction, and placed on ice before extracting the protein. The protease inhibitor, phosphatase inhibitor and PMSF were added to the lysis buffer immediately before use. Cells were collected in PBS within the hypoxia chamber and taken out in a closed tube to centrifuge. After centrifugation, the cells were returned to the chamber where the PBS was decanted and the lysis buffer added.

2.9.3 Protein Quantification with the BCA Assay

2.9.3.1 Principle

This colorimetric assay is based on the reduction of Cu^{2+} to Cu^{1+} by protein in an alkaline solution [223] by certain amino acid residues [224]. The Cu^{1+} is then detected using bicinchoninic acid (BCA). A purple reaction product is formed by chelation of two molecules of BCA with one Cu^{1+} . This product absorbs at 562 nm in a linear fashion with increasing protein concentrations. A set of protein standards is prepared and assayed and the protein concentration in the samples are reported relative to the standard curve.

2.9.3.2 Protocol

A set of protein standards were prepared by using a BSA stock vial containing 2,000 $\mu\text{g}/\text{mL}$ BSA which was serially diluted with deionized water (Table 2.18). The BCA working reagent was prepared fresh for each determination. The working reagent was prepared by mixing 50 parts of Reagent A with 1 part of Reagent B to yield a clear green solution.

Ten μL of each standard/sample was pipetted in duplicate in the wells of an ELISA plate (Nunc, Thermofisher, Denmark). To this, 200 μL of the working reagent was added, and the plate was covered and shaken on a plate shaker for 30 seconds. The plate was then incubated at 37°C for 30 mins, cooled and read on a plate reader (Dynex Technologies, US) at 550 nm. The working range of the assay was 125 – 2,000 $\mu\text{g}/\text{mL}$. The standard curve was analysed and sample protein concentrations were quantified relative to the curve using Revelation software (Dynex Technologies, US).

Table 2.18. Concentrations of BSA in the BCA Assay Standards. A stock of BSA was serially diluted to give a range of concentrations used to make a standard curve. The protein concentration of each sample was then given relative to the standard curve.

Vial	Volume Diluent (Water) (μL)	Volume and source of BSA (μL)	Final BSA Concentration ($\mu\text{g}/\text{mL}$)
A	0	300	2,000
B	125	375	1,500
C	325	325	1,000
D	175	175 of Dilution B	750
E	325	325 of Dilution C	500
F	325	325 of Dilution E	250
G	325	325 of Dilution F	125
H	400	100 of Dilution G	25
I	400	0	0

2.9.4 Western Blots

2.9.4.1 Rig Set-up

Western blots were carried out on 12% gels. Separating and stacking gels (Table 2.19) were prepared and poured freshly for each experiment. Separating gels were poured and left to set for 30 mins. Once set, stacking gels was poured on top of the separating gel and a comb placed between the plates. Once set, the comb was removed and the gel was placed in the rig. Care was taken to ensure they were tightly locked in to prevent any leaking of running buffer (Table 2.20). Once they were in the gel rig they were placed in the tank and running buffer was poured between the plates. The rig was left for 5 mins and checked for any evidence of leakage. Extra running buffer was poured into the tank to ensure the gels remained in full contact with it during electrophoresis.

Table 2.19. Components of Separating and Stacking Gels for Western Blot. Gels were made up of acrylamide, tris buffer, distilled water, SDS (sodium dodecyl sulphate), AMPS (ammonium persulphate) and TEMED (N, N, N', N' tetramethylethylenediamine).

Gel	Acrylamide (40%)	Tris 1.5M pH 8.0	Tris 0.5M pH 6.5	H ₂ O	SDS (10%)	AMPS (10%)	TEMED
Separating (12%)	4.8ml	4.0 mL	0.0 mL	5.4 mL	160 µL	80 µL	16 µL
Stacking (4%)	800µl	0.0 mL	2.0 mL	5.12 mL	80 µL	40 µL	8 µL

2.9.4.2 Sample Preparation and Loading

Protein samples were thawed and diluted as necessary to load 30 µg of protein/lane. Ten µL of protein was mixed with 2 µL of 6X loading buffer (Table 2.20) and boiled at 95°C for 3 mins. The lanes of the rig were gently rinsed with running buffer. A molecular weight marker (Biorad, Ireland) was loaded (5 µL) in the first lane of each gel. Samples (12 µL final volume) were loaded in each lane and the rig was connected to the power pack (Biorad, Ireland). The gel was run at 100 V for 90 mins until the proteins had separated adequately and had run the length of the gel.

Table 2.20. Components of Electrophoresis Running Buffer. Contents of 500 mL of 5X buffer, pH 8.3.

Running Buffer Component	Concentration	Weight/Volume
Tris Base	0.125 M	7.56 g
Glycine	0.96 M	36.03 g
SDS	0.5%	25 mL
Distilled water		475 mL
Total Volume		500 mL

Table 2.21. Components of 6X Laemmli (Loading) Buffer.

Component	Weight/Volume
Sodium Dodecyl Sulphate	1.2 g
Bromophenol Blue	6 mg
Glycerol	4.7 mL
Tris 0.5 M pH 6.8	1.2 mL
Distilled water	2.1 mL
Dithiothreitol	0.93 g

2.9.4.3 Wet Transfer

A wet transfer method was used from protein transfer from the gels to nitrocellulose membranes (Biorad, Ireland). Filter paper (Whatman, UK) and foam sponge pieces were pre-soaked in cold transfer buffer (Table 2.22) before running. The gels were removed from the plates and nitrocellulose soaked in transfer buffer was applied to the gels. The gels were sandwiched between layers of sponge and filter paper in the transfer apparatus before placing them within the transfer rig. The tank was filled with transfer buffer and connected to the power pack. The samples were transferred for 90 mins at 100 V. An ice pack was placed within the tank to prevent overheating of the transfer apparatus, and changed after 45 mins. Once transfer was complete, the membranes were removed and stained with Ponceau S (Sigma-Aldrich, UK) for one minute to check that transfer had completed successfully and to check for even protein loading between lanes. The ponceau stained membranes were photographed (Las 4000 Luminescent Image Analyser, Fujifilm, UK) before continuing.

Table 2.22. Components of Transfer Buffer. Contents of 1X Transfer Buffer, pH 8.2, stored at 4°C.

Transfer Buffer Component	Volume/Weight
Tris	6.06 g
Glycine	28.8 g
Methanol	400 mL
Distilled water	1600 mL
Total volume	2 L

2.9.4.4 Blocking and Antibody Staining

The membranes were blocked using 5% skimmed milk in PBS (Oxoid, Thermofisher, Denmark) 0.1% Tween (Sigma-Aldrich, UK) (PBST) for 2 hours on an orbital shaker (Stuart Scientific, UK) at 4°C for 2 hours. Primary antibodies were made up in 5% skimmed milk in PBST to the desired concentration. Blocking milk was poured off and the antibody was applied to the membranes. They were incubated overnight at 4°C on the orbital shaker. Following the overnight incubation, the primary antibody was removed and stored at -20°C. The membranes were washed 3 times for 10 mins each with wash buffer (Table 2.23). The secondary antibody was made up to the desired concentration in 3% skimmed milk in PBST and incubated with the membranes at room temperature on the orbital shaker for 1 hour. The membranes were washed again 3 times for 10 mins each.

Table 2.23. Components of Wash Buffer.

Component of Wash Buffer	Volume
PBS	500 mL
0.3% Tween	1.5 mL
Total volume	~500 mL

2.9.4.5 Detection

Luminol (Santa Cruz, US) was prepared and incubated with the blot for 1 minute, manually rotating the blot so that it was entirely covered. The blot was brought to the developer. A light image was taken of the blots to ensure correct focusing before taking chemiluminescent images. Exposures were taken every 10 seconds for one minute, every minute for 5 mins and every 5 mins for 15 mins. If no signal was detected, Amersham ECL Advance (GE Healthcare, UK) was used in the same manner as luminol to enhance the image detection.

2.9.4.6 Control Antibody

After detection of the chemiluminescent image, blots were blocked in skimmed milk for 2 hours and reprobbed with β -actin antibody (Sigma-Aldrich) overnight at 4°C. They were washed as previous and incubated with a secondary antibody conjugated to alkaline phosphatase (AP) for one hour at room temperature. They were washed again and the antibody was detected using an AP-specific detection system, to avoid detection of signal from the previous target.

Chapter 3

Hypoxia Induces Chemoresistance in
an Ovarian Cancer Cell Line Model

3.1 Introduction

3.1.1 Chemoresistance

Chemoresistance is a phenomenon in which tumour cells do not respond to the action of chemotherapy drugs. It is observed in many cancer types including breast [225], pancreatic [226], prostate [227], colon [228] and ovarian [229]. It is a significant problem facing medical oncologists, as chemoresistance inevitably leads to a poorer outcome for their patients. Chemoresistance can be intrinsic i.e. the tumour cells are resistant before they ever receive chemotherapy, or it can be acquired – following a successful chemotherapy regimen, recurrent tumour cells are no longer sensitive to drug treatments. Intrinsic chemoresistance has been linked to tumour cell interactions with stroma [230] and has been observed in up to half of breast cancer patients [231] and approximately a fifth of ovarian cancer patients [128]. Acquired chemoresistance has been linked to a myriad of genetic cellular changes including heightened expression of the multidrug resistance protein P-glycoprotein [232], alternative splicing of mRNA transcripts [233], DNA methylation [234] and hypoxia [235]. There is an on-going search for biomarkers which may shed light on mechanisms of chemoresistance, and lead to development of novel therapies and personalized drug regimens.

3.1.2 Models of Chemoresistance

In order to effectively study how chemoresistance occurs, it is necessary to have appropriate models of chemoresistance to work with. There are many cell and animal models of chemoresistance in the literature. It is important to understand how chemoresistance is achieved in these models in order to understand how experimental procedures are influencing this, and thus thorough characterization of these models is essential [236]. Models of chemoresistance have been developed for many cancer types such as liposarcoma [237] hepatocellular carcinoma [238] and ovarian carcinoma [236]. In this study a cisplatin resistant ovarian carcinoma model was used. The A2780 cell line was established from tumour tissue from an

untreated patient. The cisplatin-resistant derivative, A2780cis was established by growing the A2780 cells in increasing stepwise concentrations of cisplatin and was initially characterised in 1987 [239]. This model has since been used in a variety of studies in determining the activity and resistance profiles of novel platinum and non-platinum agents in ovarian cancer [240-243]. It has also been used to investigate mechanisms of platinum resistance such as cellular drug efflux [244,245], micro RNAs (miRNAs) [246] and, in a recent publication by our group, platelet adhesion [58]. A2780cis have also been shown to be carboplatin-resistant [240,247]. Carboplatin is the platinum drug received by most ovarian cancer patients in first line therapy due to the reduced levels of toxicity associated with it compared to cisplatin [248], however, cisplatin resistance is more commonly studied in terms of ovarian cancer with three times as many articles published in relation to cisplatin. Cisplatin is also used in the treatment of advanced ovarian cancer as well as in the treatment of many other cancers including lung, oesophageal, testicular and advanced bladder cancer, thus determining methods of resistance to cisplatin is not just applicable to ovarian cancer but to a wide range of malignancies.

3.1.3 Cisplatin

Cisplatin (Figure 3.1) is an inorganic platinum agent which forms intra- and inter-strand crosslinks in GC-rich regions of DNA [249]. When these links are not repaired, it causes the cell to arrest and enter apoptosis. When cisplatin is administered, it is transported in the blood bound to plasma proteins [250]. Once it has arrived at the cell membrane, its uptake is mediated through the copper transporter CTR1 [251]. Chloride (Cl⁻) concentrations within the cell facilitate the release of Cl⁻ groups from cisplatin and their replacement with water. The major DNA adducts formed by cisplatin are 1,2 intra-strand cross-links with adjacent guanine nucleotides and to a lesser extent adenosine-guanine adducts [252]. These adducts affect cellular functioning in two ways. Firstly, they inhibit normal replication of DNA by preventing DNA polymerase from functioning [253] leading to collapse of the replication fork. Secondly, these lesions are detected by ATM and ATR kinases

which phosphorylate intermediates Chk1 and Chk2 [254]. Chk1 and Chk 2 then phosphorylate and activate p53 leading to apoptosis [254].

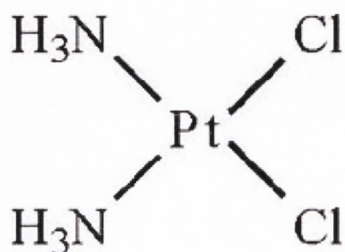


Figure 3.1. Structure of Cisplatin. Cisplatin is an octahedral Platinum (IV) complex. Only the *cis* isomer (pictured) has cytotoxic abilities. The *trans* isomer, in which a chloride and amine group are interchanged does not have the same functionality as cisplatin.

3.1.4 Cisplatin Resistance

Cisplatin resistance is mediated through several different mechanisms. These can be categorized into mechanisms which reduce the amount of drug entering the cell, mechanisms which reduce the activity of the drug within the cell, and mechanisms which increase the amount of drug pumped out of the cell.

3.1.4.1 Reducing Cisplatin Entry

Reduced accumulation of cisplatin in cancer cells is thought to be one reason for resistance [255]. For a long time, cisplatin was thought to enter cells passively [249]. However, studies in the yeast *Saccharomyces cerevisiae* have demonstrated that the copper transporter γ CTR1 was also responsible for cisplatin transport into the cell [256]. Furthermore, reduced expression of CTR1, has been associated with reduced cisplatin uptake in a cisplatin-resistant small cell lung cancer model [255]. Conversely, transfection of these cisplatin-resistant cells with CTR1 was shown to

increase cisplatin uptake [255]. *In vitro* experiments using small cell lung cancer cell lines have shown cisplatin resistant cells to express lower levels of CTR1 mRNA and that these cells had a reduced uptake of cisplatin compared to cells with high levels of CTR1 expression [255]. Low expression of CTR1 in ovarian tumour specimens has been linked to resistance to platinum chemotherapy and faster progression of disease [257].

3.1.4.2 Reducing Cisplatin Effectiveness Within the Cell

Once inside the cell, cisplatin can bind to proteins such as glutathione and metallothioneins, and it is thought that once bound to these molecules, cisplatin is rendered inactive [258]. Indeed, *in vitro* studies have shown an association between cisplatin resistance and increased intracellular glutathione concentration [259,260]. Clinical studies have shown high expression of glutathione-s-transferase, an enzyme which catalyses the detoxification of compounds by glutathione, to be associated with poorer survival in ovarian cancer patients [261]. Low expression of metallothionein and thioredoxin, another redox protein, has been associated with better overall survival and longer progression free survival in ovarian cancer patients [262], while high expression of glutathione peroxidase 3 has been observed in ovarian clear cell carcinoma [263], a type of ovarian cancer noted for resistance to platinum chemotherapy [94].

As the principal action of cisplatin is to create apoptosis-inducing lesions in DNA, another method by which cells circumvent its action is to step up DNA repair mechanisms. This allows the cell to simply repair the damage inflicted by cisplatin and to continue to divide. Several different mechanisms are involved in the repair of cisplatin-generated lesions including homologous recombination, nucleotide excision repair and mismatch repair. Homologous recombination (HR) is a technique used by cells to repair double stranded breaks in DNA. HR is a complex process, in which a protein complex containing Rad50 recognises the break in DNA and recruits another protein complex containing other members of the Rad family which then

catalyses the repair process [264]. Inter-strand cross links formed by cisplatin can be repaired using nucleotide excision repair (NER). In this process, a protein complex containing XPF and ERCC1 facilitates excision of the cross linked region, and allows full repair of the site by HR [264]. Ovarian cancer patients harbouring mutations in BRCA1/2 are often more sensitive to platinum-based therapy, as these proteins are important players in the HR process [265]. Interestingly, secondary acquired mutations in BRCA1/2 which render them active again have been linked to chemoresistance in ovarian cancer [266].

3.1.4.3 Increasing Cisplatin Efflux

Several different membrane transporters have been implicated in cisplatin resistance through increasing drug efflux from the cell. The ATPase copper transporters ATP7A and ATP7B have been associated with cisplatin resistance [267]. Increased levels of ATP7A have been linked with cisplatin resistance in ovarian cancer cell lines [268] and poorer outcome in ovarian cancer patient samples [269]. Recently, a novel transporter, LAPT4B, was shown to be associated with cisplatin resistance both through interaction with the multi-drug resistance gene, P-glycoprotein and through activation of the Akt signalling pathway [270].

3.1.4.4 Hypoxia and Cisplatin Resistance

Hypoxia has been shown to induce resistance to cisplatin in a number of different cell types. In a glioma cell line, cells became 2 – 3-fold more resistant to cisplatin following exposure to hypoxia for 24 hours [186]. In testicular germ cell carcinoma, cells became 2 – 8-fold more resistant to cisplatin following treatment with the drug in hypoxia for 72 hours [191]. A study using colon carcinoma cell lines showed that cisplatin resistance was only induced under hypoxia in a cell line containing mutated p53 and a functioning DNA repair response, thus highlighting the importance of p53 in the hypoxic response to cisplatin [187]. Repeated exposure to hypoxia which leads to cisplatin resistance has been linked to up-regulation of BCL-XL, an anti-apoptotic protein [271]. Hypoxia has also been shown to increase expression of P-

glycoprotein [272] and other multidrug resistance genes [273]. It has also been shown to enhance the Akt signalling pathway, which has been implicated in chemoresistance in a number of cancers [273]. Cisplatin resistance induced by hypoxia has also been linked to a number of other molecular markers such as PIM-1, a kinase which regulates apoptosis and the cell cycle [274], DRP1, a dynamin family protein which is involved in organelle fission [275], STAT3, a signalling protein [189], NFκB, a transcription activator [276], ERCC1 a DNA repair protein [277], CBR1, a carbonyl reductase enzyme [278] and CycB, a chaperone protein [279]. Autophagy induced by hypoxia has also been implicated as a resistance mechanism to cisplatin treatment [280]. Thus hypoxia has been linked to cisplatin resistance through a wide variety of different cellular adaptations, and is an important player in chemoresistance of solid tumours such as ovarian cancer. Furthermore, knockdown of HIF-1α has been shown to increase sensitivity of cells to cisplatin in a number of cell lines including malignant glioma [281], oral squamous cell carcinoma [188] and fibrosarcoma [178]. Hypoxia-induced cisplatin resistance has been shown to be independent of P-glycoprotein expression [186,282] and nitric oxide production [283]. It has been linked to HIF-1α-stimulated erythropoietin production in cervical cancer [284], suppression of apoptosis through targeting of Cytochrome C in normal rat epithelium [271] and cyclophilin A expression in pancreatic cancer [285]. In hepatocellular carcinoma cell lines, the Akt pathway was implicated in chemoresistance induced by HIF-1α [273]. Thus there are many potential pathways involved in cisplatin resistance that may be at play in our model system.

3.1.4.5 Cisplatin Resistance, Hypoxia and Ovarian Cancer

There have been many studies examining the effects of cisplatin on ovarian cancer cell lines. These look at drug treatment length [286], synergistic effects of cisplatin in combination with other agents [287-294], investigation of efficacy of new chemotherapeutic drugs [295-299], characterization of cell lines [300-302] and evaluation of different forms of gene therapy [303-305]. However, there are relatively few studies solely looking at the effects of hypoxia on the response to

cisplatin in ovarian cancer cell lines, and only one other to date using the MTT assay to measure changes in chemoresistance [306]. Most studies looking at the effect of hypoxia on cisplatin investigate the effects on molecular biomarkers associated with clinical outcome within the cell rather than at resistance levels *per se*. It has been shown that L1-CAM, a membrane glycoprotein, can protect ovarian cancer cells from apoptosis induced by hypoxia and by cisplatin [307]. Cisplatin has also been shown to decrease vascular endothelial growth factor (VEGF) mRNA levels through binding to a hypoxia-responsive element (HRE) within its promoter, and that HIF-1 α can restore VEGF expression [308]. Interestingly, short exposure to a high dose of cisplatin has been shown to inhibit HIF-1 α activity and to reduce VEGF and CA9 expression in a number of ovarian cancer cell lines [309]. STAT3, a transcriptional activator, has been shown to influence proliferation of ovarian cancer cells in hypoxia and inhibition of it increases sensitivity to cisplatin in A2780 cells [189]. Hypoxia induced with the mimetic agent CoCl₂ was shown to increase resistance to cisplatin in CI3K cells, through inhibition of expression and activity of HIF-1 α [306].

Cisplatin is a DNA-damaging agent which acts through formation of inter-strand and intra-strand adducts which send the cell into apoptosis through activation of p53 and certain MAP kinases such as ERK, JNK and p38 [310]. Hypoxia has been shown to increase cellular levels of p53 – elevated p53 protein levels were detected in human normal and cancer cell lines with up to 22 hours of exposure to hypoxia [311], however, many human cancers have a defective p53 pathway, and p53-null cells have been shown to be resistant to apoptosis from hypoxia [312]. Furthermore, hypoxia has been shown to select for cells with decreased apoptotic potential within tumours due to deficiencies in p53 [312]. Hypoxia has been shown to induce resistance to cisplatin in a number of cancers such as glioma [186], testicular carcinoma [191], non-small cell lung carcinoma [185] and gastric cancer [280].

3.1.5 Paclitaxel

Microtubules are hollow cylindrical structures which make up part of the cell's cytoskeleton, and have many important cellular functions such as maintaining cell shape and polarity, transport of secretory vesicles and distribution of chromosomes during mitosis [313]. Microtubules are composed of α , β tubulin subunits and are constantly in a state of flux, polymerizing at one end (addition of new subunits) and depolymerising at the other end (removal of old subunits) [314]. Paclitaxel (Figure 3.2) is a natural product derived from the western yew tree, *Taxus brevifolia* [315]. It binds to polymerized microtubules [316], and stabilizes them, leading to a mitotic block at anaphase [317]. This induces cellular death by apoptosis [318]. Paclitaxel is given to most ovarian patients as part of their first-line chemotherapy regimen.

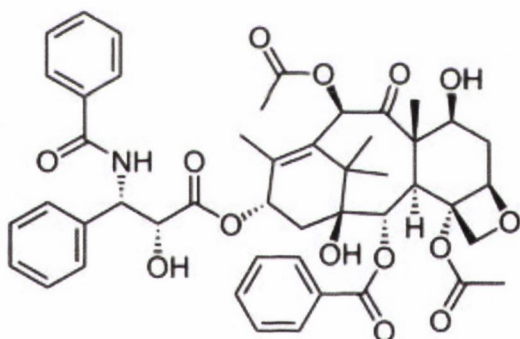


Figure 3.2. Structure of Paclitaxel. Paclitaxel is a derivative of the bark of the Pacific Yew tree. It has a complex structure with several stereocentres.

3.1.6 Paclitaxel Resistance

Resistance to paclitaxel is achieved in a number of ways.

3.1.6.1 Tubulin Modification

One way in which cells become resistant to paclitaxel is altering their expression of tubulin isotypes. It has been shown in a variety of cell line models that increased expression of particular isotypes of class II, III and IV β -tubulin is associated with resistance to paclitaxel [319-322]. Paclitaxel cannot bind as efficiently to class III β -tubulin, thus the drug's activity is reduced leading to increased resistance [323]. The human epidermal growth factor (EGF) receptor has been shown to modulate the expression of class IV β -tubulin [324]. The EGF receptor has been implicated in the pathogenesis of many cancers including ovarian cancer [325]. The use of siRNA to silence these tubulin isotypes increases resistant cells' sensitivity to paclitaxel [326]. However, although *in vitro* experiments have demonstrated the effect of isotype expression on paclitaxel resistance, a study which grew xenografts of human ovarian cancer specimens was not able to correlate tubulin isotype expression with resistance – thus it was initially unclear whether it had a role in clinical paclitaxel resistance [327]. However more recent studies have linked low levels of class III tubulin expression with longer progression free intervals and longer overall survival in lung cancer [328] and ovarian cancer [329]. In addition to differential isotype expression, acquired mutations of tubulin can also modulate paclitaxel resistance [330,331], although the role of mutations has been controversial due to the presence of tubulin pseudogenes [332].

3.1.6.2 Tau and other Microtubule-Associated Proteins

Microtubule-associated proteins (MAPs) are proteins which can interact with microtubules and have a variety of functions. Tau is a MAP which binds to microtubules and stabilizes them. Low expression of Tau has been shown to identify patients who are more sensitive to paclitaxel treatment in breast cancer both in cell

lines and in clinical samples [333-335]. However, another study which analysed three separate cohorts of breast cancer patients found high Tau expression to be an indicator of better response, and associated Tau expression with oestrogen receptor (ER) negative breast tumours [336]. Thus, the role of Tau in breast cancer is unclear. Low Tau expression has also been linked to better response to paclitaxel in gastric cancer [337]. High expression of another MAP, MAP2, has been linked to paclitaxel sensitivity in breast cancer [338] and MAP4 over-expression has been associated with paclitaxel sensitivity in cell lines [339,340].

3.1.6.3 P-glycoprotein

P-glycoprotein is an ABC transporter encoded by the multi-drug resistance gene, MDR1. It acts as an efflux pump, removing drugs from the cell and causing resistance to a wide range of cytotoxic agents [341]. In ovarian cancer, its expression has been linked to increased risk of brain metastasis [342], shorter overall survival [261] and disease progression [343].

3.1.6.4 Hypoxia and Paclitaxel Resistance

The role of hypoxia in resistance to paclitaxel has not been as widely investigated as cisplatin. However, hypoxia has been shown to cause paclitaxel resistance in cell line models of testicular cancer [191], breast cancer [344], lung cancer [345] and ovarian cancer [346]. Studies in a number of different cancer types have identified possible mechanisms by which hypoxia induces paclitaxel resistance including activation of the antiapoptotic protein Bad via the Akt pathway [347], alteration of microtubule morphology [345], overexpression of the microtubule-associated protein SEPT9 [348], induction of expression of tubulin isotypes associated with resistance [349], and activation of the ERK pathway [350]. It has been shown in *in vivo* models that paclitaxel administered under normal oxygen conditions improves radiosensitivity of murine mammary tumours, while it has no effect on radiosensitivity if administered in hypoxia [351,352]. Furthermore, *in vitro* studies of testicular carcinoma [191], breast cancer [344] and cervical cancer [350]

demonstrated reduced effectiveness of paclitaxel when cells were cultured with the drug in hypoxia. A detailed study by Merighi *et al.* showed that increased resistance to paclitaxel in glioblastoma was mediated by activation of the Akt signalling pathway [347]. Potential biomarkers which have been associated with hypoxia and resistance to paclitaxel include a member of the septin family, SEPT9 [348] expression of a specific tubulin isotype, TUBB3 [349], and cell-cycle affecter cyclin B1 [353]. An elegant study using RNA interference techniques in 2007 convincingly demonstrated that HIF-1 α induces resistance to paclitaxel in orthotopic models of lung cancer [345]. Similarly, Huang *et al.* have shown that HIF-1 α induces paclitaxel resistance in one of the ovarian carcinoma cell lines used in this study, A2780, through arresting the cells at the G₀/G₁ phase of the cell cycle [346]. Inhibition of apoptosis through HIF-1 has also been shown to induce resistance to paclitaxel in a breast cancer cell line model [354]. Thus similarly to cisplatin, hypoxia has been shown to induce resistance to paclitaxel in a variety of different ways.

3.1.7 Aim

As it has been shown that hypoxia can induce resistance to both cisplatin and paclitaxel in a variety of cell types, the aim of this chapter was to evaluate the effect of hypoxia on chemoresistance in our ovarian cancer cell line model (A2780/A2780cis). The specific objectives of the chapter were:

- i) To examine the effect of hypoxia exposure on cisplatin and paclitaxel resistance
- ii) To examine the effect of hypoxia on hypoxia 'naïve' cells i.e. cells never exposed to hypoxia before treatment
- iii) To examine HIF-1 α expression in normoxic and hypoxic conditions in our cell lines

3.2 Methods

3.2.1 Cell Culture

Human epithelial ovarian cancer cell lines A2780 (cisplatin-sensitive) and A2780cis (cisplatin-resistant) were cultured in a humidified atmosphere at 37°C as described in Chapter 2.

3.2.2 Drug and Vehicle Control Formulation

Cisplatin (Hospira, Warwickshire, UK) and paclitaxel (Actavis, Devon, UK) were kindly donated by the compounding unit in St. James's Hospital. Cisplatin was received as a 1 mg/mL solution and paclitaxel was received as a 6 mg/mL solution. Both were stored at room temperature in the dark in accordance with the manufacturers' instructions. Drugs were freshly diluted in media to the desired stock concentration for each experiment (100 µM cisplatin, 1000 nM paclitaxel). The vehicle control for paclitaxel was kindly supplied by Actavis. Cisplatin vehicle control was prepared in media. The vehicle control formulations are outlined in Table 3.1.

Table 3.1. Components of Vehicle Controls for Cisplatin and Paclitaxel.

Vehicle	Components
Cisplatin	1 mg/mL mannitol; 9 mg/mL sodium chloride
Paclitaxel	Cremophor EL [®] , anhydrous citric acid, ethanol

3.2.3 MTT Assays

The MTT assay was used to determine the rate of cell proliferation and cell viability as described in Chapter 2. Preliminary experiments were carried out to determine the correct seeding density for each of the cell lines in 96-well plates. Experiments were also carried out to determine the most appropriate duration of drug treatment for both cell lines. When the optimal seeding density and drug treatment period were decided, the hypoxia matrix was carried out. Response to drug treatment was

measured by changes in the IC₅₀ (inhibitory concentration 50 – the concentration of drug required to kill 50% of cells).

3.2.3.1 Optimization of Seeding Density

As cytotoxic drugs are generally most potent in actively dividing cells, it was necessary to seed cells at a concentration in which cells would be in the exponential phase of growth during treatment. In order to determine the optimal seeding density for each cell line, different concentrations of cells were plated in a log-scale (Table 3.2) in 96-well plates (Biosciences, Ireland) and incubated overnight at 37°C to adhere. The following day cell proliferation was assessed using the MTT assay. This was carried out for three experimental oxygen conditions - normal oxygen (21% O₂, 5% CO₂), acute hypoxia (4 hours, 0.5% O₂, 5% CO₂) and chronic hypoxia (5 days, 0.5% O₂, 5% CO₂) to ensure similar growth characteristics for each condition. Hypoxic exposure was carried out in an In Vivo hypoxic chamber (Fannin Healthcare, Ireland). All experiments were carried out for at least n=3.

Table 3.2. List of Seeding Densities Assayed to Determine the Optimum Cell Concentration for Cytotoxicity Assays.

	Cells/mL
1	1x10 ⁷
2	3x10 ⁶
3	1x10 ⁶
4	3x10 ⁵
5	1x10 ⁵
6	3x10 ⁴
7	1x10 ⁴
8	3x10 ³

3.2.3.2 Optimization of Drug Treatment Period

Both cell lines were plated in 96-well plates at a concentration of 1×10^5 cells/mL and incubated overnight at 37°C to adhere. They were then treated with a range of concentrations of cisplatin or paclitaxel (Table 3.3) for 24, 48, 72 or 96 hours. Following incubation with the drug for the respective time period, cell viability was assessed using an MTT assay. The vehicle controls were checked for toxicity, however both vehicles were found to be non-toxic within the range of concentrations used (Appendix). The outside wells of all 96-well plates were not used to avoid any effects of evaporation. All experiments were carried out for at least $n=3$.

Table 3.3. Concentrations of Cytotoxic Drugs Cisplatin and Paclitaxel.
Concentrations of cytotoxic drugs used for MTT assays.

Cisplatin	Paclitaxel
100 μ M	500 nM
30 μ M	150 nM
10 μ M	50 nM
3 μ M	15 nM
1 μ M	5 nM
0.3 μ M	1.5 nM
0.1 μ M	0.5 nM
0.03 μ M	0.15 nM
0.01 μ M	0.05 nM
0 μ M	0 nM

3.2.3.3 Hypoxia Matrix Experiments

In order to best represent the numerous potential clinical scenarios, a matrix of various combinations of hypoxia and drug treatment was composed (Table 3.4).

A2780 and A2780cis cell lines were subjected to a range of hypoxia conditions before and/or during treatment with cisplatin or paclitaxel, summarized in Table 3.4 and Figure 3.3. Cells were grown in normal oxygen conditions (normoxia) or exposed to hypoxia (pre-treatment O₂ conditions) and then treated with cisplatin or paclitaxel for 72 hours in hypoxia or normoxia (treatment O₂ conditions). Also, in order to evaluate the effect of transient hypoxia on response to chemotherapy, hypoxia was introduced during drug treatments in cells which had not been pre-exposed – ‘hypoxia-naïve’ cells. Cells were either treated with hypoxia for the treatment duration (72 hours) or had hypoxia introduced during treatment, at 24 hours or 48 hours. As the hypoxia chamber was a non-sterile environment, hypoxic plates to be drug treated were removed from the chamber and brought to the laminar flow hood for the drugs to be added. This was carried out promptly, and cells were returned to the chamber immediately following treatment. Cells were removed from the hypoxia chamber for a maximum of 20 mins. Following incubation with the drug an MTT assay was carried out to assess cell viability. All experiments carried out for at least n=3.

Table 3.4. Hypoxia Matrix Conditions. Cells were subjected to hypoxia or normoxia before and/or during treatment. Cells were either pre-exposed to hypoxia for a short (4 hours) or long (5 days) period and subsequently treated with cytotoxic drugs for 72 hours. Cells were exposed to hypoxia at various timepoints during the treatment period – Day 1 (i.e. for the full 72 hours of treatment) Day 2 (for the last 48 hours) or Day 3 (for the last 24 hours).

Pre-treatment	Treatment Day 1 (0 – 24h)	Treatment Day 2 (24 – 48h)	Treatment Day 3 (48 – 72h)
Normoxia	Normoxia	Normoxia	Normoxia
Normoxia	Hypoxia	Hypoxia	Hypoxia
Normoxia	Normoxia	Hypoxia	Hypoxia
Normoxia	Normoxia	Normoxia	Hypoxia
4 hours hypoxia	Normoxia	Normoxia	Normoxia
4 hours hypoxia	Hypoxia	Hypoxia	Hypoxia
5 days hypoxia	Normoxia	Normoxia	Normoxia
5 days hypoxia	Hypoxia	Hypoxia	Hypoxia

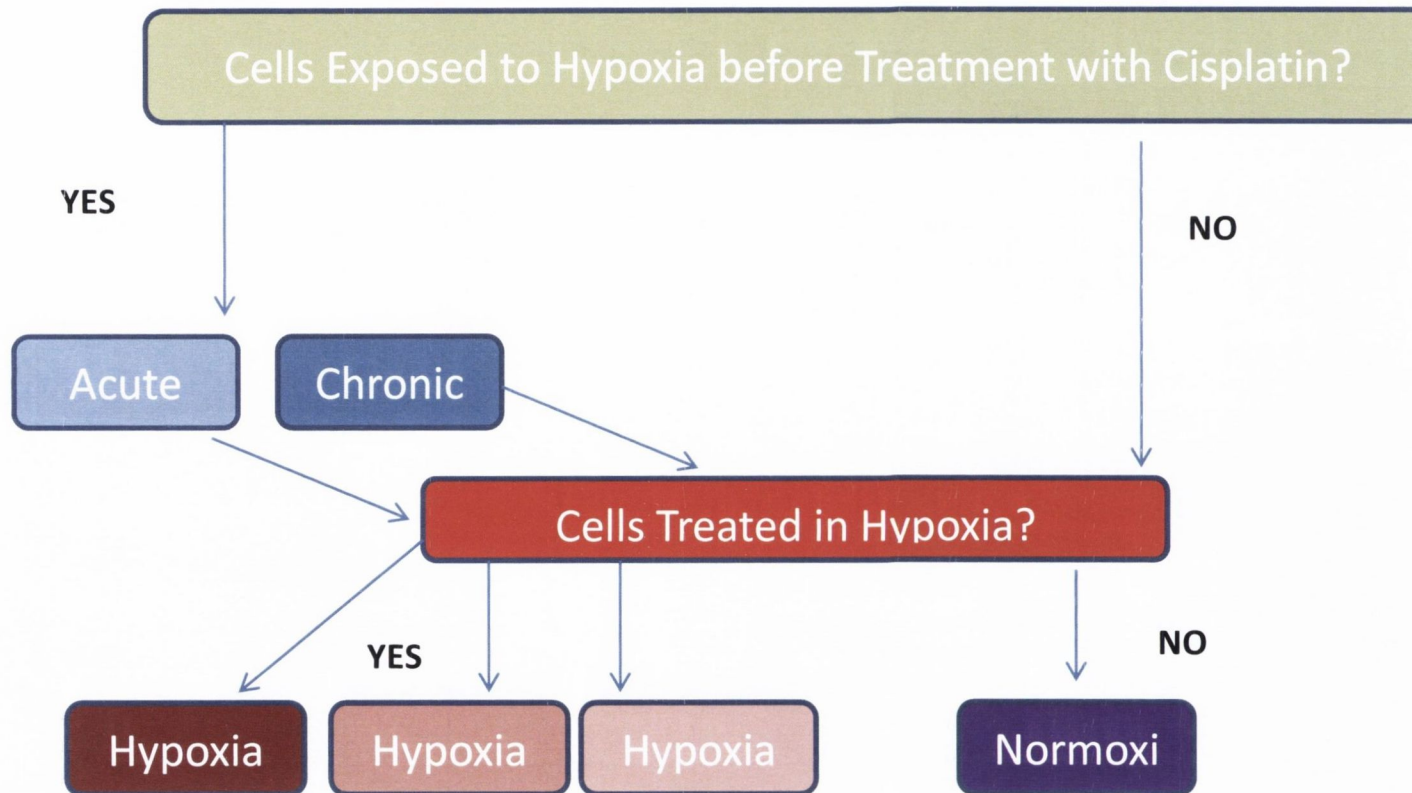


Figure 3.3. Schematic of Hypoxia Matrix Conditions. The hypoxia matrix was designed on three levels. Cells were either maintained in normal oxygen conditions or exposed to acute or chronic hypoxia before treatment. Cells were either then treated in normal oxygen or hypoxia. Finally, cells which were not exposed to hypoxia before treatment were exposed to hypoxia for part or all of the treatment period.

3.2.4 Timecourse of HIF-1 α Expression in Hypoxia

As protein expression of HIF-1 α is a marker of the hypoxic response in cells, we carried out a time course of HIF-1 α expression using western blots. Cells were exposed to hypoxia for the various time-periods used for the hypoxia matrix – 4 hours, 72 hours and 5 days. Protein was extracted in the hypoxia chamber as described in Chapter 2 and 30 μ g run on 12% gels, transferred and probed for HIF-1 α (Table 3.5) using Luminol. β -actin was used as an endogenous control. A positive control was prepared by exposing A2780cis cells to 50 μ M CoCl₂ for 24 hours. CoCl₂ stabilizes expression of HIF-1 α in normal oxygen conditions.

Table 3.5: Antibodies for HIF-1 α Timecourse. Mouse α -HIF-1 α was the primary antibody for HIF-1 α . A horse radish peroxidase (HRP)-conjugated primary antibody was used as a secondary antibody. After Luminol detection of HIF-1 α , the blots were blocked again in 3% skimmed milk and reprobed using β -actin. A secondary antibody conjugated to alkaline phosphatase (AP) was used to detect β -actin to prevent detection of the HIF-1 α antibody.

Antibody	Clone	Dilution
HIF-1 α	54, BD Biosciences	1:250
α -mouse HRP-conjugated secondary antibody	A6782, Sigma Aldrich	1:1000
β -actin	A5441, Sigma Aldrich	1:10,000
α -mouse AP-conjugated secondary antibody	A4312, Sigma Aldrich	1:1000

3.2.5 Statistical Analyses

Results were plotted and statistical analyses were carried out using GraphPad Prism Software, Version 5.03 (GraphPad Software Inc, US). Non-linear regression was used to analyse the growth curves. 100% was set as the average absorbance of untreated cells, and all other points on the graph were calculated with the following equation:

$$\% \text{ Survival} = \frac{\text{Absorbance of Treated Cells}}{\text{Absorbance of Untreated Cells}} \times 100$$

Student's t-tests on the IC₅₀ values were used to evaluate the effect of hypoxia on response to the chemotherapy drugs [355]. Significance was set at p<0.05.

3.3 Results

3.3.3 Characteristics and Morphology of A2780 and A2780cis Cell Lines

A2780 is an epithelial ovarian cancer cell line which grows as a monolayer in tissue culture flasks. A2780cis is a cisplatin resistant daughter cell line of A2780. It was created by culturing A2780 cells in increasing stepwise concentrations of cisplatin over time [239]. A2780cis are cross-resistant to carboplatin and can up-regulate DNA repair mechanisms [239]. They also have higher levels of GSH, a mechanism known to induce resistance to platinum agents.

A2780 are small, spherical cells with a translucent granular cytoplasm on light microscopy (Figure 3.4). They tend to grow in groups, and need to be seeded quite densely. A2780cis are very similar in morphology, however they have a larger proportion of elongated cells (Figure 3.4). A2780cis need more space for optimal growth and do not reach the same confluency as A2780cis.

3.3.2 Hypoxia and Morphology of A2780 and A2780cis

Exposure of the cells to hypoxia did not affect the morphological appearance or growth characteristics of A2780 or A2780cis cell lines (Figure 3.5).

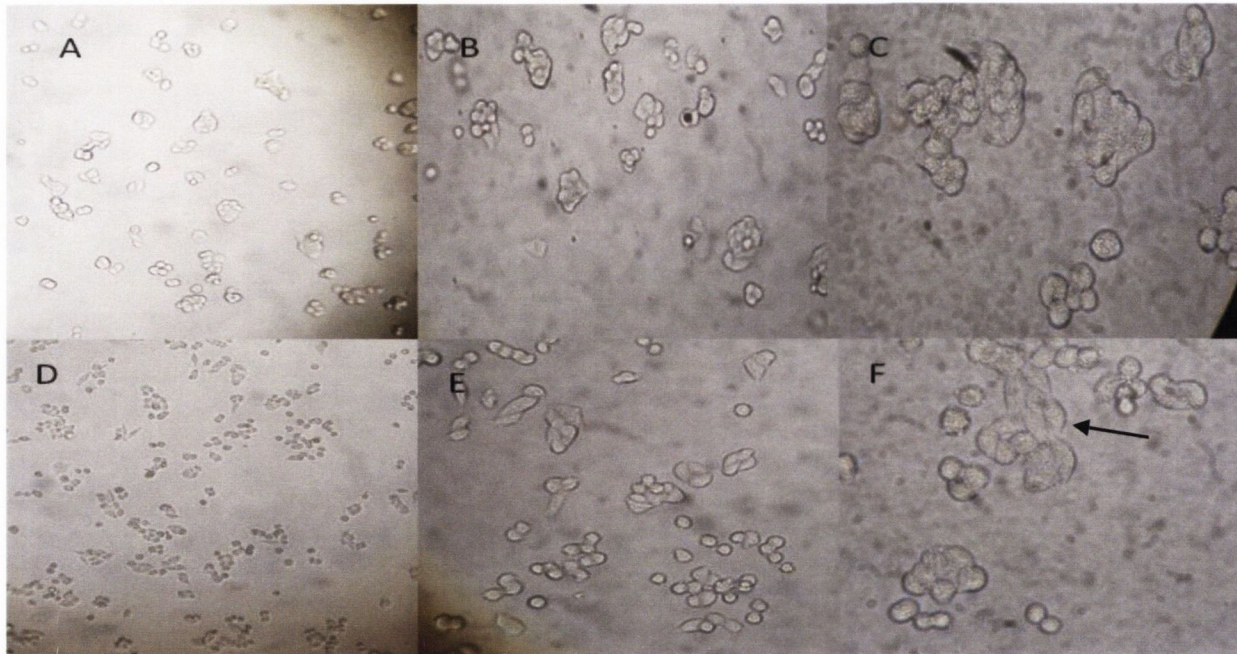


Figure 3.4. Light Images of A2780 and A2780cis cell Lines. Light images taken of A2780 (A, B and C) and A2780cis (D, E and F) taken at 10x, 20x and 40x magnification. Both cell lines were small with translucent granular cytoplasm under phase contrast microscopy. A2780cis contained a population of elongated cells (arrow), whereas A2780 contained spherical cells only.

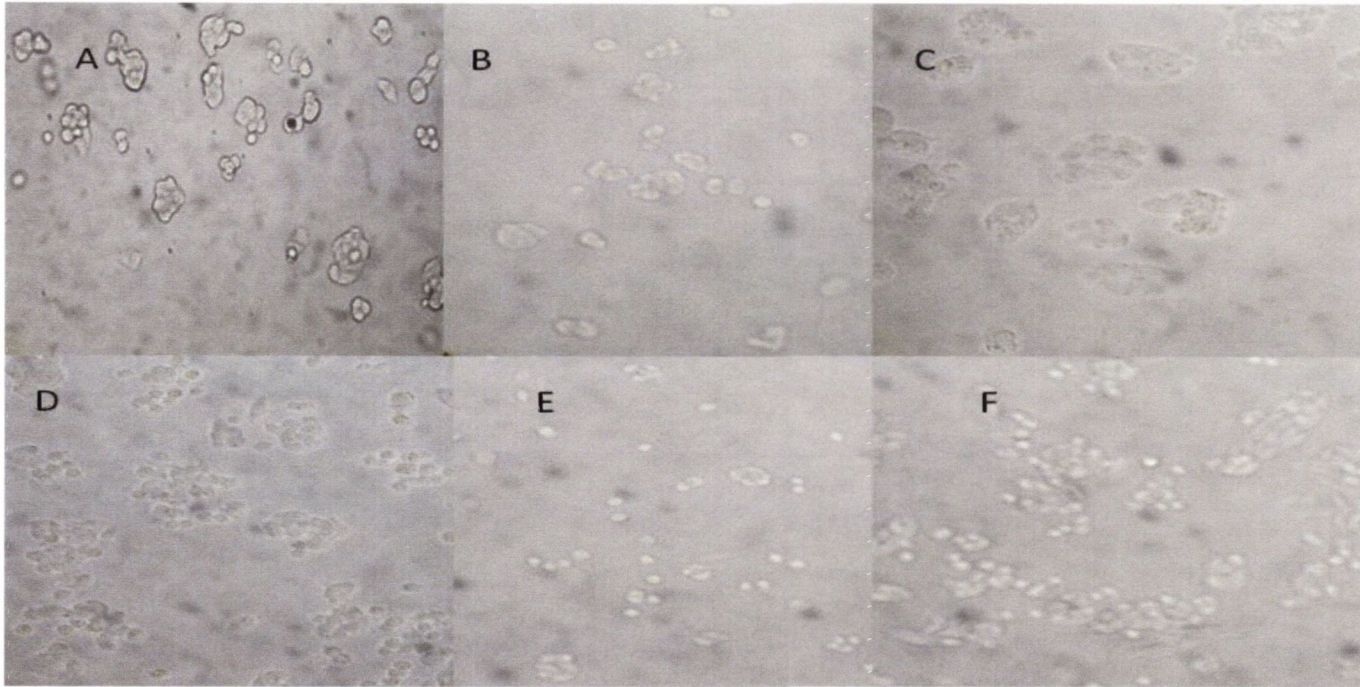
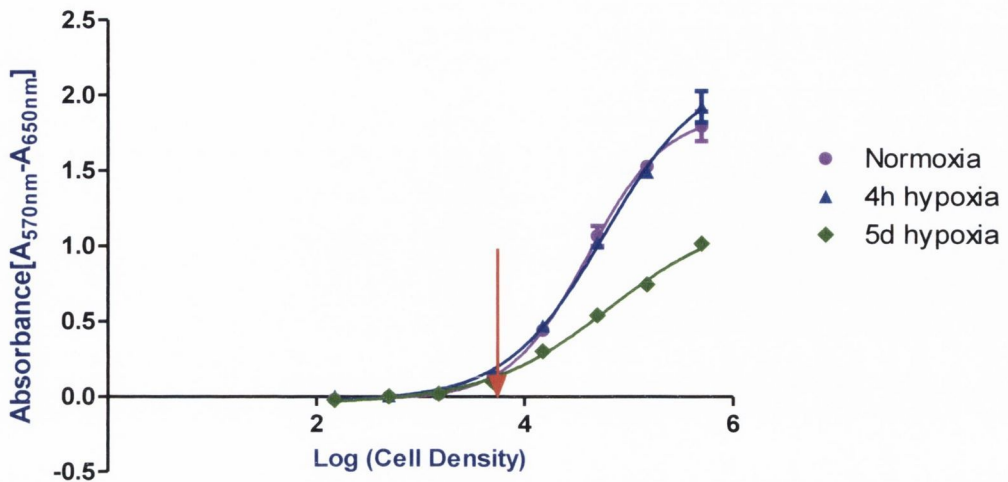


Figure 3.5. Light Images of A2780 and A2780cis cells Exposed to Hypoxia. Light images of A2780 cells (A, B and C) and A2780cis (D, E and F) exposed to hypoxia for 4 hours, 72 hours or 5 days (A, B and C). Neither cell line demonstrated any obvious changes in size or shape when exposed to hypoxia. Both cell lines retained their morphology and growth characteristics under hypoxic conditions.

3.3.3 Optimization of Seeding Density

The optimum cell seeding density was determined as the density at which cells began to enter their exponential phase of growth at the beginning of the treatment period, as this ensures that the cells remain in the exponential phase for as long as possible while being treated. For the cisplatin-sensitive cell line, A2780, this was determined to be Log(cell concentration) of 3.69 corresponding to 5000 cells/well (Figure 3.6A). This was also found to be the case for A2780 cells exposed to acute and chronic hypoxia for 4 hours and 5 days respectively (Figure 3.6A). The optimum cell seeding density for the cisplatin-resistant cell line, A2780cis, was also found to be Log(cell concentration) of 3.69, corresponding to 5000 cells/well (Figure 3.6B).

A



B

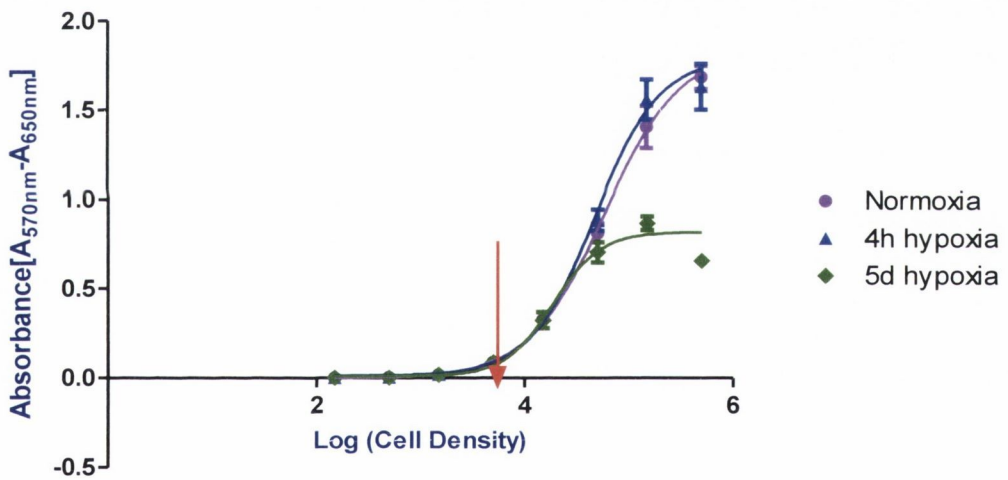


Figure 3.6. Optimal Seeding Density for A2780 and A2780cis Cell Lines. As cells are generally most responsive to cytotoxic drugs during the exponential growth phase, it was decided to use the seeding density in which the cells were entering this phase (red arrow). This was a log(cell density) of 3.69 cells for A2780 (A) and A2780cis (B), which corresponded to a number of 5,000 cells/well. n = 3

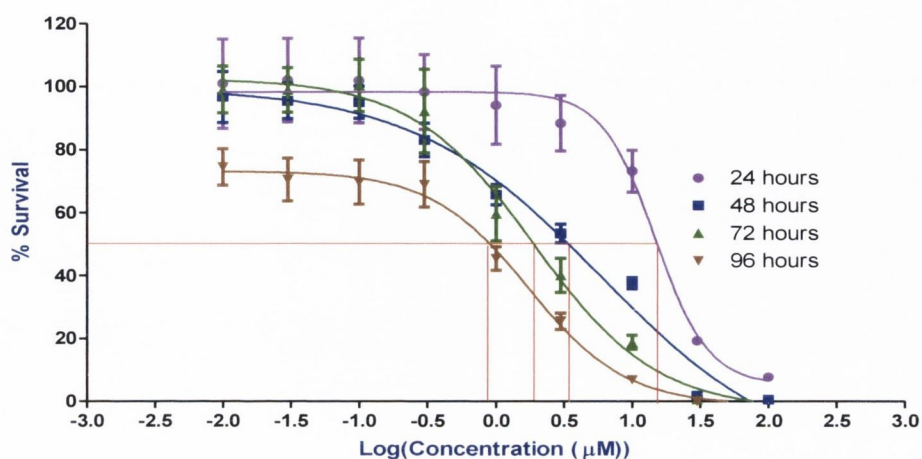
3.3.4 Optimization of Treatment Period

Figure 3.7A shows the results for treating A2780 cells in normoxia with varying concentrations of cisplatin or paclitaxel for 24, 48, 72 and 96 hour time points. Ideally the cells should be treated with the lowest concentration of drug for the shortest period of time. The optimum length of cisplatin treatment was decided as 72 hours because it gave a low IC_{50} value, and there was very little difference between the 72 hour and 96 hour values. The results for A2780cis are shown in Figure 3.8. It was decided to use the same timepoint for A2780 and A2780cis cells, to maintain a consistent experimental design. The range of IC_{50} values observed for the different timepoints are displayed in Table 3.6. The optimal time period for treatment with paclitaxel was also taken as 72 hours as it gave the lowest IC_{50} . (Figures 3.7B, 3.8B). Similarly to cisplatin, the sensitive and resistant lines were treated with paclitaxel for the same length. IC_{50} values for paclitaxel are summarized in Table 3.6.

Table 3.6. IC_{50} Values Obtained when Treating A2780 and A2780cis with Cisplatin and Paclitaxel for Various Timepoints. The timepoint which required the least amount of drug for the least time was used – 72 hours.

Cell Line/Drug	24 hours	48 hours	72 hours	96 hours
A2780/Cisplatin (μ M)	5.8	3.0	1.9	1.8
A2780/Paclitaxel (nM)	4.0	3.1	3.4	2.7
A2780cis/Cisplatin (μ M)	16.3	12.0	9.1	6.9
A2780cis/Paclitaxel (nM)	5.1	3.4	2.7	2.0

A



B

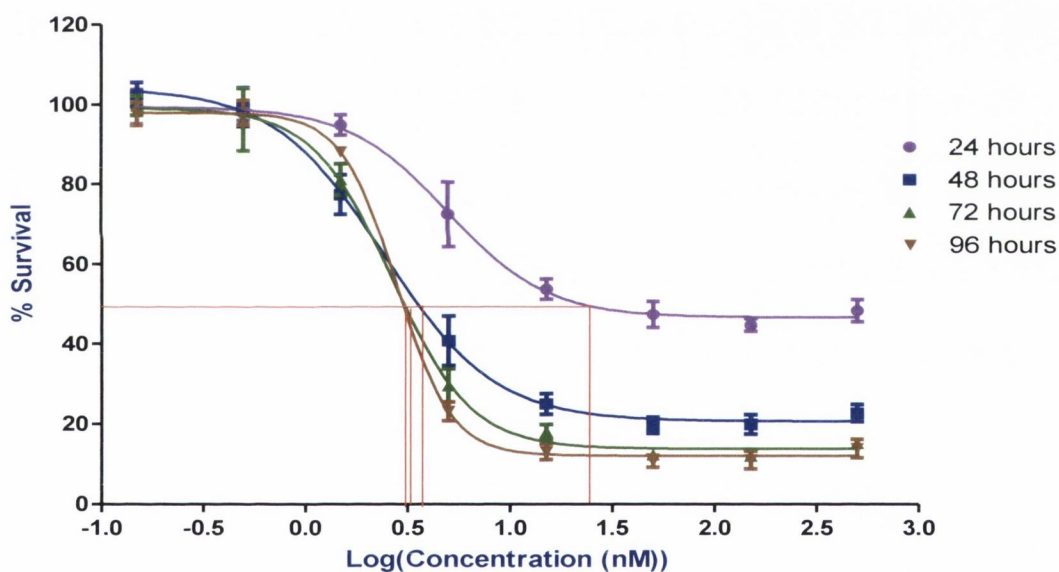


Figure 3.7. Treatment Periods for A2780 Cells with Cisplatin and Paclitaxel. A2780 cells were treated with cisplatin (A) or paclitaxel (B) for 24, 48, 72 or 96 hours. The optimum treatment length was determined as that which gave the lowest IC_{50} value for the relatively shortest period. The optimum treatment length was determined as 72 hours (green), for both cisplatin and paclitaxel. $n = 3$

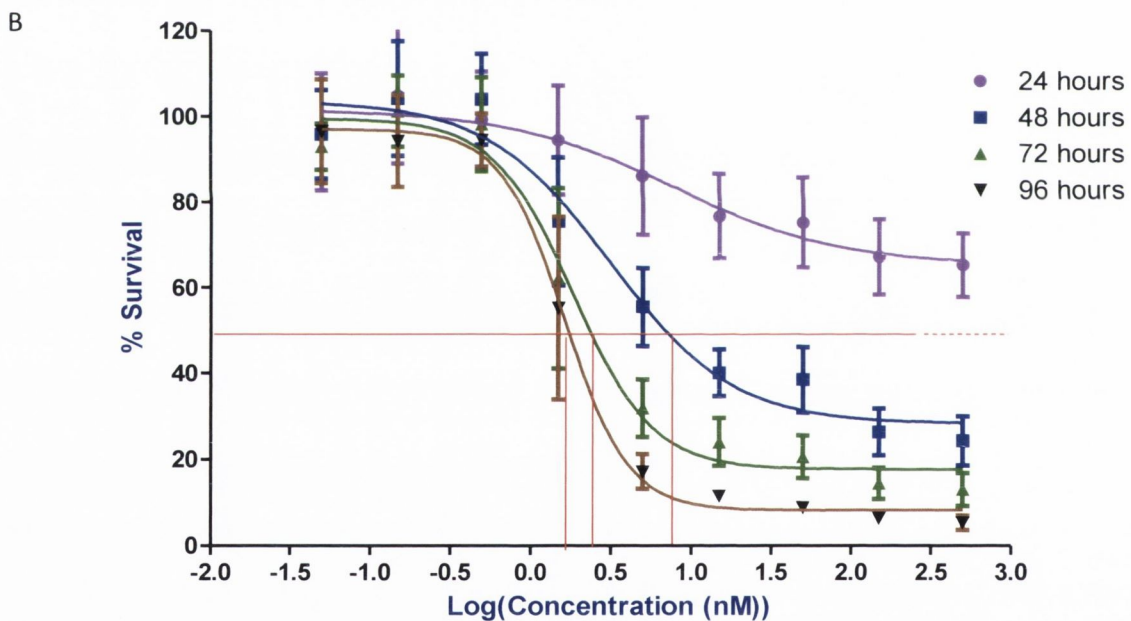
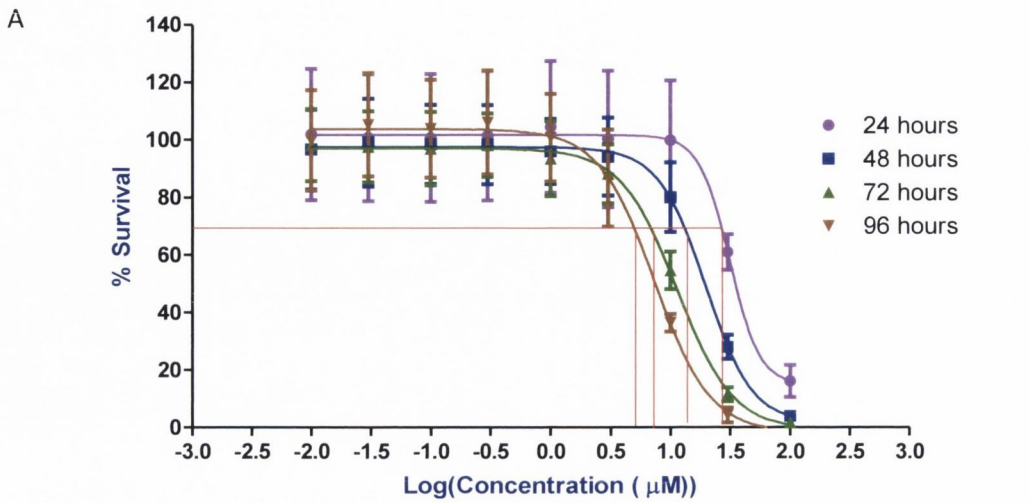


Figure 3.8. Treatment Periods for A2780cis Cells with Cisplatin and Paclitaxel. A2780cis cells were treated for 24, 48, 72 and 96 hours with cisplatin (A) or paclitaxel (B). The optimum treatment length was determined as 72 hours to be consistent with the A2780 cells. $n = 3$

3.3.5 Hypoxia Matrix Experiments

3.3.5.1 Effect of Cisplatin on Morphology of A2780 and A2780cis in Normoxia and Hypoxia.

Treatment of both A2780 (Figure 3.9) and A2780cis (Figure 3.10) with cisplatin in normoxia and hypoxia induced a number of visually assessed morphological changes associated with apoptosis including rounding-up of the cells, shrinkage and condensation of the nuclei, leading to karyorrhexis, or breakdown of the nuclei. In A2780cis cytoplasmic changes were also obvious, including development of protrusions from the cytoplasmic membrane.

3.3.5.2 Comparison of Drug Sensitivity/Resistance in A2780 and A2780cis in Normal Oxygen Conditions

A2780cis were 9-fold more resistant to cisplatin than A2780 (Figure 3.11). This was highly statistically significant, $p < 0.001$. They also showed a trend towards being more resistant to paclitaxel than A2780, however this did not reach significance (Figure 3.12).

3.3.5.3 Acute Hypoxia Increases Resistance to Cisplatin and Paclitaxel in A2780 Cells

Exposure of A2780 cells to hypoxia for four hours before treatment increased the IC_{50} value for cisplatin (Figure 3.13). This indicated increased resistance to cisplatin following acute hypoxia exposure. When the treatment period was also carried out in hypoxia, the IC_{50} was 8-fold higher than the cells which were normoxic. This was statistically significant, $p < 0.001$. If the treatment period was carried out in normoxia, the resistance was attenuated (2.4-fold), however this was still significant when compared to the normoxic group ($p < 0.05$).

Cells which were treated with paclitaxel following acute exposure to hypoxia showed a trend towards increased resistance, however this was not statistically significant (Figure 3.14). Cells which were treated with paclitaxel showed much

greater variability in response than cells treated with cisplatin, as evidenced by the larger error bars (Figure 3.14).

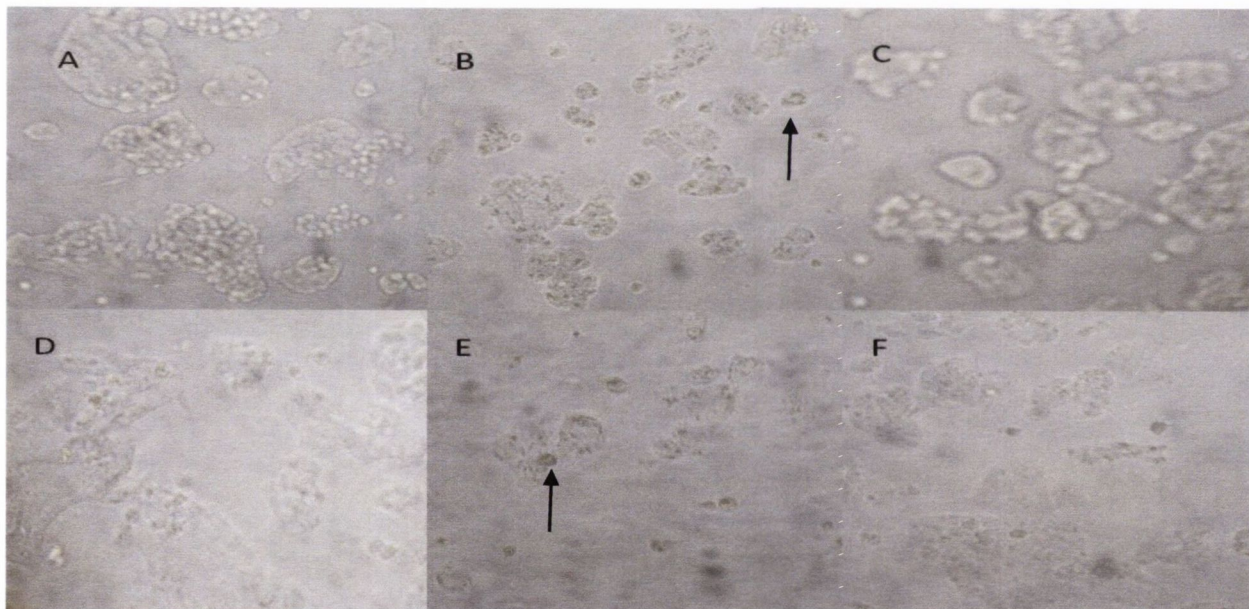


Figure 3.9. Effect of Cisplatin on Morphology of A2780 in Normoxia and Hypoxia. A2780 cells in normal media (A, D), cisplatin (B, E) and vehicle control solution (C, F) in normoxia (top row) and hypoxia (bottom row). While the vehicle control had no effect on the morphology of A2780 in either normoxia or hypoxia, addition of cisplatin lead to apoptotic features including condensation of the nuclei (arrow). Cellular features induced by cisplatin treatment were similar in normoxia and hypoxia.

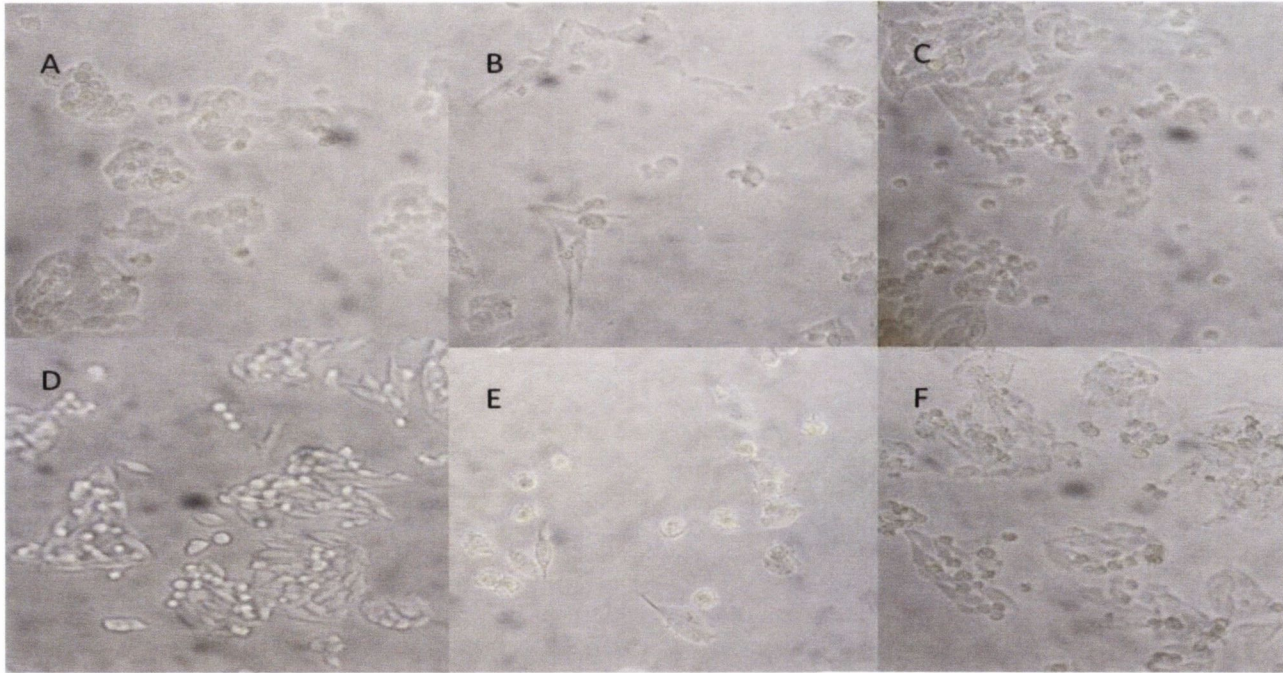
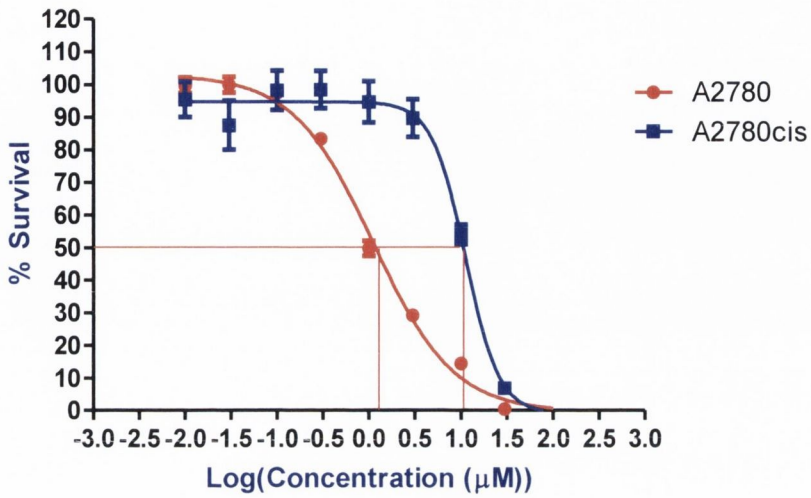


Figure 3.10. Effect of Cisplatin on Morphology of A2780cis in Normoxia and Hypoxia. A2780cis cells maintained in normal media (A, D), cisplatin (B, E) or vehicle control solution (C, F) in normoxia (top row) or hypoxia (bottom row). While the vehicle control did not induce significant changes to the morphology of A2780cis, cisplatin induced apoptotic changes such as cell shrinkage.

A



B

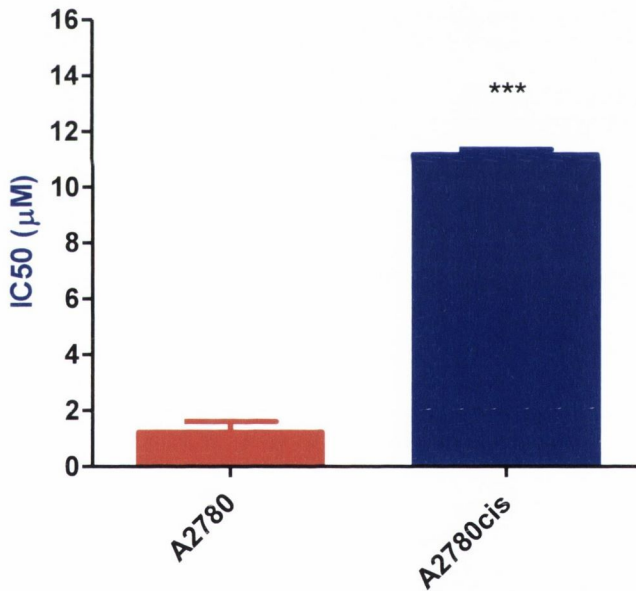
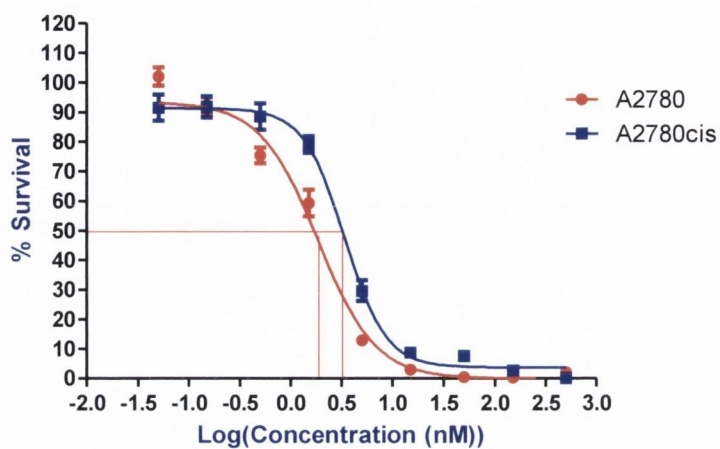


Figure 3.11. A2780cis are more Resistant to Cisplatin than A2780. Dose response curve (A) and bar chart (B) showing cisplatin resistance profiles of A2780 and A2780cis. A2780cis were 9-fold more resistant to cisplatin than A2780 in normal oxygen conditions. ***p<0.001 n = 3

A



B

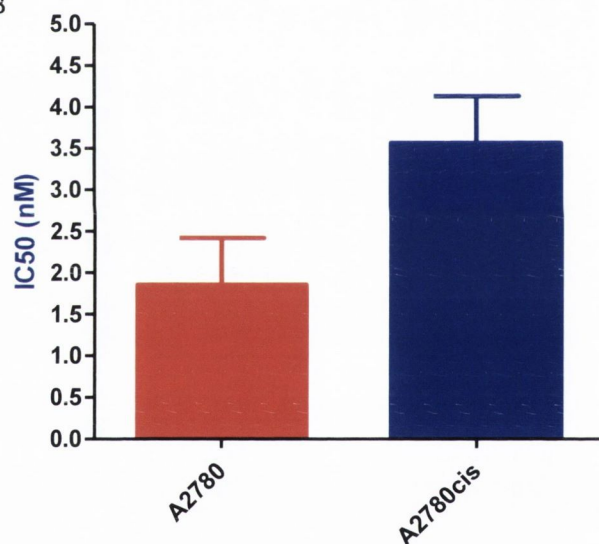
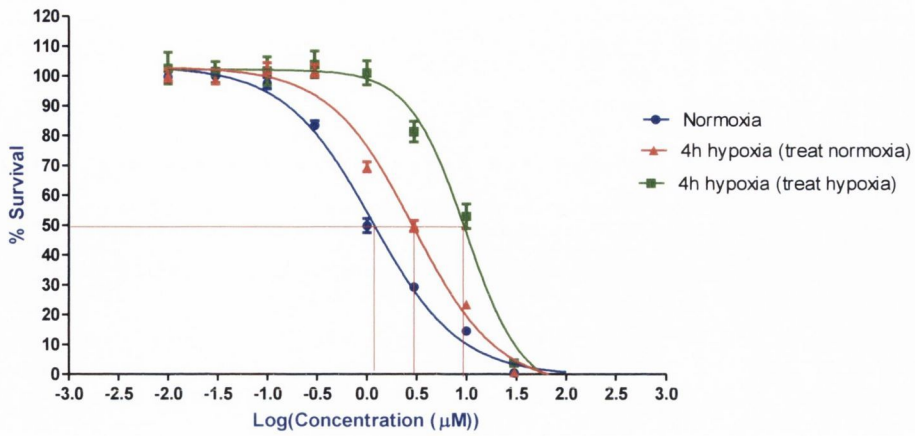


Figure 3.12. A2780 and A2780cis show Similar Resistance Profiles to Paclitaxel. Dose-response curve (A) and bar chart (B) displaying resistance profiles to paclitaxel. Both cell lines showed similar resistance to paclitaxel. A2780cis seemed to trend towards increased resistance in comparison to A2780, although it was not statistically significant. n = 3

A



B

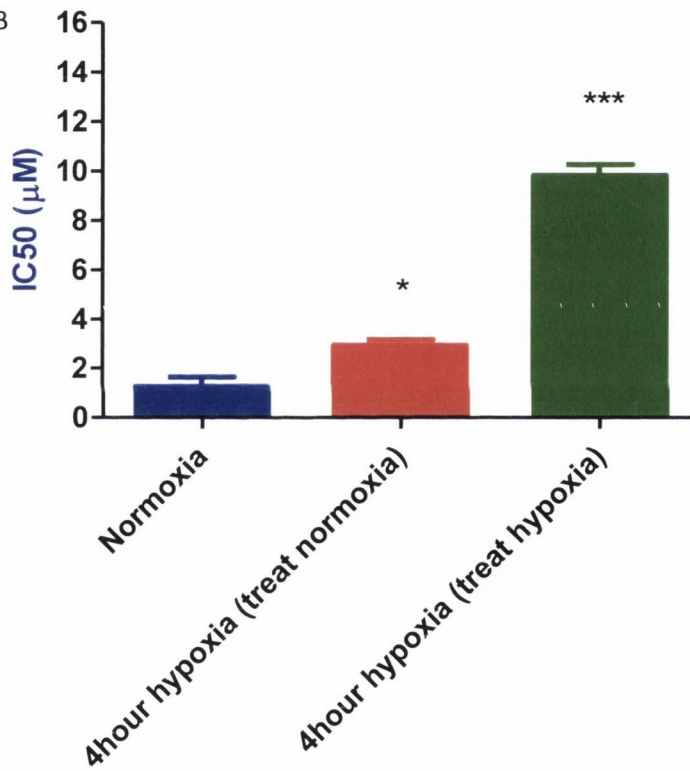
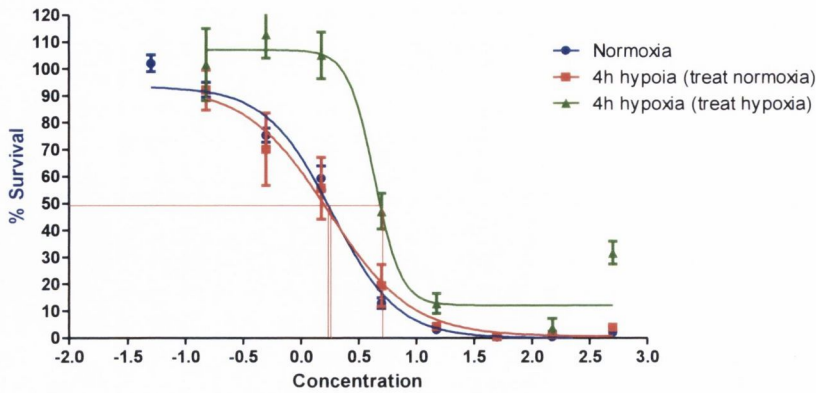


Figure 3.13. Acute Hypoxia Increases Resistance to Cisplatin in A2780. Acute pre-exposure to hypoxia (4 hours) before treatment with cisplatin for 72 hours in normoxia or hypoxia was shown to increase resistance to cisplatin, measured by increase in IC_{50} . This increase was greatest in cells which were treated in hypoxia. * $p < 0.05$ *** $p < 0.001$. $n = 3$

A



B

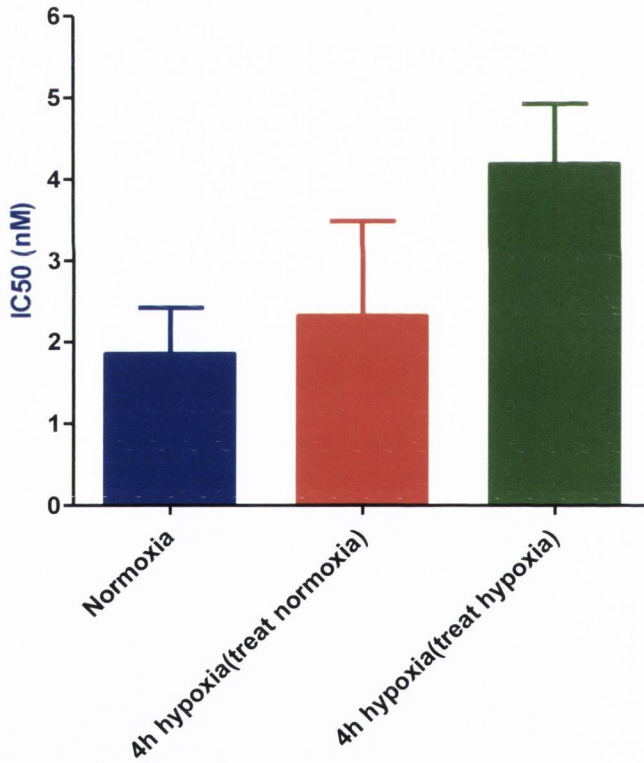


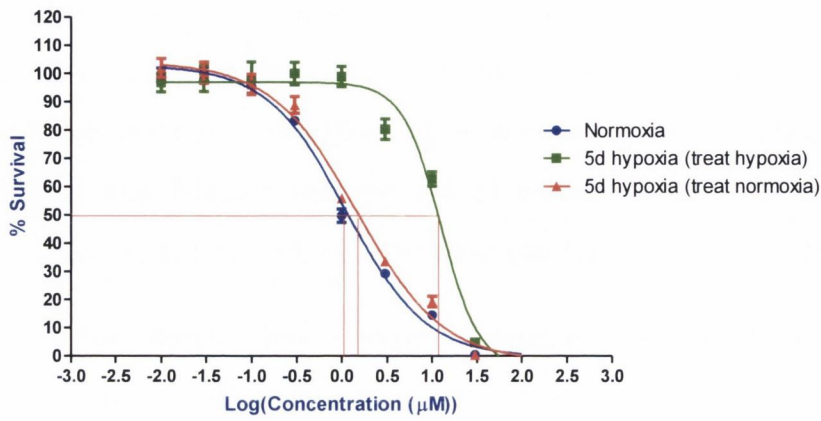
Figure 3.14. Acute Hypoxia Increases Resistance to Paclitaxel in A2780. Cells exposed to acute hypoxia before treatment trended towards increased resistance. These cells showed much greater variability in their response to paclitaxel than cisplatin, thus although a trend can be seen, the results were not statistically significant. n = 3

3.3.5.4 Chronic Hypoxia Increases Resistance to Cisplatin and Paclitaxel in A2780 Cells

Pre-exposing cells to chronic hypoxia (5 days) increased resistance to cisplatin (Figure 3.15). Chronic hypoxic exposure resulted in almost a 10-fold increase in IC_{50} . This increased resistance was only seen when the cells were also treated in hypoxia. Cells which were chronically exposed to hypoxia but treated with cisplatin in normoxia showed comparable sensitivity to cisplatin as the non-hypoxic cells.

A2780 which were chronically exposed to hypoxia and treated with paclitaxel showed a trend towards increased resistance, however the increase was not statistically significant (Figure 3.16). This was likely due to the increased variability observed when treating cells with paclitaxel.

A



B

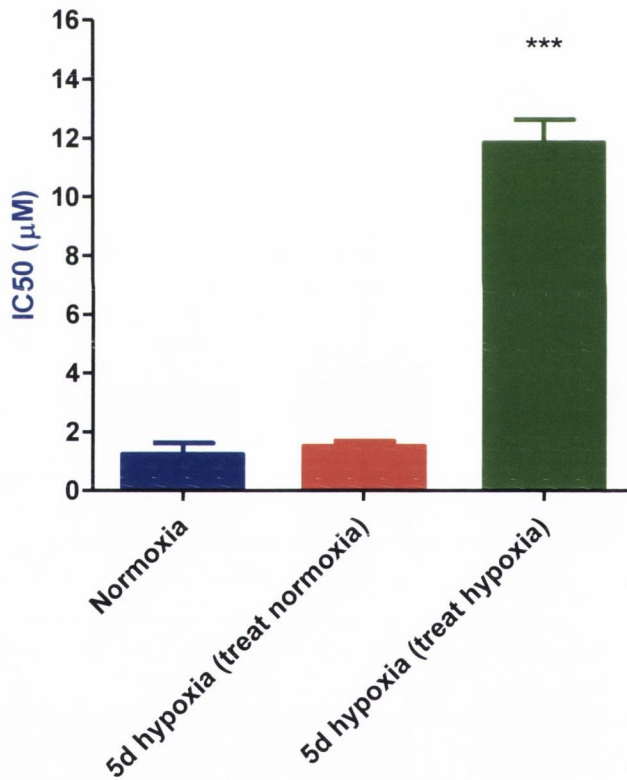
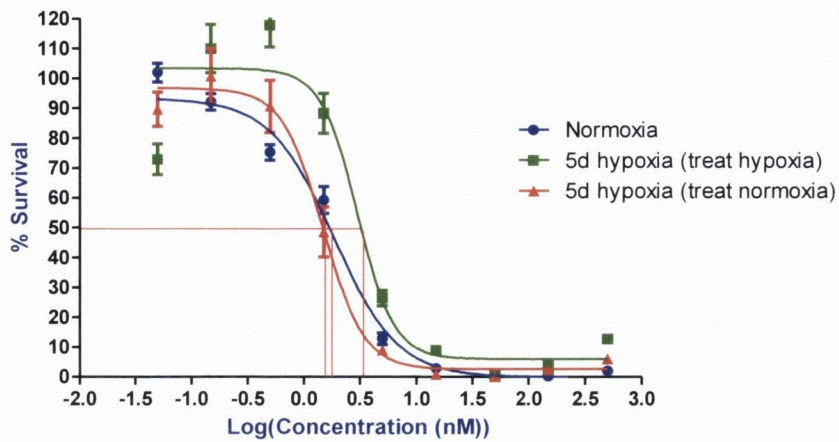


Figure 3.15. Chronic Hypoxia Increases Resistance to Cisplatin in A2780. Dose-response curve (A) and bar graph of IC₅₀ values (B) demonstrating increased resistance to cisplatin following chronic hypoxic exposure. This was statistically significant in cells which were treated in hypoxia. *** p < 0.001 n = 3

A



B

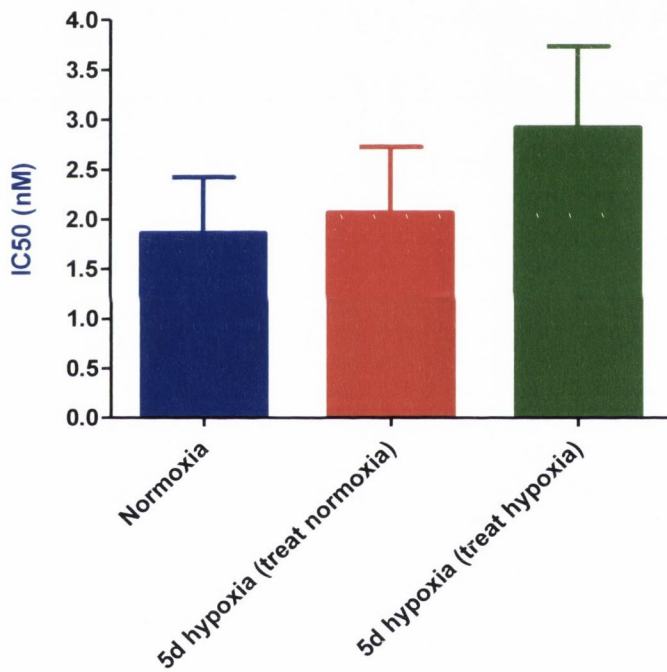
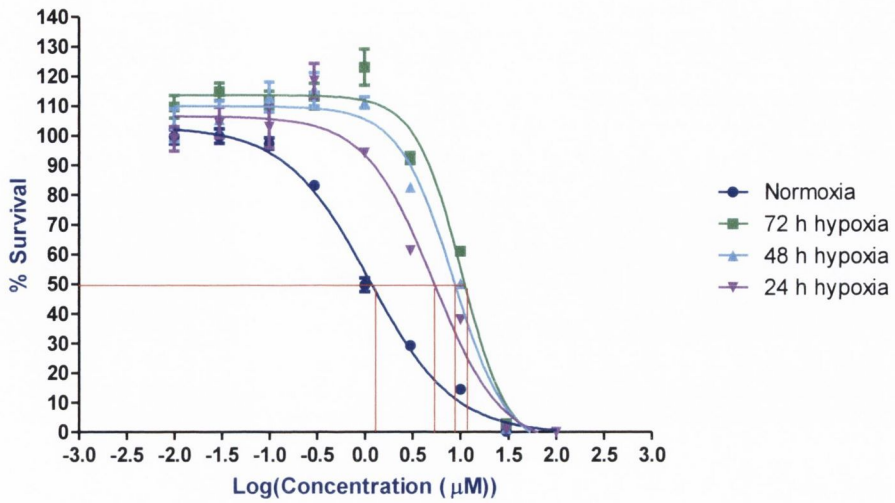


Figure 3.16. Chronic Hypoxia Increases Resistance to Paclitaxel in A2780. Cells which were chronically exposed to hypoxia showed a trend of increased resistance to paclitaxel. This was not statistically significant, however this is likely due to the increased variability in response to paclitaxel observed in A2780. n = 3

3.3.5.5 Treating A2780 in Hypoxia Increases Resistance to Cisplatin and Paclitaxel

Cells which were grown in normal oxygen and treated in hypoxia showed increased resistance to cisplatin. Cells which had the full 72 hour treatment in hypoxia showed levels of resistance which were comparable with resistance seen in the chronic hypoxia cells (Figure 3.17). The level of resistance increased with increasing length of time in hypoxia during the drug treatment. Cells which were treated with paclitaxel in hypoxia again demonstrated a trend towards increased resistance however this was not statistically significant (Figure 3.18).

A



B

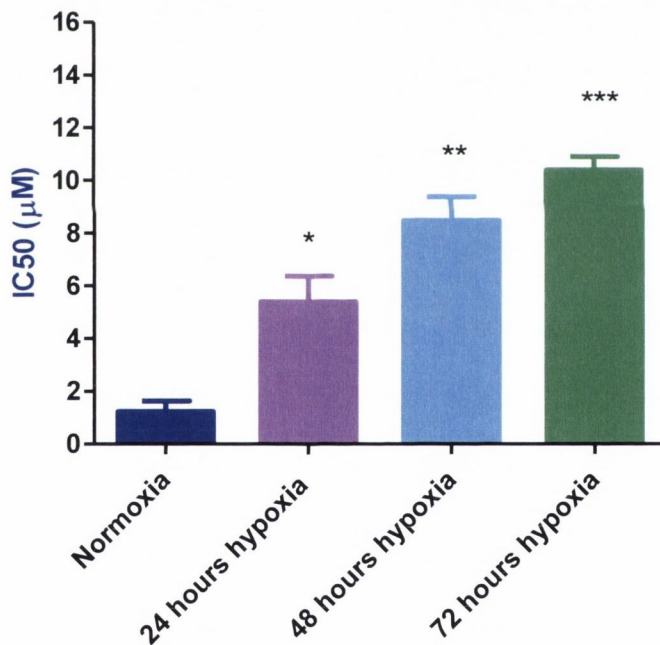


Figure 3.17. Treating A2780 in Hypoxia Increases Resistance to Cisplatin. Cells which were not pre-exposed to hypoxia were treated with cisplatin in hypoxia. Hypoxia was introduced at the beginning of treatment or at timepoints during the treatment. The longer the cells were in hypoxia during treatment, the higher the increase in IC_{50} . * $p < 0.05$ ** $p < 0.01$ *** $p < 0.001$ $n = 3$

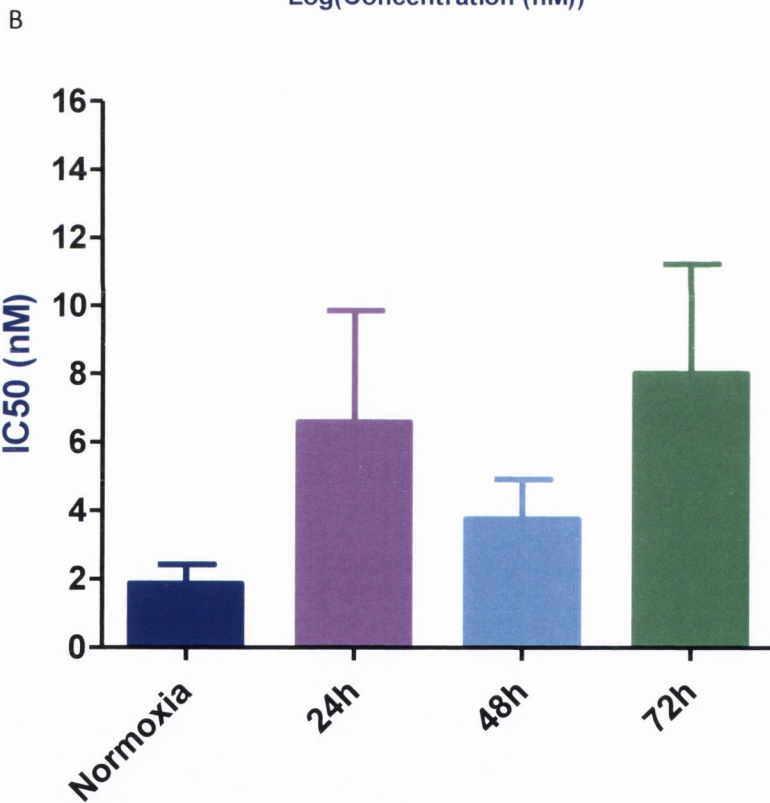
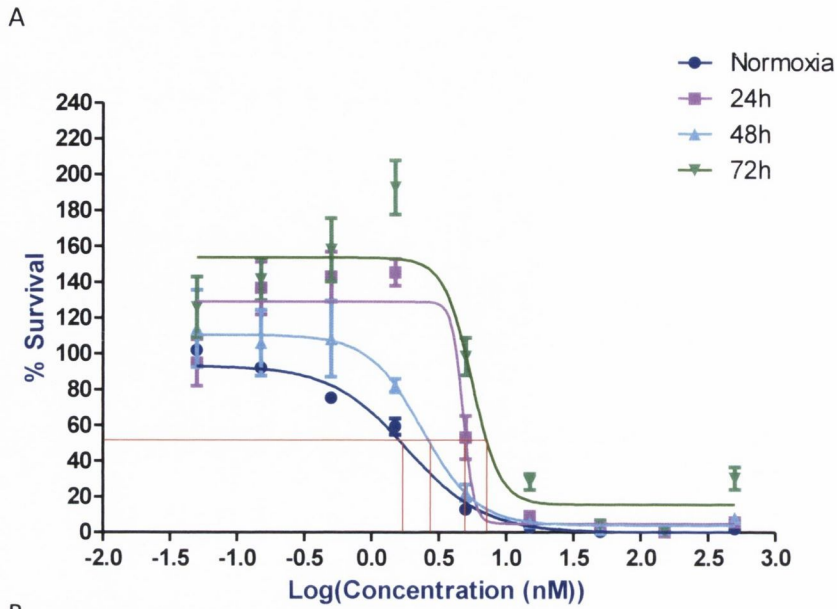
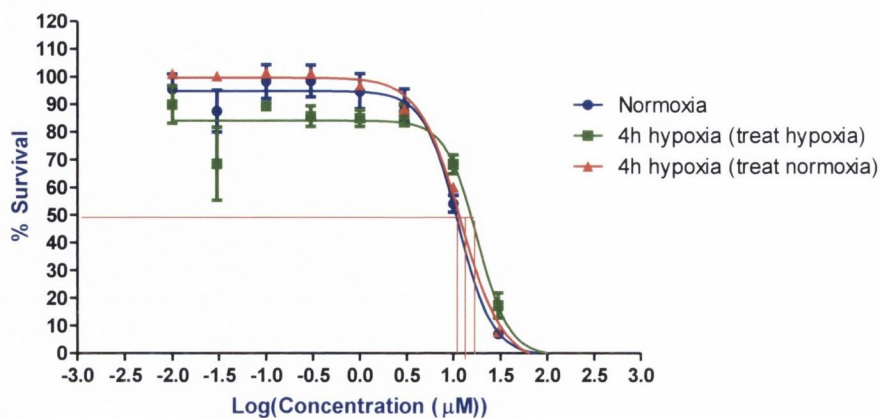


Figure 3.18. Treating A2780 in Hypoxia Increases Resistance to Paclitaxel. Cells which were not pre-exposed to hypoxia were treated with paclitaxel in hypoxic conditions. Hypoxia was introduced either at the beginning of treatment or at a timepoint during treatment. Although there was a trend towards increased resistance when treated in hypoxia, this did not reach statistical significance. $n = 3$

3.3.5.6 Acute Hypoxia Increases Resistance to Cisplatin but not Paclitaxel in A2780cis Cells

A2780cis which were exposed to hypoxia for four hours before treating with cisplatin showed further 8-fold increased resistance (Figure 3.19). This was statistically significant $p < 0.05$. This resistance was seen in cells which were also treated in hypoxia – cells which were exposed to hypoxia for a brief period before drug treatment in normoxia did not show increased resistance to cisplatin. A2780cis exposed to acute hypoxia did not show increased resistance to paclitaxel (Figure 3.20).

A



B

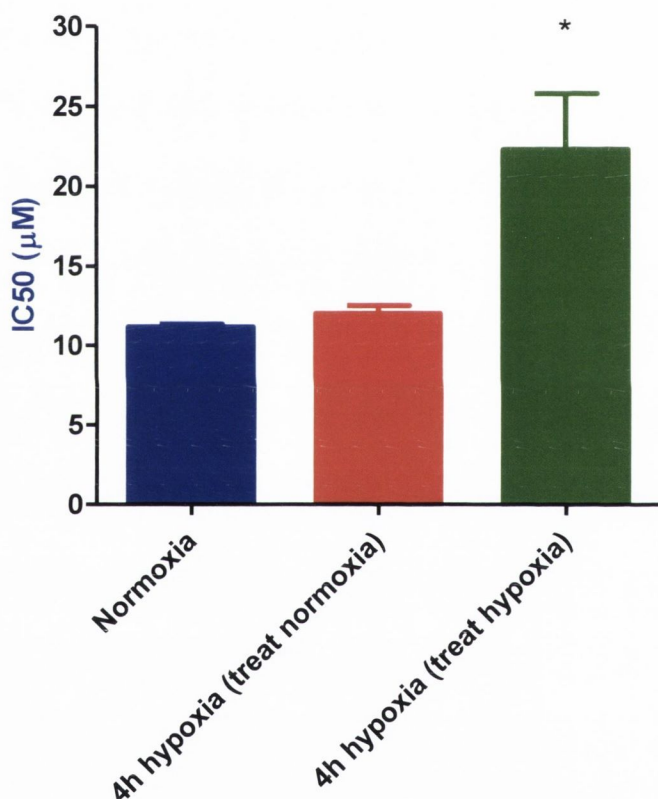
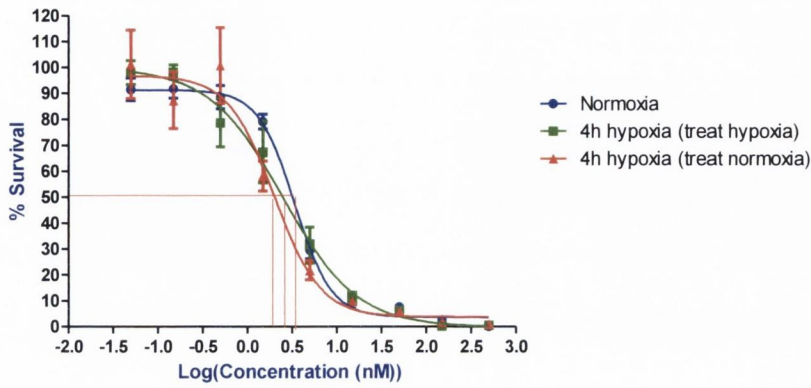


Figure 3.19. Acute Hypoxia Increases Resistance to Cisplatin in A2780cis. Dose response curves and bar graphs detailing response of A2780cis to cisplatin following hypoxia. Exposure of A2780cis to hypoxia for four hours before treatment increased resistance to cisplatin when the cells were also treated in hypoxia for 72 hours. This resistance was not present if cells were treated in normoxia. * $p < 0.05$ $n = 3$

A



B

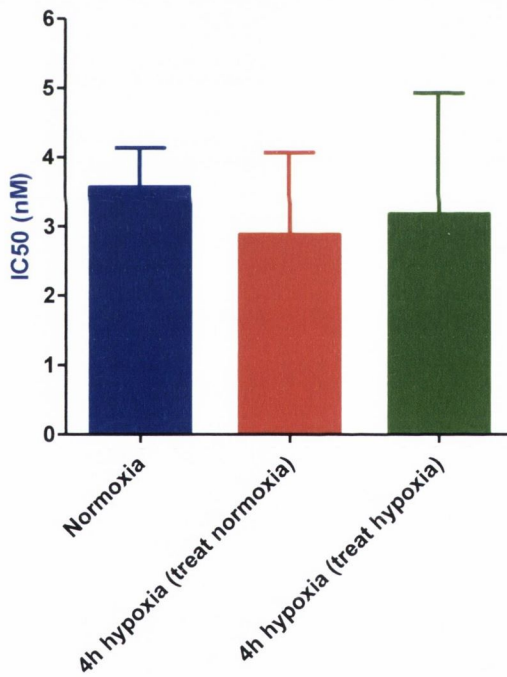
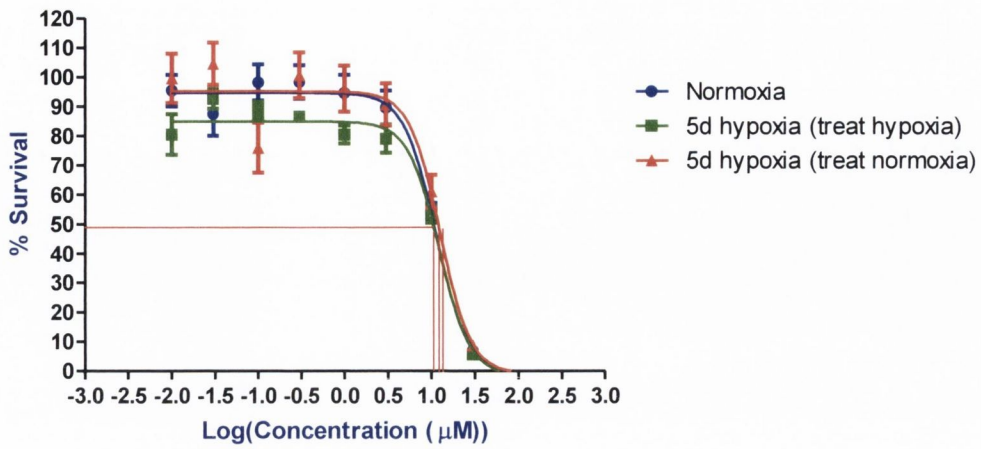


Figure 3.20. Acute Hypoxia does not Increase Resistance to Paclitaxel in A2780cis. Exposure of A2780cis to acute hypoxia before treatment with cisplatin did not increase resistance. Treatment of cells in normoxia or hypoxia following pre-exposure to acute hypoxia did not affect resistance to cisplatin. n = 3

3.3.5.7 Chronic Hypoxia Increases Resistance to Cisplatin but not Paclitaxel in A2780cis Cells

Exposing A2780cis to hypoxia for five days before treatment with cisplatin increased resistance (Figure 3.21). The increase was small yet significant ($p < 0.05$). This increase in resistance to cisplatin was only observed if cells were treated with cisplatin in hypoxia in addition to chronic exposure before treatment. Increased resistance to cisplatin was not observed if cells were treated in normoxia, even after chronic exposure to hypoxia previously. Chronic exposure to hypoxia before drug treatment did not affect the response to paclitaxel in A2780cis (Figure 3.22).

A



B

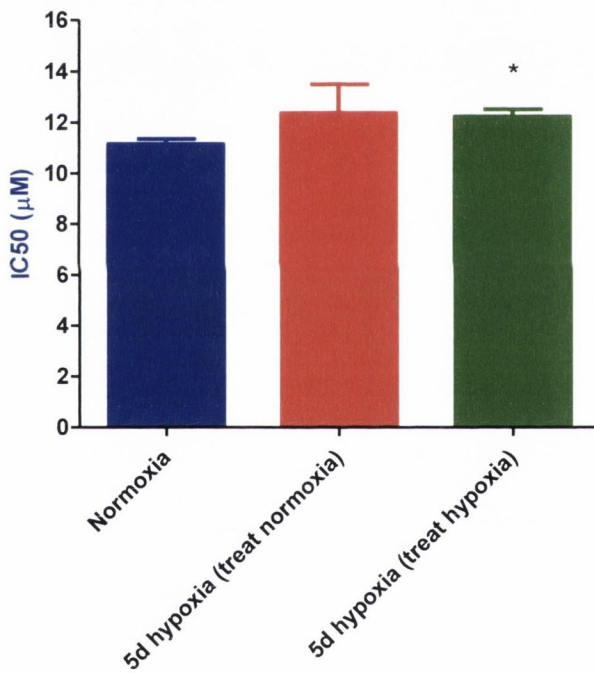
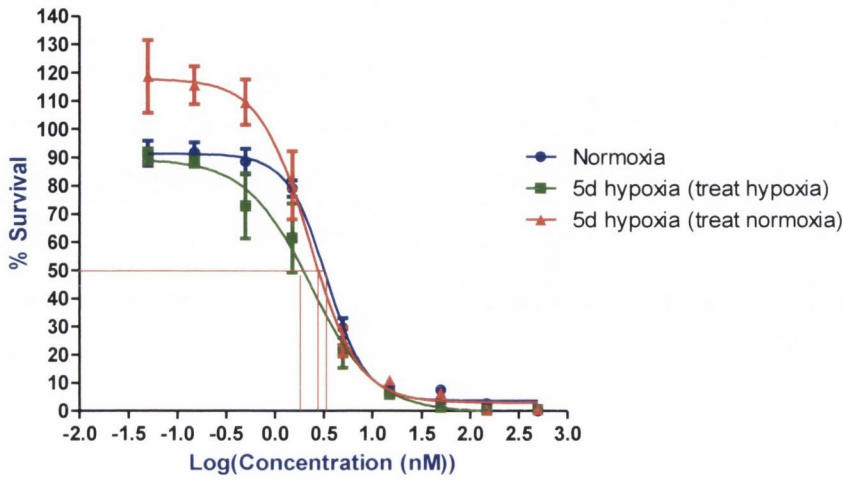


Figure 3.21. Chronic Hypoxia Increases Resistance to Cisplatin in A2780cis. Cells which were exposed to hypoxia for 5 days before treatment in hypoxia displayed increased resistance to cisplatin. This increased resistance was attenuated in cells which were treated in normoxia. * $p < 0.05$ $n = 3$

A



B

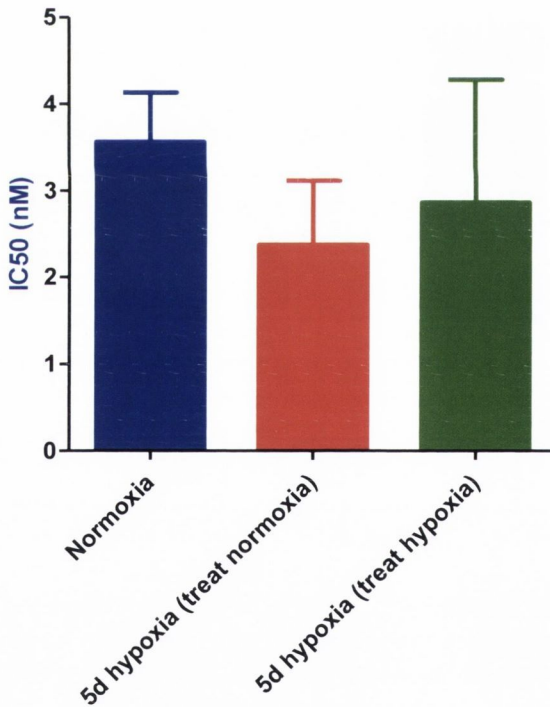
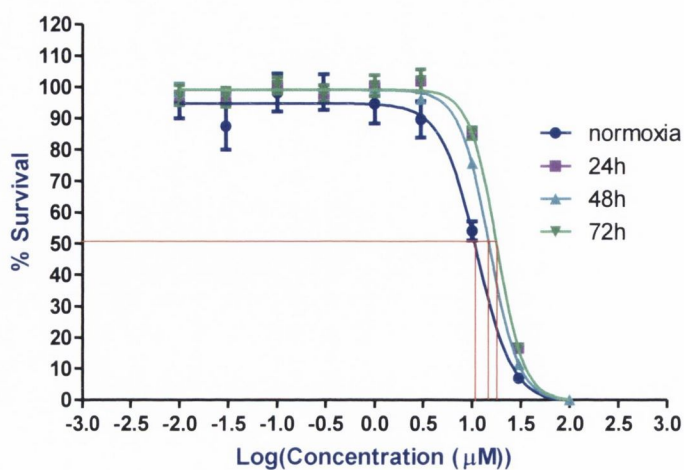


Figure 3.22. Chronic hypoxia does not Increase Resistance to Paclitaxel in A2780cis. Exposure of A2780cis to chronic hypoxia before drug treatment did not affect their response to paclitaxel. Treatment of cells in hypoxia or normoxia did not affect response to paclitaxel. n = 3

3.3.5.8 Treating A2780cis in Hypoxia Increases Resistance to Cisplatin but not Paclitaxel

Cells which were not previously exposed to hypoxia were treated with cisplatin or paclitaxel in hypoxic conditions. Cells were either placed in hypoxia at the beginning of the drug treatment or they were placed in hypoxia at timepoints during the treatment. Drug treatment in hypoxia increased the resistance of A2780cis to cisplatin ($p < 0.01$, Figure 3.23). Treatment of A2780cis with paclitaxel in hypoxia did not affect the resistance levels (Figure 3.24).

A



B

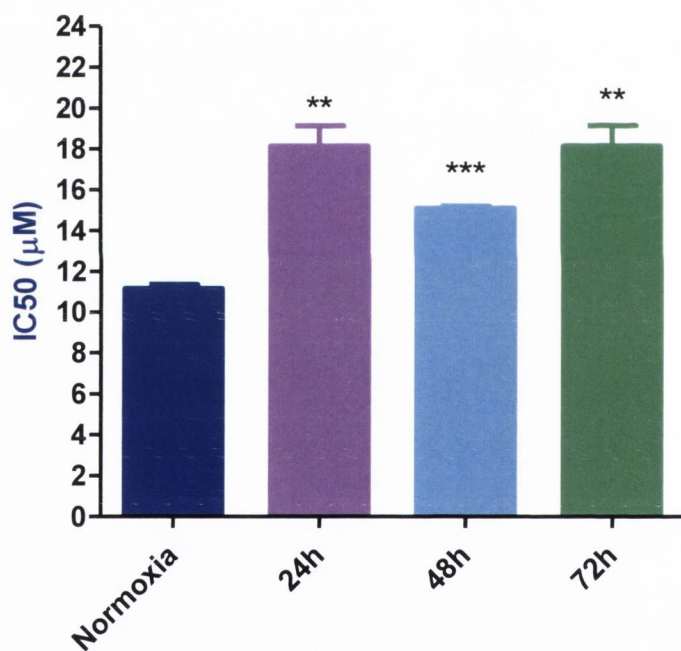
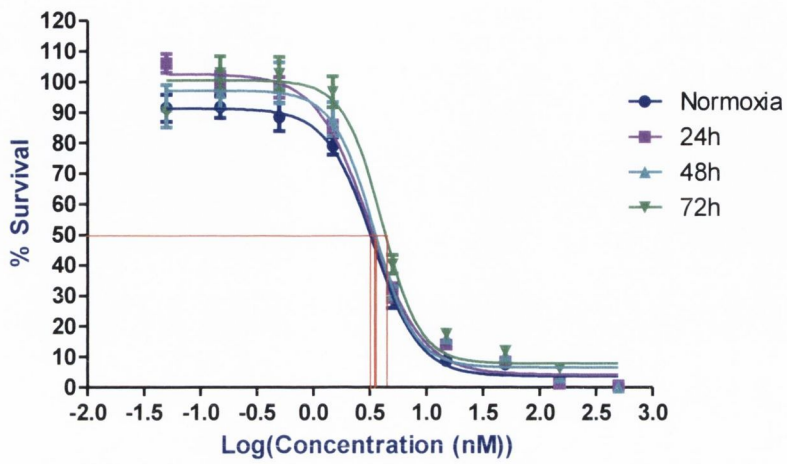


Figure 3.23. Treating A2780cis in Hypoxia Increases Resistance to Cisplatin. A2780cis cells which were not previously exposed to hypoxia were placed in hypoxia during drug treatment. Resistance to cisplatin was increased when treated in hypoxia compared to treatment in normoxia. Increased resistance was seen when cells were in hypoxia for any length of the treatment (24 hours, 48 hours or 72 hours). ** $p < 0.01$ *** $p < 0.001$ $n = 3$

A



B

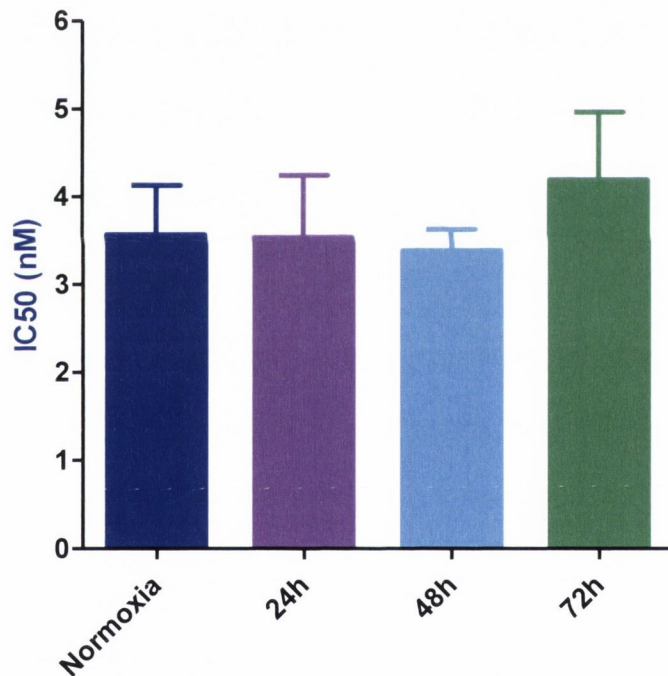


Figure 3.24. Treating A2780cis in Hypoxia does not Increase Resistance to Paclitaxel. A2780cis which were not previously exposed to hypoxia were treated with cisplatin either for the full duration of treatment (72h) or for periods during treatment (24 or 48h). Treatment in hypoxia did not affect resistance of A2780cis to paclitaxel. n = 3

3.3.6 Timecourse of HIF-1 α Expression in A2780 and A2780cis

Expression of HIF-1 α protein was measured using Western Blot. HIF-1 α protein expression was absent in normoxic cells, however was present from 4 hours in cells exposed to hypoxia. It displayed a similar pattern of expression in both A2780 and A2780cis, although it seemed to have a slight decrease in expression at 72 hours in A2780cis (Figure 3.25).

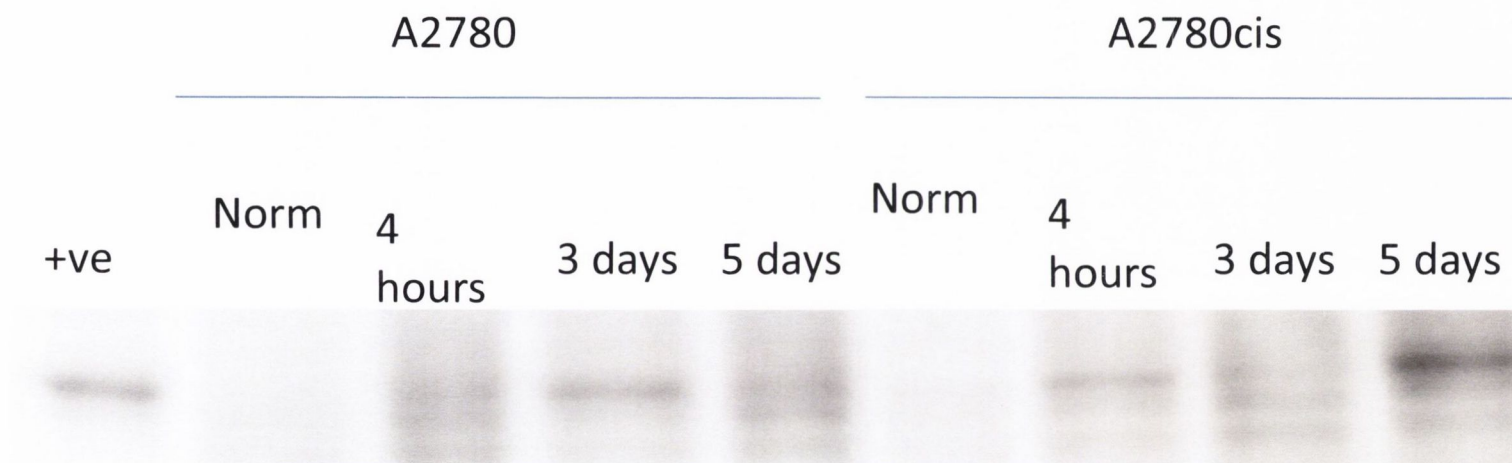


Figure 3.25. Timecourse of Expression of HIF-1 α in A2780 and A2780cis. HIF-1 α protein expression was virtually absent in normoxic cells, however it was present from 4 hours in cells exposed to hypoxia. A positive control of A2780cis treated with 50uM of CoCl₂ was used to show the bands at the correct position on the gel, 120kDa. n = 3

3.4 Discussion

Chemoresistance is a major problem affecting ovarian cancer patients. Hypoxia has been implicated in development of chemoresistance in a number of cancer types including breast [354,356,357], prostate [358], colon [359], liver [273,278,280] and ovarian [189,346]. Studies analysing how hypoxia affects the response of different models to chemotherapeutics usually use either MTT assays or clonogenic assays to measure sensitivity/resistance. In this study, we chose the MTT assay to measure resistance due to its ease of use and relatively short assay time.

There is conflicting evidence in the literature on tumour HIF-1 α expression and its link to a clinical response. An early study by Birner *et al.* showed that HIF-1 α expression alone was of no use as an indicator of response to chemotherapy in ovarian cancer [360]. A similar study in 2008 also claimed that expression of HIF-1 α could not be linked to response to platinum-based therapy in ovarian carcinoma, although high expression levels of HIF-1 α were associated with poorer overall survival [199]. A study by Daponte *et al.* also correlated HIF-1 α expression with poorer overall survival in ovarian carcinoma [200]. Interestingly however, protein expression of HIF-1 α has also been correlated to better overall response in late stage epithelial ovarian carcinoma specimens [201]. Thus hypoxia is shown to affect the resistance of many solid tumours to both cisplatin and paclitaxel through a variety of mechanisms – mainly those which affect the manner in which the drug exerts its effects. However, the clinical effect of this is still unclear – while many studies demonstrate a poorer outcome for patients with hypoxic tumours, others have shown hypoxic tumours to confer a survival advantage. However, these studies have used HIF-1 α or other surrogate markers of hypoxia such as VEGF to link hypoxia to survival or other clinical responses – it may be that these are unsuitable markers for this type of analysis. In this chapter we aimed to determine the effect of hypoxia on response to chemotherapy in our model, and to determine the significance of timing/duration of hypoxia.

We developed a hypoxia matrix in order to best represent possible clinical scenarios in patient care. Many studies investigating hypoxia and chemoresistance look at the introduction of hypoxia during treatment [185,191,272,361] however we felt it would be of use to look at the introduction of hypoxia at various different stages of treatment. Furthermore, there are few peer-reviewed articles examining the effect of hypoxia on chemoresistance in ovarian cancer cell lines. We considered four types of patient scenarios when designing the different points of the hypoxia matrix:

1. A patient with a small tumour which has not been hypoxic before or during chemotherapy.
2. A patient with a large tumour, receiving neoadjuvant chemotherapy before debulking. These patients often have a large tumour and a build-up of ascitic fluid [362]. This type of tumour is likely to have been chronically hypoxic before receiving chemotherapy, and is hypoxic when chemotherapy begins. As the tumour shrinks, regions may return to normal oxygenation, and receive chemotherapy under normal oxygen conditions.
3. A patient with a relatively large tumour, which is removed before receiving adjuvant chemotherapy. If there is any tumour remaining (i.e. the patient was suboptimally debulked), this tumour may have been chronically hypoxic before removal of the bulk of the tumour, or it may become acutely hypoxic due to growth in the interval between surgery and commencement of chemotherapy.
4. A patient with a tumour which undergoes transient hypoxia due to abnormal vasculature compressing blood vessels – they are exposed to hypoxia followed by rapid reoxygenation.

‘Acute’ and ‘chronic’ hypoxia were defined as 4 hours and 5 days respectively, in accordance with definitions in the literature [363,364]. We found that cells which were acutely hypoxic showed very similar proliferation curves to normoxic cells. While they all entered the exponential phase of growth at the same seeding density,

chronically hypoxic cells tended to grow faster than normoxic or acutely hypoxic cells, thus the proliferation curve tended to plateau faster for chronically hypoxic cells. Thus, the chronically hypoxic cells did not remain in the exponential phase of growth for as long as the other cells, and it was necessary to seed the cells at a low density in order to maintain the exponential phase for as long as possible during treatment.

In this study, exposing both the parent A2780 cells and the daughter A2780cis cells to acute or chronic hypoxia increased resistance to cisplatin, in accordance with a previous study in ovarian cancer cell lines by Su *et al.* [306]. This resistance was greatest when the cells were also cisplatin-treated in hypoxia, however it was attenuated when the treatment was carried out in normal oxygen conditions. Reoxygenation following hypoxic exposure has been shown to restore sensitivity to radiation therapy in breast cancer [365] and gastric cancer [366], although as yet has not been shown to affect chemosensitivity. However, a previous study using a breast cancer model also found no cisplatin resistance in cells which had been exposed to hypoxia followed by drug treatment in normal oxygen [282]. Although HIF-1 α protein had been expressed from 4 hours, tissue reoxygenation following periods of hypoxia has long been known to cause damage to cells due to production of free radicals [367]. It is likely that some of the cell death seen in the cells treated in normoxia is due to reoxygenation injury.

In the cisplatin-sensitive A2780, the highest level of cisplatin resistance was seen in cells chronically exposed to hypoxia pre-treatment and then treated in hypoxia (~10-fold). A2780 cells which were acutely exposed to hypoxia pre-treatment and treated in hypoxia were 8-fold more resistant to cisplatin than normoxic cells. Thus, the resistance of A2780 to cisplatin increased over time in hypoxia. This may be due to changes in molecular signalling occurring over time within the cells and it has long been known that concentrations of signalling molecules within cells can increase with prolonged hypoxic exposure [368]. A study examining the effect of acute and chronic hypoxia on mitomycin C sensitivity in colon carcinoma found that one

particular biomarker of mitomycin C sensitivity was elevated in acute hypoxia yet reduced in chronic hypoxia, mirroring the sensitivity profile of the cells as measured by MTT [369], therefore it has been previously shown that changes in molecular molecules within the cell can be related to resistance to chemotherapy. Studies in animal models have also demonstrated biochemical differences between tumours which are acutely or chronically hypoxic [370] and *in vitro* studies have shown that induction of ion channels involved in signalling leading to gene expression are activated over time in hypoxia [371]. Thus it is clear that cells under longer periods of hypoxia are constantly being stimulated to express different levels of molecules which can be linked to resistance.

A2780cis displayed a more modest yet significant fold change in resistance of 2-fold for cells acutely exposed to hypoxia before treatment and 1.1-fold for cells chronically exposed. Thus the cisplatin resistance profile of A2780cis (i) is not as drastically affected by hypoxia as A2780, and (ii) does not display the same pattern as A2780. The fact that there is a much lesser increase in cisplatin resistance in A2780cis indicates that hypoxia may be inducing the same or similar changes within the cells to induce cisplatin resistance as chronic exposure to cisplatin. It is possible that the lesser resistance in the chronically hypoxia-exposed A2780cis is linked to the decrease in HIF-1 α expression noted on Western Blot after 72 hours hypoxic exposure, however HIF-1 α expression had increased at 5 days hypoxia. However, as noted above, there are diverse cellular changes occurring over time in hypoxia, and it may be that in this cell line, the resistance to cisplatin is being dampened. One possible reason for this is overactivation of prolyl hydroxylase (PHD) enzymes in A2780cis in chronic hypoxia. PHD enzymes normally act to degrade the HIF-1 α protein in normal oxygen conditions. In acute hypoxia, these enzymes are inactivated, allowing accumulation of the HIF-1 α protein. However, a study in 2008 by Ginouves *et al.* showed that over time in hypoxia, PHDs can become overactivated [372]. The authors showed that this protects cells from necrosis, and can occur *in vitro* and *in vivo*.

Treatment of the hypoxia 'naïve' cells with cisplatin in hypoxia demonstrated increased resistance to cisplatin in both cell lines. Even if cells were only exposed to hypoxia for part of the treatment period they were still significantly more resistant to cisplatin than cells treated in normal oxygen. A2780 and A2870cis cells which were not pre-exposed to hypoxia yet treated in hypoxia for the duration of treatment were 8.6-fold and 1.6-fold more resistant to cisplatin respectively. Thus in A2780 cells, the level of resistance observed in cells treated only in hypoxia was very similar to the levels in the acutely hypoxic cells. This is not surprising, as the acutely hypoxic cells had only a very short exposure to hypoxia before treatment. The level of resistance increased with increasing time in hypoxia during treatment. Thus it can be seen that the level of cisplatin resistance increased over time in hypoxia in the A2780, and reduced over time in hypoxia in A2870cis.

Although a trend for increased resistance to paclitaxel could be observed in A2780 for all hypoxic exposures, this did not reach statistical significance. This is likely due to the increased variability observed for the paclitaxel IC₅₀ values. For example, in A2780 cells exposed to acute hypoxia followed by paclitaxel treatment in normoxia, the IC₅₀ value ranged from 0.4 nM to 4 nM, an increase of 10-fold. Cremophor EL® is the main diluent used for paclitaxel formulation. Previous studies have found that Cremophor EL® can affect the activity of paclitaxel in a number of cell lines, and at high levels can antagonize the effects of paclitaxel [373]. As Cremophor EL® is a thick viscous mixture and is difficult to accurately pipette, it is possible that in the small volumes that were used for this study, variations in the amount of Cremophor EL® that was used for making up stock solutions could have contributed to the variability observed. However, this was also a phenomenon observed by others in our group using paclitaxel prepared in dimethylsulfoxide (DMSO). Thus, this may be a problem with the use of paclitaxel in cell culture-based research which should be considered when planning experiments.

A2780 cells which were exposed to hypoxia before and/or during treatment, showed a trend towards increased resistance to paclitaxel. A previous study using

A2780 cells has shown increased resistance to paclitaxel with increasing hypoxia levels [346]. They were also able to show that this resistance was abrogated when siRNA for HIF-1 α was introduced to the cells, thus indicating that HIF-1 α was indeed responsible for this resistance. Hypoxic A2780 cells have been shown to express TUBB3, a tubulin isotype which is linked to paclitaxel resistance, via HIF-1 α activation [349]. Thus this may be one way in which these cells are becoming more resistant to paclitaxel. However, there is little information in the literature of the effects of hypoxia on paclitaxel sensitivity in this cell line. It is likely that other mechanisms such as activation of the Akt and ERK pathways may be contributing to the resistance observed, as has been seen in other cell models.

The sensitivity of A2780cis to paclitaxel was not influenced by hypoxia. There was no trend observed for any of the hypoxic interventions carried out. As A2780cis is part of a cisplatin resistance model, it is not commonly used in the literature to study paclitaxel resistance. However, there have been a few papers which have used this model to study cross-resistance of novel chemotherapeutic agents which are similar in action to paclitaxel. A2780cis has been shown to have a relatively similar sensitivity profile to paclitaxel as A2780, as we observed [374,375]. Currently there are no articles in the literature which examine the effect of hypoxia on paclitaxel resistance in A2780cis. We have shown that hypoxia does not increase paclitaxel resistance in these cells while greatly increasing cisplatin resistance.

Western blots for HIF-1 α protein expression were carried out for A2780 and A2780cis in normoxia and hypoxia. A positive control was formed by exposing cells to 50 μ M of cobalt chloride (CoCl₂) for 24 hours before carrying out protein extraction. CoCl₂ is a divalent cation which is capable of stabilizing HIF-1 α under normal oxygen conditions [376]. There is conflicting evidence on the expression of HIF-1 α in normoxia in the A2780 cell line in the literature. We found HIF-1 α not to be expressed under normal oxygen conditions. This is in contrast to previous studies which have shown A2780 [377] and A2780cis cells to express high levels of HIF-1 α under normal culture conditions [378,379]. It may be that the antibodies used by

these papers were more sensitive than our antibody, and could pick up lower concentrations of HIF-1 α protein present. Other studies have shown minimal to no expression of HIF-1 α in normoxia, in accordance with our study [346,349,380]. In our study, HIF-1 α expression was induced as early as four hours after the cells were placed in hypoxia. Increases in HIF-1 α expression have been noted from as early as 30 mins of hypoxic exposure [381]. In A2780 cells, we saw that HIF-1 α protein expression was fairly constant between 4 hours and 5 days of hypoxic exposure. In A2780cis however, there was a drop in HIF-1 α expression at 72 hours, although this was recovered after 5 days. It is unclear why this occurred, although if the cells were becoming desensitized to the activity of PHD enzymes as discussed previously, it may be that this mechanism is reversible, or that the cells alter signalling mechanisms/biological activity in order to circumvent this. In addition, at certain timepoints there was a laddering effect observed around the band position of HIF-1 α . This has been observed in many studies of HIF-1 α protein expression, in a variety of different tissue types and with different antibodies [182,382-386]. There are several causes of multiple bands on Western blots including non-specific antibodies, over-concentrated antibody, protein digestion, post-translational modifications e.g. glycosylation and splice variants. The fact that this multi-banding has been observed in several independent studies indicates that it may be more than a technical issue. Indeed several splice variants of the HIF-1 α gene have been reported [387]. HIF-1 α polymorphisms have been linked to more aggressive tumour biology in prostate cancer [388]. Polymorphisms of the HIF-1 α protein have been shown to have clinical significance in head and neck squamous cell carcinoma [389], renal cell carcinoma [390] and oesophageal carcinoma [391].

3.5 Summary

This chapter set out to investigate the effect of hypoxia on cisplatin and paclitaxel resistance in the ovarian cancer cell line model A2780 and A2780cis. We have shown that:

1. A2780 cells exposed to hypoxia increase resistance to cisplatin over time.
2. A2780cis cells exposed to hypoxia also increase resistance to cisplatin.
3. The response of A2780 cells to cisplatin is more greatly affected by hypoxia than A2780cis.
4. A2780 cells show a trend towards increased resistance to paclitaxel in hypoxia.
5. The response of A2780cis to paclitaxel is not affected by hypoxia.
6. HIF-1 α protein is expressed in both cell lines in hypoxic conditions, although the pattern of expression varies slightly between the cell lines.

However, although the experiments in this chapter have shown how hypoxic exposure affects resistance to chemotherapeutic drugs, it is unclear what the reasons for the differences are. In the following chapter, RNA is extracted from both cell lines under hypoxic and normoxic conditions and interrogated on Affymetrix Human Gene Arrays, in order to identify genes or pathways that could influence the resistance observed.